

Advancing block-oriented modeling in process control

by

Stephanie Diane Loveland

A dissertation submitted to the graduate faculty
in partial fulfillment of the requirements for the degree of

DOCTOR OF PHILOSOPHY

Major: Chemical Engineering

Program of Study Committee:
Derrick K. Rollins, Sr., Major Professor
Gerald M. Colver
Rodney O. Fox
Carolyn Heising
Andrew C. Hillier

Iowa State University

Ames, Iowa

2008

Copyright © Stephanie Diane Loveland, 2008. All rights reserved.

UMI Number: 3307080

INFORMATION TO USERS

The quality of this reproduction is dependent upon the quality of the copy submitted. Broken or indistinct print, colored or poor quality illustrations and photographs, print bleed-through, substandard margins, and improper alignment can adversely affect reproduction.

In the unlikely event that the author did not send a complete manuscript and there are missing pages, these will be noted. Also, if unauthorized copyright material had to be removed, a note will indicate the deletion.



UMI Microform 3307080
Copyright 2008 by ProQuest LLC
All rights reserved. This microform edition is protected against
unauthorized copying under Title 17, United States Code.

ProQuest LLC
789 East Eisenhower Parkway
P.O. Box 1346
Ann Arbor, MI 48106-1346

To Brian, Joshua, Nathanael and LilyAnna

ABSTRACT	V
CHAPTER 1. INTRODUCTION	1
1. GENERAL INTRODUCTION	1
2. ADVANCED CONTROL TECHNIQUES	2
3. MOTIVATION AND DISSERTATION ORGANIZATION	3
4. REFERENCES	4
CHAPTER 2. BACKGROUND	6
1. MODEL TYPES	6
2. HAMMERSTEIN AND WIENER MODELS	6
2.1. H-BEST	9
2.2. W-BEST	11
3. OTHER BLOCK-ORIENTED MODELS	14
4. STATISTICAL DESIGN OF EXPERIMENTS	15
5. REFERENCES	17
CHAPTER 3. PRELIMINARY INVESTIGATIONS	21
1. MOTIVATION FOR RESEARCH	21
2. SCOPE OF RESEARCH	23
3. PRELIMINARY WORK	24
3.1. EXAMPLE 1: SIMULATED NL PROCESS	24
3.2. EXAMPLE 2: SIMULATED LNL PROCESS	26
3.3. EXAMPLE 3: INTERACTIVE EFFECTS OF INPUTS	28
3.4. EXAMPLE 4: A PILOT-SCALE DISTILLATION PROCESS	30
4. DISSERTATION RESEARCH	37
5. REFERENCES	38
CHAPTER 4. NONLINEAR MULTIPLE INPUT FEEDFORWARD CONTROL UNDER BLOCK-ORIENTED MODELING	40
1. BACKGROUND	40
2. METHODOLOGY	42
2.1. BUILDING THE PROPOSED LNL MODEL	42
2.2. GENERAL FEEDFORWARD CONTROL	44
2.2. PROPOSED FEEDFORWARD CONTROL METHODOLOGY	45
3. THE PROCESS STUDIED	47
4. THE FEEDFORWARD-FEEDBACK CONTROLLER	54

5. COMPARISON OF FEEDBACK ONLY CONTROLLER WITH FEEDFORWARD/FEEDBACK CONTROLLER	55
6. CONCLUSIONS	57
7. REFERENCES	57

CHAPTER 5. DEVELOPMENT OF NONLINEAR FEEDFORWARD CONTROL FROM CLOSED-LOOP FREELY-EXISTING TYPE DATA WITH APPLICATION TO A PILOT-SCALE DISTILLATION COLUMN

1. INTRODUCTION	60
2. METHODOLOGY	63
2.1 MODELING METHODOLOGY	63
2.1.1. The Wiener model	64
2.1.2. Procedure for Model-Building	66
2.2. FEEDFORWARD CONTROL METHODOLOGY	67
2.2.1. General Feedforward Controller Methods	67
2.2.2. Proposed Feedforward Controller Methodology	69
3. THE DISTILLATION PROCESS	71
3.1. OPEN-LOOP MODEL BUILDING	71
3.1.1. Training Phase	71
3.1.2. Testing Phase	80
3.2. CLOSED-LOOP FEEDBACK CONTROL AND MODEL BUILDING	83
3.3. IMPLEMENTATION OF THE PROPOSED FEEDFORWARD/FEEDBACK CONTROL SCHEME	87
3.4. PI CONTROLLER VS. FFPI CONTROLLER PROCESS RESPONSES	88
4. CONCLUSIONS	91
5. ACKNOWLEDGEMENTS	91
6. REFERENCES	92

CHAPTER 6. CONCLUSIONS AND FUTURE WORK

1. CONCLUSIONS	95
2. FUTURE WORK	97
3. REFERENCES	98

ACKNOWLEDGEMENTS

99

ABSTRACT

The increasing pressure in industry to maintain tight control over processes has led to the development of many advanced control algorithms. Many of these algorithms are model-based control schemes, which require an accurate predictive model of the process to achieve good controller performance. Because of this, research in the fields of nonlinear process modeling and predictive control has advanced over the past several decades.

In this dissertation, a new method for identifying complicated block-oriented nonlinear models of processes will be proposed. This method is applied for LNL and LLN “sandwich” block-oriented models and will be shown to accurately predict process response behavior for a simulated continuous-stirred tank reactor (CSTR) and a pilot-scale distillation column. In addition, it will be shown to effectively model the pilot-scale distillation column using closed-loop, highly correlated input data.

Using the block-oriented models identified, a new feedforward control framework has been developed. This feedforward control framework represents the first that compensates for multiple input disturbances occurring simultaneously. Only a single process model is needed to account for all measured disturbances. In addition, it allows a plant engineer to develop the predictive model of the process from plant historical data instead of introducing a series of disturbances to the process to try to identify the model. This has the potential to considerably reduce the cost of implementing an advanced control scheme in terms of time, effort and money. The proposed feedforward control framework is tested on a simulated CSTR process in Chapter 4, and on a pilot-scale distillation column in Chapter 5.

CHAPTER 1. INTRODUCTION

1. General Introduction

In industry, it is desirable to have good control of processes to maintain both operational safety and product quality standards. The field of process control has evolved over time to meet these ever-changing standards. A process control system must monitor process outputs and implement input changes based on the current process conditions [1]. In the past few decades, many different advanced control algorithms have been developed. Among these are several types of model-based control algorithms, including Smith predictors, feedforward controllers and model predictive control (MPC) schemes [2]. As more and more industries apply the concepts to their processes, the limitations and strengths of model-based control have been seen under many conditions.

The application of any model-based control strategy requires determination of an accurate process model. Controller performance is highly dependent upon the model that is chosen to predict process behavior. The procedures used for developing the process model can be time-consuming and costly, and generally require that the process be perturbed in order to determine cause-and-effect behavior between the process inputs and outputs.

There are many challenges to developing accurate process models. Many chemical and biological systems exhibit some type of nonlinear behavior, but model-based control schemes have often used linear models to reduce the computational load on the control system. This can be sufficient when the process is operated over a small range of inputs [3, 4]. Real process systems also often exhibit complex dynamic responses to changes in the process inputs, including nonlinear dynamics, which can make the process response prediction even more difficult. Several types of nonlinear models have been proposed to

address some of these challenges. These include Radial Basis Functions (RBFs) and Artificial Neural Networks (ANNs) [5, 6], ARMAX models [7, 8, 9], Genetic Algorithms [10], Feedforward Neural Networks (FNNs) [11] and Block-Oriented Models (BOMs) [12-17].

2. Advanced Control Techniques

Among the different advanced control methodologies, the topic of feedforward control is one of the oldest. The basic concept was applied as early as 1925 to level control systems for boiler drums [2]. However, it wasn't widely used in industry until the 1960s [18]. Since then, it has been applied in many types of chemical processes, including boilers, evaporators, solids dryers, direct-fired heaters and waste neutralization plants [19].

The concept of feedforward control allows for theoretically perfect control of a process system. Using measured values of process input disturbances (loads), corrective action can be taken before the process output deviates from its desired set point. However, because not all disturbances can be measured efficiently or in a timely manner and the model used may not be perfect, it is usually used in conjunction with feedback control, which compensates for any deviation of the output variable from its set point, regardless of what caused the deviation [2].

Most feedforward control schemes approximate the feedforward controller by a linear model [20], but nonlinear process models can also be used [21, 22]. A feedforward control law for each disturbance variable is typically determined separately, and interactive behavior between these input variables is not addressed.

3. Motivation and Dissertation Organization

Because the application and performance of any model-based control scheme is highly dependent upon the predictive model that is used, the model identification step is critical. In addition, the ability of a model-based control scheme to address nonlinear and interactive process response behaviors to accurately predict process outputs is vitally important. Given that most applications of feedforward control do not address these behaviors, the focus of this research has been to develop accurate, compact nonlinear process models that are applied easily in a feedforward control scheme to improve control of a process. The nonlinear process models used are block-oriented models (BOMs) which are capable of addressing both interactive input behaviors and nonlinearities, as well as complex process dynamics. Of particular interest are the Hammerstein, Wiener and sandwich block-oriented models.

This dissertation is organized as follows. Chapter 2 will give an overview of model types, with particular attention being paid to block-oriented models. The H-BEST and W-BEST modeling methodologies developed by Rollins et al. [13, 16] will be presented, and will be followed by a brief discussion on the use of statistical design of experiments in model identification procedures. In Chapter 3, preliminary work using simulated processes that are Hammerstein, Wiener and sandwich BOMs will be introduced. Chapter 4 is a paper presenting a new method for using the LNL “sandwich” type BOM in a feedforward/feedback control scheme, and applies this to a simulated continuous-stirred tank reactor (CSTR). Chapter 5 is a paper that will present a methodology for applying the W-BEST modeling methodology to a real distillation process in both open- and closed-loop modes. In addition, the identified model will be used in a feedforward/feedback control

scheme on the distillation column, and compared with standard feedback control. Finally, Chapter 6 will give general conclusions about the work discussed and propose future research avenues.

4. References

- [1] Ogunnaike, B.A. and W.H. Ray, *Process Dynamics, Modeling and Control*, Oxford University Press, Inc., New York, 1994.
- [2] Seborg, D.E., T.F. Edgar and D.A. Mellichamp, *Process Dynamics and Control*, 2nd edition, John Wiley and Sons, 2003 {check date}
- [3] Clarke, D.W., C. Mohtadi and P.S. Tuffs, "Generalized Predictive Control- Part 1: The Basic Algorithm," *Automatica*, Vol. 23, pp. 137-148, 1987.
- [4] Muske, K.R. and J.B. Rawlins, "Model Predictive Control with Linear Models," *AIChE Journal*, Vol. 39, pp. 262-287, 1993.
- [5] Alexandridis, A. and H. Sarimveis, "Nonlinear Adaptive Model Predictive Control Based on Self-Correcting Neural Network Models," *AIChE Journal*, Vol. 51. No. 9, September 2005.
- [6] Fischer, M., O. Nelles and R. Isermann, "Adaptive Predictive Control of a Heat Exchanger Based on a Fuzzy Model," *Control Engineering Practice*, Vol. 6, pp. 259-269, 1998.
- [7] Di Palma, F., L. Magni, "A Multi-Model Structure for Model Predictive Control," *Annual Reviews in Control*, Vol. 28, pp. 47-52, 2004.
- [8] Gao, J, R. Patwardhan, K. Akamatsu, Y. Hashimoto, G. Emoto, S.L. Shah, B. Huang, "Performance Evaluation of Two Industrial MPC Controllers," *Control Engineering Practice*, Vol. 11, pp.1371-1387, 2003.
- [9] Havlena, V. and J. Findejs, "Application of Model Predictive Control to Advanced Combustion Control," *Control Engineering Practice*, Vol. 13, pp. 671-680, 2005.
- [10] Al-Duwaish H. and Naeem, Wasif , "Nonlinear Model Predictive Control of Hammerstein and Wiener Models Using Genetic Algorithms," *Proceedings of the 2001 IEEE International Conference on Control Applications*, September 5-7, 2001, Mexico City, Mexico

- [11] Gao, F., F. Wang and M. Li, "Predictive Control for Processes with Input Dynamic Nonlinearity," *Chemical Engineering Science*, Vol. 55, pp. 4045-4052, 2000.
- [12] Pearson, R.K. and B.A. Ogunnaike, "Nonlinear Process Identification," *Nonlinear Process Control*, Prentice-Hall PTR, Upper Saddle River, NJ, pp. 11-110, 1997.
- [13] Rollins, D.K., N. Bhandari, A.M. Bassily, G.M. Colver and S. Chin, "A Continuous-Time Nonlinear Dynamic Predictive Modeling Method for Hammerstein Processes," *Industrial and Engineering Chemistry Research*, Vol. 42, No. 4, pp. 861-872, 2003.
- [14] Greblicki, W., "Continuous-Time Hammerstein System Identification," *IEEE Transactions on Automatic Control*, Vol. 45, No. 6, pp. 1232-1236, 2000.
- [15] Bhandari, N. and D.K. Rollins, "Continuous-Time Hammerstein Nonlinear Modeling Applied to Distillation," *AIChE Journal*, Vol. 50, No. 2, pp. 530-533, 2004.
- [16] Bhandari, N. and D.K. Rollins, "A Continuous-Time MIMO Wiener Modeling Method," *Industrial and Engineering Chemistry Research*, Vol. 42, No. 22, pp. 5583-5595, 2003.
- [17] Chin, S., N. Bhandari and D.K. Rollins, "An Unrestricted Algorithm for Accurate Prediction of MIMO Wiener Processes," *Industrial and Engineering Chemistry Research*, Vol. 43, pp. 7065-7074, 2004.
- [18] Shinskey, F.G., *Process Control Systems: Application, Design, and Tuning*, 4th ed. McGraw-Hill, New York, 1996, Chapter 7.
- [19] Shinskey, F.G., M.F. Horddeski and B.G. Liptak, "Feedback and Feedforward Control", in *Instrument Engineer's Handbook: Vol. 2, Process Control*, 3rd ed., B.G. Liptak (Ed.), Chilton Book Col, Radnor, PA, 1995, Section 1.8.
- [20] Zhang, J. and R. Agustriyanto, "Inferential Feedforward Control of a Distillation Column," *Proceedings of the American Control Conference*, pp. 2555-2560, Arlington, VA, June 25-27, 2001.
- [21] Smith, C.A. and A.B. Corripio, *Principles and Practice of Automatic Process Control*, Wiley, New York, 1985. Smith & Corripio
- [22] Luyben, W.L., *Process Modeling, Simulation and Control for Chemical Engineers*, 2nd ed., McGraw-Hill, New York, 1990. Luyben, W.L.

CHAPTER 2. BACKGROUND

1. Model Types

Any model-based control scheme that is implemented requires some predictive model of the process being controlled. The ability of the control algorithm to maintain adequate control of the process is highly dependent upon the ability of the model to accurately predict the process behavior. Most chemical processes exhibit some type of nonlinear behavior; however, in order to simplify the computational efforts of the controller, many of the model-based control schemes have used a linear process model, which can be sufficient for processes which operate over a small region [1, 2].

Over the past decade, advances in computational technology have allowed for the introduction of nonlinear models to be used for the process response prediction [3-7]. Some authors have proposed using multiple linear models for the process, separating them into operating regions within the process [8, 9]. Others have used nonlinear models, and the types of nonlinear models that have been used include Radial Basis Functions (RBF) and Artificial Neural Networks (ANN) [7, 8], ARMAX models [9, 10, 11], Genetic Algorithms (GA) [12] and Feedforward Neural Networks [13].

2. Hammerstein and Wiener Models

The model identification process varies depending upon the type of model used. Many of the nonlinear models mentioned previously use a pseudo-random sequence (PRS) of input changes to estimate model parameters. This can allow for good estimation of dynamic or non-linear effects but does not effectively account for interactive effects among multiple inputs [14]. In addition to the types of models previously mentioned, a class of models known as block-oriented models (BOM) has been developed. The Hammerstein model is

one of the most common types, and it combines static nonlinearity with linear dynamics. It can be represented in block form, as described by Pearson and Ogunnaike [15] and is shown as Fig. 1 below. Another common BOM is the Wiener model, which also combines the static nonlinearity with linear dynamics, but the order of the blocks is reversed.

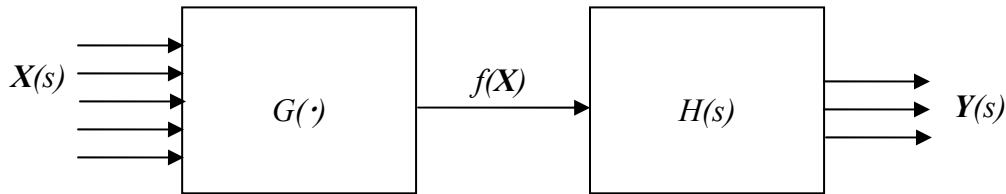


Figure 1: A description of a MIMO Hammerstein model as it appears in Pearson and Ogunnaike [15]. The input vector \mathbf{X} passes through a static map, resulting in the vector $f(\mathbf{X})$, which can be nonlinear. This vector then passes through the linear dynamic map and produces the output vector \mathbf{Y} .

Much has been discussed about these types of systems. Most of the models that have been proposed use discrete-time modeling, which places this type of approach into the class of NARMAX models [16]. While these have the capability of addressing any non-linear and interactive effects, they are usually developed assuming all these terms are zero, due to the enormous parameter identification burdens that exist [14].

There have been some who have successfully identified continuous-time Hammerstein and Wiener models and used them for prediction [16-20]. Among these, there exists an identification method that uses statistical design of experiments (SDOE) [21, 22] which has been proven to be a more efficient method of identifying process parameters [21, 23]. These types of models have successfully been used to represent several types of nonlinear processes, including pH neutralizations, distillation columns and continuous-stirred tank reactors (CSTR) [24].

The first papers discussing the use of Hammerstein models appeared in 1966 by Narendra and Gallman [25]. They have become increasingly popular because of their simple structure and ability to effectively model many types of nonlinear processes. Rollins et al. (1998) [26] developed a continuous-time Hammerstein modeling method that gives an explicit algorithm for the continuous-time, integrated form of the model and takes full advantage of SDOE [21]. This method was developed using a single-input, single-output (SISO) study on a CSTR [26], and has been named the Hammerstein Block-oriented Exact Solution Technique (H-BEST) because it has been shown to give an exact solution for a true Hammerstein process [8]. This method has been shown to be an accurate method of modeling both open- and closed-loop processes [27] and they contain a substantial amount of intelligent information about the process as well [14]. The algorithm and its applications will be discussed in more detail below.

Two general methods are typically used to identify Wiener models [14]. These are parametric and non-parametric methods. The primary difference between these two methods is that the non-parametric method results in a purely empirical model of the process, while the parametric method assumes some particular structure for both the static nonlinearity and the linear dynamics. The model identification for the parametric form then just requires estimation of the parameters. An exact solution for a true Wiener process was developed by our research group and is known as the Wiener Block-oriented Exact Solution Technique, or W-BEST. It follows a parametric approach to model identification and has been shown to accurately model both single-input, single-output (SISO) and multiple-input, multiple-output (MIMO) CSTR processes [14, 19]. It will be presented and discussed in more detail below.

2.1. H-BEST

The H-BEST algorithm was first introduced by Rollins et al. in 1998, and at the time it was known as the semi-empirical technique, or SET [26]. It was the first explicit continuous-time algorithm used to predict the output response of a Hammerstein process to a step change in the input that was able to fully exploit SDOE. At the time of its introduction, the authors were unaware that the method was an exact solution for a true Hammerstein process. In 2002, the mathematical proof that it was indeed an exact solution was discovered and its name was updated to H-BEST to reflect this. The H-BEST algorithm for a single step input change to the process can be written as

$$y(t) = f(u(t); \beta) \cdot g(t; \tau) \mathcal{S}(t) \quad (1)$$

where β is the vector of coefficients, $\mathcal{S}(t)$ is the unit step function, and the dynamics are described by $g(t; \tau)$, defined as

$$g(t; \tau) = \mathcal{L}^{-1}[G(s) \cdot U(s)] = \mathcal{L}^{-1}\left\{G(s) \cdot \frac{1}{s}\right\} \quad (2)$$

where \mathcal{L}^{-1} is the inverse Laplace transform operator. For a series of step input changes, the

H-BEST solution can be written as

$$y(t) = \begin{cases} f(u(0); \beta) \cdot g(t; \tau); & 0 \leq t < t_1 \\ y(t_1) + [f(u(t_1); \beta)y(0) - y(t_1)] \cdot g(t - t_1; \tau); & t_1 \leq t < t_2 \\ \vdots \\ y(t_{i-1}) + [f(u(t_i); \beta)y(0) - y(t_{i-1})] \cdot g(t - t_i; \tau); & t_i \leq t \end{cases} \quad (3)$$

where the inputs and outputs are in terms of deviation variables. The process of identifying an H-BEST model can be given in four simple steps. These are as follows [14]:

- i. Determine the statistical experimental design to be used.
- ii. Run the experimental design as a series of step tests, allowing steady state to occur after each change while collecting the data dynamically over time.
- iii. Use the steady-state data to determine the ultimate response function, $f(\mathbf{v}(t))$.
- iv. Use the dynamic data to determine the dynamic response function, $g(t; \tau)$ for each output.

The H-best model is identified when the model forms for $f(\mathbf{v}(t))$ and $g(t; \tau)$ are specified and the parameter estimates are determined.

The H-BEST algorithm as described above has been applied to several different processes, including an industrial flow loop in both open- and closed-loop modes [14], a household clothes dryer [16] and a distillation column [18]. It was able to accurately model systems with various types of dynamics in these cases. However, in all the early studies done using the H-BEST modeling method, each of them was restricted to step input changes, which often do not occur in real processes. For processes where the inputs were periodic, the input to the H-BEST algorithm needed to be approximated as piece-wise step changes. If the process variables are sampled frequently enough, then there is no problem with using this type of approximation, and it was done successfully by Rollins et al. [16] in 2003. But, in some cases, it is not possible to sample frequently enough to adequately approximate the periodic input behavior, and will not produce an acceptable model of the process [24, 28].

This changed in 2004 when Zhai et al. presented a form of the H-BEST algorithm that could be used for systems with sinusoidal input sequences [29]. They were able to accurately predict the output of true SISO Hammerstein systems with both first- and second-order dynamics. In 2006, Zhai et al. also demonstrated the ability of this algorithm to accurately predict the output response of a MIMO Hammerstein system with second-order plus lead dynamics [30]. The H-BEST algorithm for a SISO system with first-order dynamics and all

variables initially at steady state is described by Eqs. 4-6 below for the time interval $t_{n-1} < t < t_n$.

$$u(t) = b_n + A_n \sin(\omega_n(t - t_{n-1})) \quad (4)$$

$$f(u(t)) = a_1 u(t) + a_2 u(t)^2, \quad (5)$$

$$y(t) = \left(a_1 b_n + a_2 b_n^2 + \frac{1}{2} a_2 A_n^2 \right) \cdot g_0(t - t_{n-1}; \tau) + (a_1 A_n + 2a_2 b_n A_n) \cdot g_s(t - t_{n-1}; \omega_n, \tau) - \frac{1}{2} a_2 A_n^2 \cdot g_c(t - t_{n-1}; 2\omega_n, \tau) + y(t_{n-1}) \cdot e^{-(t-t_{n-1})/\tau} \quad (6)$$

Where $g_0(t; \tau)$, $g_s(t; \omega, \tau)$ and $g_c(t; \omega, \tau)$ are defined as:

$$g_0(t; \tau) = 1 - e^{-t/\tau} \quad (7)$$

$$g_s(t; \omega, \tau) = \frac{1}{1 + (\omega\tau)^2} \left[\omega\tau \cdot e^{-t/\tau} - \omega\tau \cdot \cos(\omega\tau) + \sin(\omega\tau) \right] \quad (8)$$

$$g_c(t; \omega, \tau) = \frac{1}{1 + (\omega\tau)^2} \left[-e^{-t/\tau} + \omega\tau \cdot \cos(\omega\tau) + \sin(\omega\tau) \right] \quad (9)$$

In this case, the input change $u(t)$ has a sinusoidal element imposed upon a step input change. Other forms of the H-BEST algorithm for the more complicated second-order and second-order plus lead dynamics under sinusoidal input changes, as well as those for sinusoidal input changes with changing phase can be found in [29] and [30].

In addition to the work done to handle sinusoidal inputs, Rollins et al. introduced a method of handling systems that have serially correlated noise on the process measurements [31].

2.2. *W-BEST*

The W-BEST method of model identification was introduced in 2002 [14] and follows the same general procedure as that of H-BEST model identification. The static

nonlinearity is first recovered from steady-state process information, and it is assumed to be of polynomial form [12, 32, 33]. Once the static nonlinearity has been determined, the linear dynamics are determined. The form of the linear dynamic block is restricted to one of the basic types, such as first-order plus dead time (FOPDT) or second-order plus dead time (SOPDT). This is done to simplify the parameter estimation process [14, 32]. The primary difference between the W-BEST algorithm and other Wiener models is that the W-BEST algorithm is a continuous-time model of a process and can be viewed as a “gray-box” model. That is, the linear dynamic part of the system is assumed to be of some known structure, and is determined by observation of the process response to input changes. Most other Wiener models are discrete-time. The only notable exception is the Wiener model developed by Huang et al. [32], which is similar in nature to the W-BEST model but is unable to address interactions between inputs in a multiple-input system.

For a system with dead time θ and a series of step input changes u_0, u_1, \dots, u_i occurring at times $0, t_1, \dots, t_i$, respectively, the W-BEST algorithm can be described as follows [14]:

$$y(t) = f(v(t)) \quad (10)$$

$$\begin{aligned} 0 < t \leq \theta & \quad \hat{v}(t) = v(0) \\ \theta < t \leq t_1 + \theta & \quad \hat{v}(t) = v(0) + [u_0 - v(0)]g(t - \theta; \tau) \\ t_1 + \theta < t \leq t_2 + \theta & \quad \hat{v}(t) = v(t_0 + \theta) + [u_1 - v(t_0 + \theta)]g(t - (t_1 + \theta); \tau) \\ \vdots & \\ t_i + \theta < t & \quad \hat{v}(t) = v(t_{i-1} + \theta) + [u_i - v(t_{i-1})]g(t - (t_i + \theta); \tau) \end{aligned} \quad (11)$$

where the linear dynamics are described by $g(t-t_i; t)$, $v(0)$ is the initial condition for $v(t)$, and τ is the parameter vector for the dynamic system. As in the case of the H-BEST algorithm, all variables are initially at steady state and the algorithm is given for deviation variables.

This algorithm was successfully used to describe the behavior of a SISO CSTR which had second-order-plus-dead-time-plus-lead (SOPDPL) dynamics, and it proved to be better than the H-BEST algorithm for this case because of the nature of the process [14]. It was later applied to another CSTR system with seven (7) inputs and five (5) outputs by Bhandari and Rollins in 2003 [19] and was able to accurately model that system.

A restriction of the W-BEST algorithm as presented above was its inability to directly model processes with periodic input changes. Zhai et al. (2006) presented an algorithm that addresses this weakness and provides an exact solution for the Wiener system with sinusoidal input changes [37]. If the sinusoidal input change described by Eq. 4 above is introduced into the Wiener system with first-order dynamics, then the W-BEST algorithm for the interval $t_{n-1} < t < t_n$ becomes:

$$v(t) = b_n \cdot g_0(t - t_{n-1}; \tau) + A_n \cdot g_s(t - t_n; \omega_n, \tau) + v(t_{n-1}) \cdot e^{-(t-t_{n-1})/\tau} \quad (12)$$

where $g_0(t; t)$ and $g_s(t; \omega, t)$ are defined as they were in the case of the H-BEST algorithm. Other forms of the W-BEST algorithm for systems with more complex dynamics have also been presented [29, 30]. The proposed algorithms were also used to model a simulated CSTR process similar to the one used by Bhandari and Rollins (2003) [19]. In this case, sinusoidal input changes were imposed upon the step input changes and the process response was predicted and compared to the simulated process response, with good results [30]. The results were compared with those given by the piecewise step change approximation [16] and quantitatively compared using two criteria: the sum of squared prediction error (SSPE) and average relative error (ARE). For all outputs, the W-BEST algorithm with the modifications for sinusoidal input changes performed better than that of the piecewise step input change approximation [24].

Another important aspect of the work done by Zhai et al. (2006) was the recognition that any input signal that is noisy can be decomposed into a sum of sinusoidal components, and written as

$$X(t) = \sum_{j=1}^k (A_j \cos(\omega_j t) + B_j \sin(\omega_j t)), \quad (13)$$

$$0 < \omega_1 < \dots < \omega_k < \pi$$

where the A_j 's and B_j 's are uncorrelated random variables with $E[A_j]=0$, and $Var(A_j)=Var(B_j)=\sigma^2, j=1, \dots, k$ [37]. They point out that an infinite number of sinusoidal terms should be used in the above equation; however, this may be reduced to a finite number to approximate a stationary time series as long as it includes all of the major frequencies and amplitudes [34]. By using this approximation, they were able to simulate input signals that look like noisy signals in real processes. Hajjair and Eloutassi described how to extract these sinusoidal components from a noisy signal [35]. We will also use this approximation later when we are discussing a distillation column with noisy inputs.

3. Other Block-Oriented Models

While the Hammerstein and Wiener models are probably the most common block-oriented models in the literature, there are other types as well. The Uryson model consists of several Hammerstein models in parallel, driven by a common input and having the outputs summed [15, 38]. There are also “sandwich” block-oriented models, consisting of varying combinations of linear dynamic and static nonlinear blocks. These types of models can be used where a process response follows even more complex behavior and cannot be adequately described by a Hammerstein or Wiener model.

The LNL sandwich model consists of a linear dynamic block followed by a nonlinear static block followed by another linear dynamic block, and is shown in Fig. 2 below.

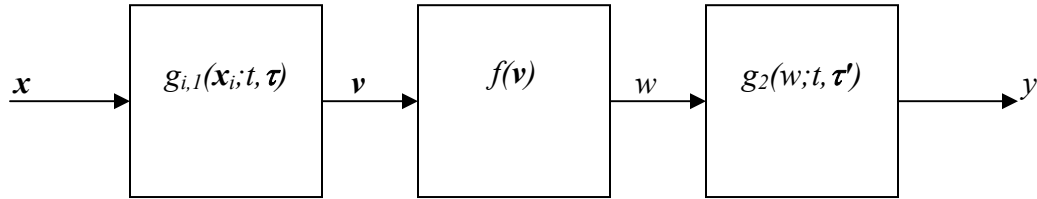


Figure 2: A block diagram of the LNL sandwich block-oriented model structure. The input vector \mathbf{x} passes through the linear dynamic block $g_{i,1}$ to give the vector \mathbf{v} , which then passes through the nonlinear static map to give w , and finally through the linear dynamic block g_2 to give the output variable y .

Chapter 4 will discuss in more detail the LNL sandwich block-oriented model, and it will be used to identify the process response of a simulated CSTR process with complex input behavior. It will also be used for developing a feedforward controller to be used to maintain control of the reactor temperature of the simulated CSTR process.

4. Statistical Design of Experiments

Although many different approaches have been proposed for addressing both Hammerstein and Wiener systems, the H-BEST and W-BEST BOM methods first exploited the use of statistical design of experiments (SDOE). The ability to use SDOE ensures that a pure cause-and-effect relationship between inputs and outputs can be obtained [23]. Most methods for identifying Hammerstein and Wiener systems make use of a pseudo-random sequence (PRS), in which a series of deterministic or random input changes occurs at fixed or randomly determined times [36]. If these changes are deterministic, then only a specified number of levels over the input space are used. For the special case of only the minimum and maximum input levels being used in the input sequence, the design is called a pseudo-random binary sequence (PRBS).

Rollins and Bhandari (2004) [21] and Bhandari and Rollins (2003) [19] have demonstrated that for a simulated process, using SDOE in the model building process gives substantially more information than a PRS design requiring the same amount of experimental test time in the identification process. To demonstrate quantitatively that SDOE is a more efficient method of obtaining significant information, Rollins et al. (2006) [23] introduced an efficiency term to compare the D-optimum criterion (see [37]) for each experimental design type, as applied to Hammerstein processes. In this way, they were able to objectively evaluate competing designs and determine which is more effective. A similar study was done by Hardjasamudra et al. (2006) for Wiener systems [22]. In both of these cases, the authors found that the dynamic parameters could be sufficiently estimated by using a PRS design, but these designs did not allow for the ultimate response behavior to be accurately predicted. Because of this, for BOM development, SDOE appears to be the better choice.

However, in many real processes, making any changes to the inputs for the purpose of developing a reliable process model can cause problems with normal operations. It is desirable to be able to easily identify the process model without causing significant upsets to the everyday operations of the process. Ideally, historical data from the plant database could be used to develop these models. There are many advantages to using this historical data: the data is readily available and generally abundant, it is collected frequently, it covers the “typical” operating space of the process, and does not require specific perturbations to be introduced, which may cause process upsets. The work done by Rollins et al. [31] which introduced a method of dealing with serially correlated noise has been extended by Rollins et al. [39] to modeling glucose response in Type 2 diabetic patients with highly correlated inputs. Chapter 5 of this dissertation will extend this work further and apply it to modeling

the process output response on a real distillation column with highly correlated inputs, and show that an accurate process model can be found using the W-BEST modeling methodology under these conditions. In addition, it will be implemented into a feedforward controller to maintain control of the process output (top tray temperature) on the distillation column.

5. References

- [1] Clarke, D.W., C. Mohtadi and P.S. Tuffs, "Generalized Predictive Control- Part 1: The Basic Algorithm," *Automatica*, Vol. 23, pp. 137-148, 1987.
- [2] Muske, K.R. and J.B. Rawlins, "Model Predictive Control with Linear Models," *AIChE Journal*, Vol. 39, pp. 262-287, 1993.
- [3] te Braake, H.A.B., E.J.L. van Can, J.M.A. Scherpen and H.B. Verbruggen, "Control of Nonlinear Chemical Processes Using Neural Models and Feedback Linearization," *Computers and Chemical Engineering*, Vol. 22, pp. 1113-1127, 1998.
- [4] Wright, G.T. and T.F. Edgar, "Nonlinear Model Predictive Control of a Fixed-Bed Water-Gas Shift Reactor: An Experimental Study," *Computers and Chemical Engineering*, Vol 18, pp. 83-102, 1994.
- [5] Bodizs, A., F. Szeifert and T. Chovan, "Convolution Model Based Predictive Controller for a Nonlinear Process," *Industrial and Engineering Chemistry Research*, Vol. 38, pp. 154-161, 1999.
- [6] Noriega, J.R. and H. Wang, "A Direct Adaptive Neural-Network Control for Unknown Nonlinear Systems and Its Application," *IEEE Transactions on Neural Networks*, Vol. 1, pp. 4-27, 1998.
- [7] Alexandridis, A. and H. Sarimveis, "Nonlinear Adaptive Model Predictive Control Based on Self-Correcting Neural Network Models," *AIChE Journal*, Vol. 51. No. 9, September 2005.
- [8] Fischer, M., O. Nelles and R. Isermann, "Adaptive Predictive Control of a Heat Exchanger Based on a Fuzzy Model," *Control Engineering Practice*, Vol. 6, pp. 259-269, 1998.
- [9] Di Palma, F., L. Magni, "A Multi-Model Structure for Model Predictive Control," *Annual Reviews in Control*, Vol. 28, pp. 47-52, 2004.

- [10] Gao, J, R. Patwardhan, K. Akamatsu, Y. Hashimoto, G. Emoto, S.L. Shah, B. Huang, "Performance Evaluation of Two Industrial MPC Controllers," *Control Engineering Practice*, Vol. 11, pp.1371-1387, 2003.
- [11] Havlena, V. and J. Findejs, "Application of Model Predictive Control to Advanced Combustion Control," *Control Engineering Practice*, Vol. 13, pp. 671-680, 2005.
- [12] Al-Duwaish H. and Naeem, Wasif , "Nonlinear Model Predictive Control of Hammerstein and Wiener Models Using Genetic Algorithms," *Proceedings of the 2001 IEEE International Conference on Control Applications*, September 5-7, 2001, Mexico City, Mexico
- [13] Gao, F., F. Wang and M. Li, "Predictive Control for Processes with Input Dynamic Nonlinearity," *Chemical Engineering Science*, Vol. 55, pp. 4045-4052, 2000.
- [14] Loveland, S.D., *Advances in Nonlinear Process Modeling Using Block-oriented Exact Solution Techniques*, M.S. Thesis, Iowa State University, Ames, Iowa 2002.
- [15] Pearson, R.K. and B.A. Ogunnaike, "Nonlinear Process Identification," *Nonlinear Process Control*, Prentice-Hall PTR, Upper Saddle River, NJ, pp. 11-110, 1997.
- [16] Rollins, D.K., N. Bhandari, A.M. Bassily, G.M. Colver and S. Chin, "A Continuous-Time Nonlinear Dynamic Predictive Modeling Method for Hammerstein Processes," *Industrial and Engineering Chemistry Research*, Vol. 42, No. 4, pp. 861-872, 2003.
- [17] Greblicki, W., "Continuous-Time Hammerstein System Identification," *IEEE Transactions on Automatic Control*, Vol. 45, No. 6, pp. 1232-1236, 2000.
- [18] Bhandari, N. and D.K. Rollins, "Continuous-Time Hammerstein Nonlinear Modeling Applied to Distillation," *AIChE Journal*, Vol. 50, No. 2, pp. 530-533, 2004.
- [19] Bhandari, N. and D.K. Rollins, "A Continuous-Time MIMO Wiener Modeling Method," *Industrial and Engineering Chemistry Research*, Vol. 42, No. 22, pp. 5583-5595, 2003.
- [20] Chin, S., N. Bhandari and D.K. Rollins, "An Unrestricted Algorithm for Accurate Prediction of MIMO Wiener Processes," *Industrial and Engineering Chemistry Research*, Vol. 43, pp. 7065-7074, 2004.
- [21] Rollins, D.K. and N. Bhandari, "Constrained MIMO dynamic Discrete-Time Modeling Exploiting Optimal Experimental Design," *Journal of Process Control*, Vol. 14, No. 6, pp. 671-683, 2004.

- [22] Hardjasamudra, A., D.K. Rollins, N. Bhandari and S. Chin, "Optimal Experimental Design for Wiener Systems," accepted by *Chemical Engineering Communications*, April, 2006.
- [23] Rollins, D.K., L. Pacheco and N. Bhandari, "A Quantitative Measure to Evaluate Competing Designs for Non-linear Dynamic Process Identification," *The Canadian Journal of Chemical Engineering*, Vol. 84, No. 4, 2006
- [24] Zhai, D., *Continuous-Time Block-Oriented Nonlinear Modeling with Complex Input Noise Structure*, Ph.D. Dissertation, Iowa State University, Ames, Iowa, 2005.
- [25] Narendra, K.S. and P.G. Gallman, "An Iterative Method for the Identification of Nonlinear Systems Using a Hammerstein Model," *IEEE Transactions on Automatic Control*, Vol. 6 (AC-11), pp. 546-550, 1966.
- [26] Rollins, D.K., J.M. Liang and P. Smith, "Accurate Simplistic Predictive Modeling of Non-linear Dynamic Processes," *ISA Transactions*, Vol. 36, pp. 293-303, 1998.
- [27] Rietz, C.A., *The Application of a Semi-Empirical Modeling Technique to Real Processes*, M.S. Thesis, Iowa State University, Ames, Iowa 1998.
- [28] Seborg, D.E., T.F. Edgar and D.A. Mellichamp, *Process Dynamics and Control*, 2nd edition, John Wiley and Sons, 2003.
- [29] Zhai, D., D.K. Rollins and N. Bhandari, "Compact Block-Oriented Continuous-Time Dynamic Modeling for Nonlinear Systems Under Sinusoidal Input Sequences," *Proceedings of the IASTED Intelligent Systems and Control Conference*, Honolulu, Hawaii, pp. 295-300, 2004.
- [30] Zhai, D., D.K. Rollins, N. Bhandari and H. Wu, "Continuous-Time Hammerstein and Wiener Modeling Under Second-Order Static Nonlinearity for Periodic Process Signals," *Computers and Chemical Engineering*, Vol. 31, pp.1-12, 2006.
- [31] Rollins, D.K., N. Bhandari, S. Chin, T. Junge and K. Roosa, "Optimal Deterministic Transfer Function Modeling in the Presence of Serially Correlated Noise," *Chemical Engineering Research and Design*, Vol. 84(A1), pp. 9-21, 2006.
- [32] Huang, H.P., M.W. Lee and Y.T. Tang, "Identification of Wiener Model Using Relay Feedback Test," *Journal of Chemical Engineering of Japan*, Vol. 31, No. 4, pp. 604-612, 1998.

- [33] Balestrino, A. and A. Caiti, "Approximation of Hammerstein/Wiener Dynamic Models," *Proceedings of the IEEE-INNS-ENNS International Joint Conference on Neural Networks*, Vol. 6, Como, Italy, pp. 70-74, 2000.
- [34] Brockwell, P.J. and R.A. Davis, *Introduction to Time Series and Forecasting*, New York: Springer, 2002.
- [35] Hajjair, A., and O. Eloutassi, "Extracting Sine Waves from Noisy Measurements and Estimating Their Parameters," *Proceeding of the IASTED Conference on Decision and Control*, pp. 341-345, 1999.
- [36] Brosilow, C. and B. Joseph, *Techniques of Model-Based Control*, Prentice Hall PTR, Upper Saddle River, NJ, pp. 387-394.
- [37] Bates, D.M. and D.G. Watts, *Nonlinear Regression Analysis and Its Applications*, John Wiley & Sons, Inc., New York, NY, pp. 121-133, 1988.
- [38] Billings, S.A., "Identification of Nonlinear Systems – A Survey," *IEE Proceedings*, Vol. 127 pt.D, No. 6, pp. 272-285, 1980.
- [39] Rollins, D.K., J. Kleinedler, A. Strohbehn, L. Boland, M. Murphy, D. Andre, D. Wolf and W.E. Franke, "Modeling Glucose Noninvasively Using Wiener Simulation Modeling for Type 2 Diabetic Patients Under Free-living Conditions," submitted to *IEEE Transactions on Biomedical Engineering*, in review.

CHAPTER 3. PRELIMINARY INVESTIGATIONS

1. Motivation for Research

The process of model identification for model-based control algorithms takes on many different forms, depending upon the type of model to be used. In this research, the focus will be on block-oriented models, which combine linear dynamic (L) and nonlinear static (N) blocks to approximate nonlinear process response behavior. Most of the methods for identifying block-oriented models make use of a pseudo-random sequence (PRS). The PRS consists of a series of deterministic or random input changes occurring at fixed or randomly determined times [1]. Studies have been done by Rollins et al. [2] and Hardjasaundra et al. [3] that showed that while dynamic parameters can be sufficiently estimated by using a PRS design, the ultimate response behavior of a process is not accurately predicted using the PRS design. This contributes to process-model mismatch that will negatively affect performance of a model-based controller.

In a real process, the inputs are usually not stepwise deterministic. They often have periodic and stochastic behavior. This has been noted and some work has been done to properly identify models for systems that have periodic inputs [4, 5] or serially correlated inputs [6, 7]. However, the general equations for model-based control do not explicitly account for these types of inputs. In addition, the inputs to a process typically have a dynamic response to controller set point changes and not an instantaneous, constant-level response. Dynamic interactions between the input variables exist in many processes, and these are also not explicitly accounted for. Instead, any dynamic or interactive behavior of the inputs contributes to mismatch of the overall process model.

To illustrate the effect of input dynamics, consider a simple two-input, one-output Hammerstein process. We could express this in block diagram form as in Fig. 1.

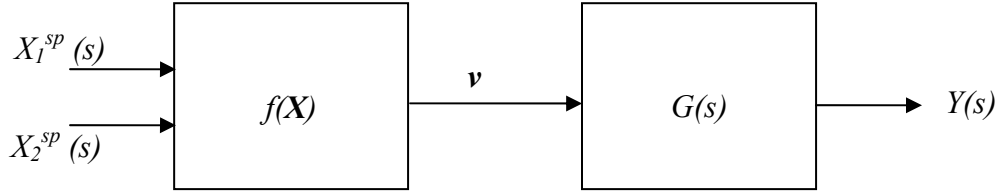


Figure 1: The block diagram for a simple two-input, one-output Hammerstein process. The inputs are represented by X_1^{sp} and X_2^{sp} , \mathbf{v} is the intermediate vector representing the static map of \mathbf{X} and Y is the output.

In this example, the set points are given by X_1^{sp} and X_2^{sp} . If there are input dynamics, then the block diagram would need to be modified, as in Fig. 2. This accounts for both input dynamics and the process dynamics. Essentially this is what is known as a sandwich block-oriented model (BOM), in which linear dynamic blocks and static nonlinearities can be assembled in any of a number of arrangements [8]. The process represented by Fig. 2 is considered an LNL sandwich process, in which the input goes through a linear dynamic block, then a nonlinear static block and finally another linear dynamic block. If the input dynamics can be separated from the process dynamics in the modeling of the process that is done for the control system, the overall control and stability of the process could be better maintained.

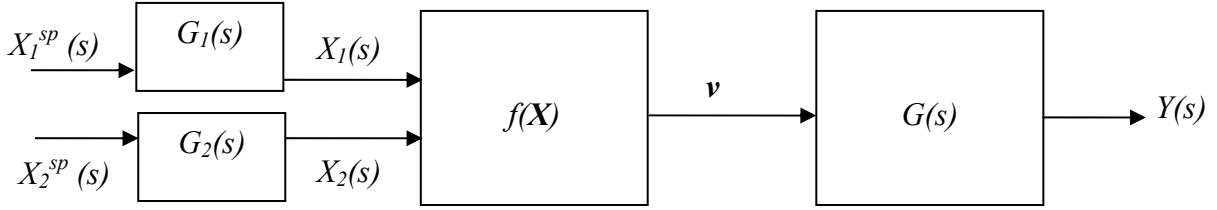


Figure 2: The block diagram for a two-input, one-output LNL sandwich process that has input dynamic behavior. The input set points have been modified to show the dynamic response of the inputs to the set point changes.

2. Scope of Research

As discussed previously, the inputs to a process are often nonstationary. If we consider this variability to be significant, we can break the input signal up into three specific parts: dynamic, periodic and stochastic contributions to noise. Mathematically, the variability can be represented by Eq. 1 below. It can also be described in block-diagram form, with the input $x_i(t)$ entering into a Hammerstein system in Fig. 3.

$$x_i(t) = w_i(t) + \varepsilon_i(t) + \xi_i(t) \quad (1)$$

where $x_i(t)$ represents the input, $w_i(t)$ represents the dynamic contribution, $\varepsilon_i(t)$ represents the stochastic contribution and $\xi_i(t)$ represents the periodic contribution to the process variability.

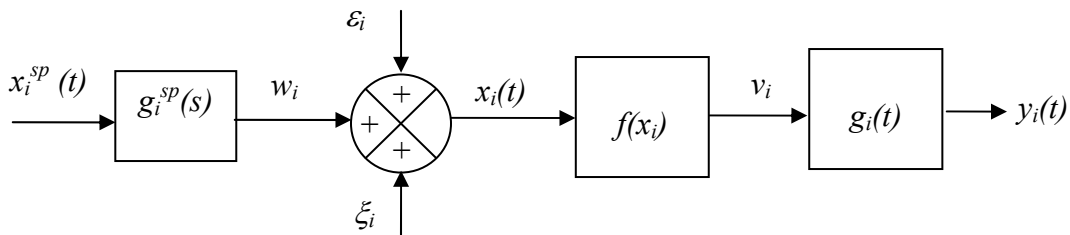


Figure 3: A block diagram representing an LNL sandwich system with input process variability consisting of three parts: dynamic, stochastic and periodic.

All three contributions to the input process variability are often due to real process variability. However, the research presented in this dissertation will focus on one of the two deterministic components, the dynamic component. The goal is to model these contributions and implement them into a model-based control scheme. Zhai [5] has proposed methods for handling the stochastic component.

The examples to be investigated include a simulated true LNL sandwich process, a simulated continuous-stirred tank reactor (CSTR) process and a real distillation process. The true LNL sandwich process will be used to illustrate the importance of understanding the input dynamics and the effects of interactive inputs. Using the simulated CSTR process, an LNL block-oriented model will be developed and implemented into a feedforward/feedback control algorithm. This will be compared to the performance of a traditional feedback controller, and is shown in Chapter 4. For the pilot-scale distillation column we will identify a Wiener block-oriented model in both open- and closed-loop modes using data typical of what could be found in a plant historical database, and implement this model into a feedforward/feedback control scheme to show the response of the process output. Comparisons will be made between this and a traditional feedback control system. This is given in Chapter 5.

3. Preliminary Work

3.1. Example 1: Simulated NL Process

To demonstrate that the dynamics of the process inputs can have a significant effect on the process response, let us consider a simple two-input, single-output NL (Hammerstein) process. This process is defined by Eqs. 2 and 3 and is illustrated by the block diagram shown in Fig. 1 above.

$$v(t) = f(\mathbf{u}(t)) \quad (2)$$

$$= a_0 + a_1 x_1 + a_2 x_1^2 + a_3 x_1 x_2 + a_4 x_2 + a_5 x_2^2$$

$$v(t) = \begin{cases} 0; & t < \tau_w \\ \tau \frac{dw(t)}{dt} + w(t); & t \geq \theta_w \end{cases} \quad (3)$$

In this case, all initial conditions and derivatives are equal to zero, $a_0 = 2.0$, $a_1 = 0.5$, $a_2 = 0.75$, $a_3 = 1.0$, $a_4 = 2.5$, $a_5 = -0.5$, $\tau_w = 5.0$ and $\theta_w = 2.0$. An arbitrary set of input set point changes were made to the process using a random number generator with a uniform distribution. This input sequence is shown in Fig. 4. If these set point changes are the true input changes to the process, then the output response to the changes is given in Fig. 5.

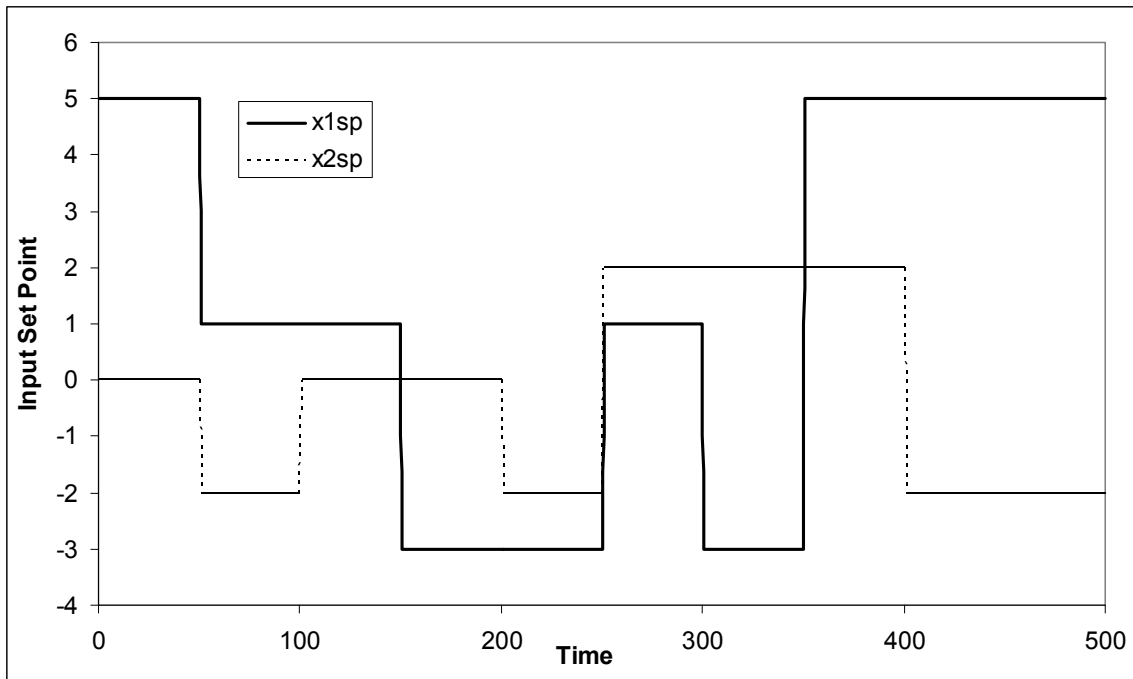


Figure 4: The set point changes made to the inputs x_1 and x_2 used in the simulated NL process described by Eqs. 2 and 3.

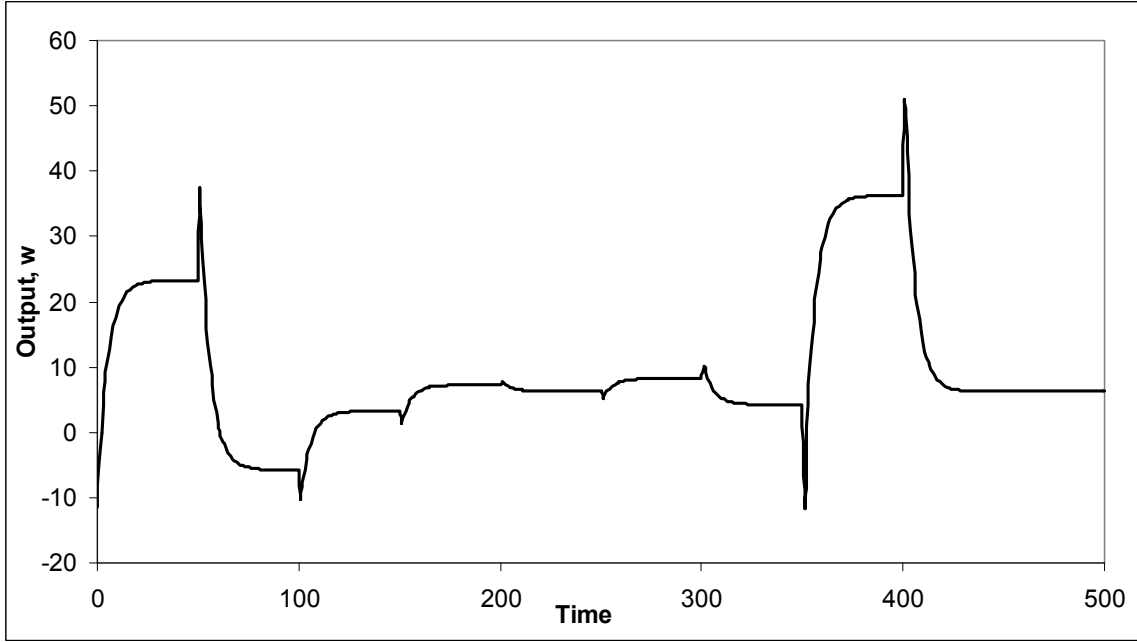


Figure 5: The simulated NL process output response to the input changes that are shown in Figure 4.

3.2. Example 2: Simulated LNL Process

In many cases, however, there is dynamic behavior in the measured input to a process as compared to the changes in the input set points that occur. The process is then an LNL process, depicted in Fig. 2 above. Suppose that each of the two inputs in our NL process exhibit simple second-order overdamped dynamic behavior, as represented in Eqs. 4 and 5 below:

$$G_1(s) = \frac{x_1}{x_1^{sp}} = \frac{1}{(\tau_1 s + 1)(\tau_2 s + 1)} \quad (4)$$

$$G_2(s) = \frac{x_2}{x_2^{sp}} = \frac{1}{(\tau_3 s + 1)(\tau_4 s + 1)} \quad (5)$$

where x_i and x_i^{sp} represent the i^{th} input and i^{th} input set point values, respectively. In the example given, $\tau_1 = 1.0$, $\tau_2 = 2.5$, $\tau_3 = 4.0$ and $\tau_4 = 7.5$.

Graphically, the dynamic change in the inputs is shown in Fig. 6. We can see that the input to the process is now much different than what was given by the set point changes alone. Because of this, the output response of the process is also significantly different, and is shown in Fig. 7.

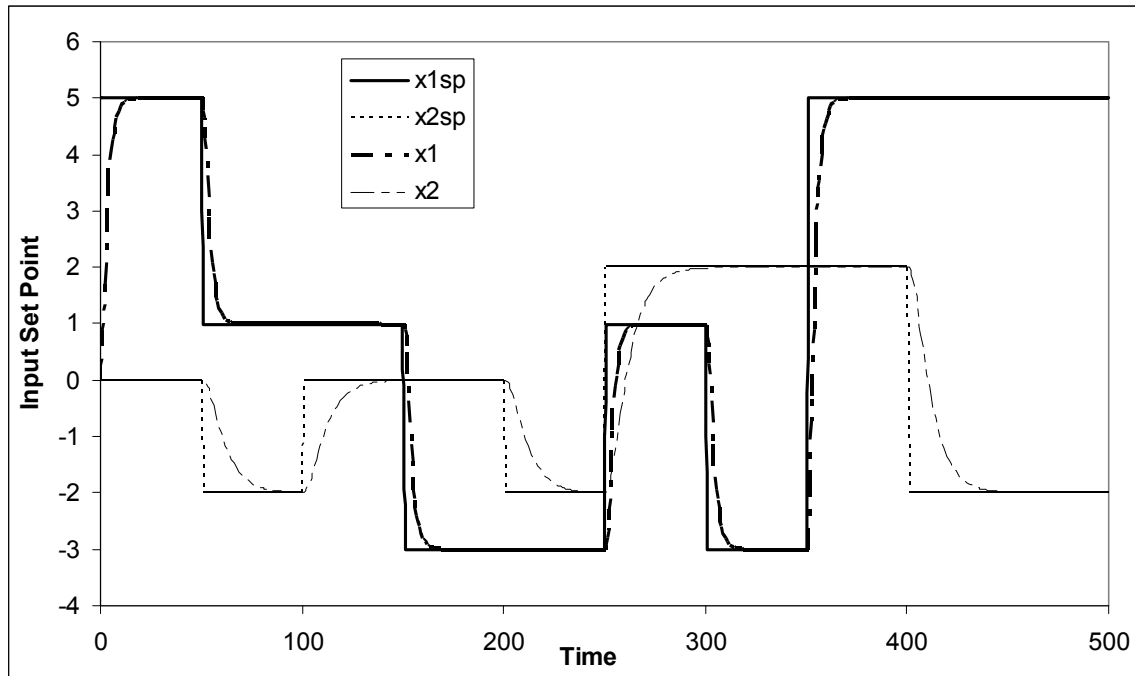


Figure 6: The inputs x_1 and x_2 are shown along with their set point changes. Each of the inputs has a second-order overdamped dynamic response to the change in set point.

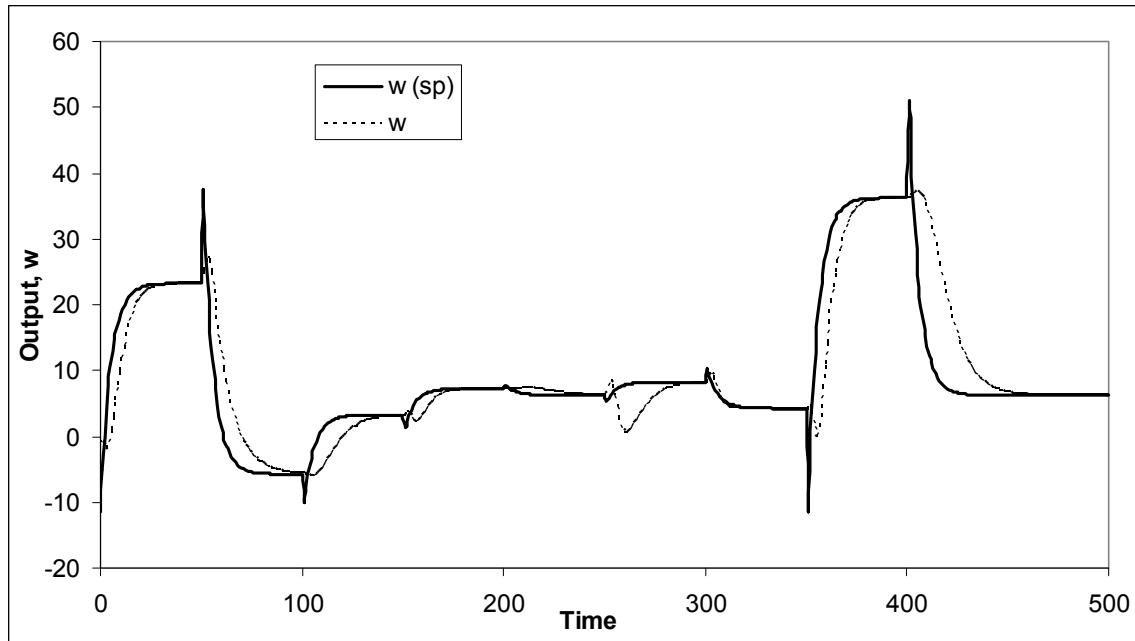


Figure 7: The simulated process output response, w , shown for both the pure set point changes (the NL process) and for inputs that have a dynamic response to the set point changes (the LNL process).

3.3. Example 3: Interactive Effects of Inputs

In addition to the dynamic behavior of inputs that can exist, there can also be interactive effects of the inputs on the process. The steady-state interactions are addressed in BOM by the nonlinear static block, which can be any nonlinear function. In the simulated LNL process that we have been discussing, this can be easily seen by holding one of the inputs constant while changing the other one. That is, if we use the same input sequence for x_1 that we have already introduced in Fig. 4 but keeping x_2 constant, we can see the process response to the changes in x_1 . The ultimate response of the process to these changes is shown in Fig.8. Note that since the lines are not parallel, there is an interaction between the two inputs. The same is true if we hold x_1 constant while changing x_2 .

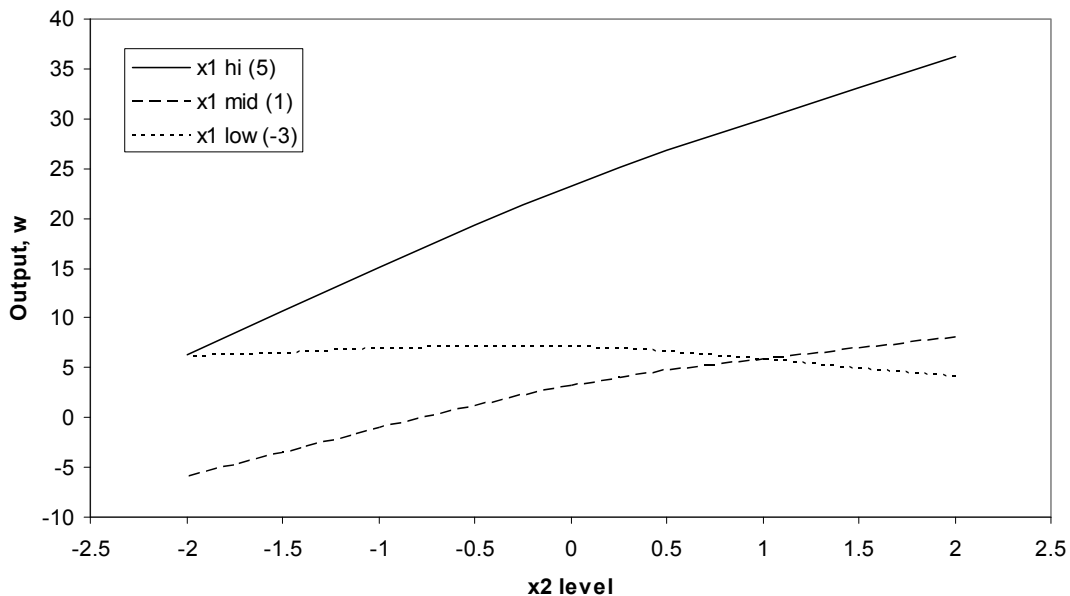


Figure 8: The ultimate response of the output, w , given by the simulated LNL process to changes in the two inputs, x_1 and x_2 . The intersection of the lines demonstrates an interaction between the two inputs.

This interaction also has an effect on the dynamics of the process. We can see in Fig. 9 that the dynamics vary depending on whether x_1 , x_2 or both are changing.

Again, by understanding the dynamics of the interactions between the two inputs and modeling these explicitly using an LNL BOM, we should be able to maintain better control of the process than if we use a Hammerstein or Wiener model within a model predictive control scheme.

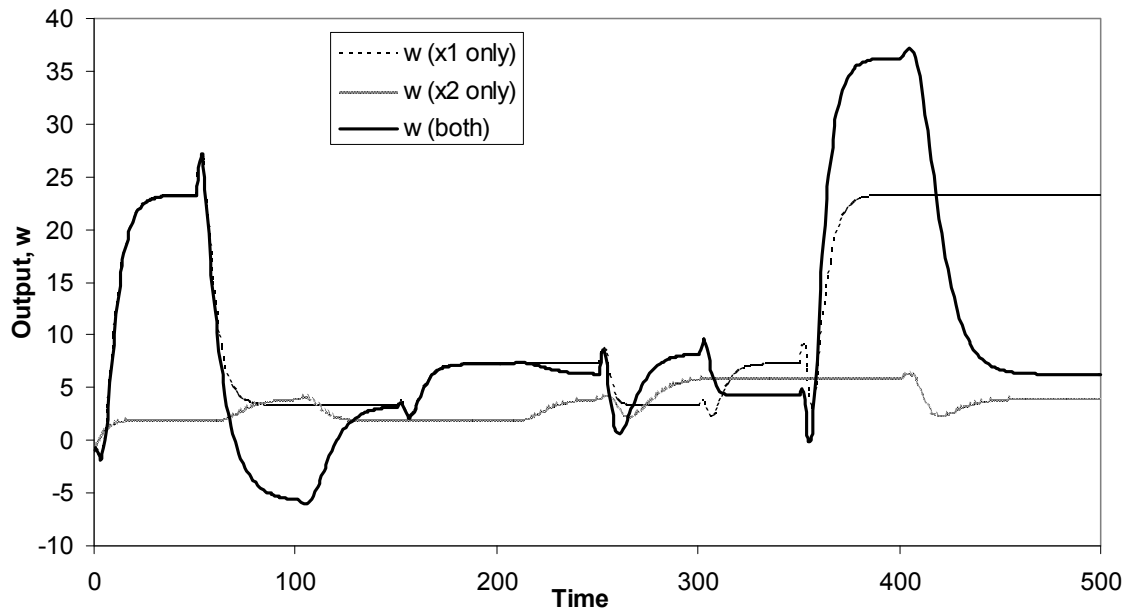


Figure 9: The simulated LNL process output response to input changes in x_1 only, x_2 only, and both x_1 and x_2 . This shows the interactive effect that changing both input variables has on the output, w .

3.4. Example 4: A Pilot-Scale Distillation Process

Tests were conducted on a pilot-scale distillation column to demonstrate the dynamic behavior of the inputs on a real process. The column is used to separate a mixture of methanol and water, and is shown schematically in Fig. 10. The column consisted of 12 sieve trays and had an inside diameter of 6 inches.

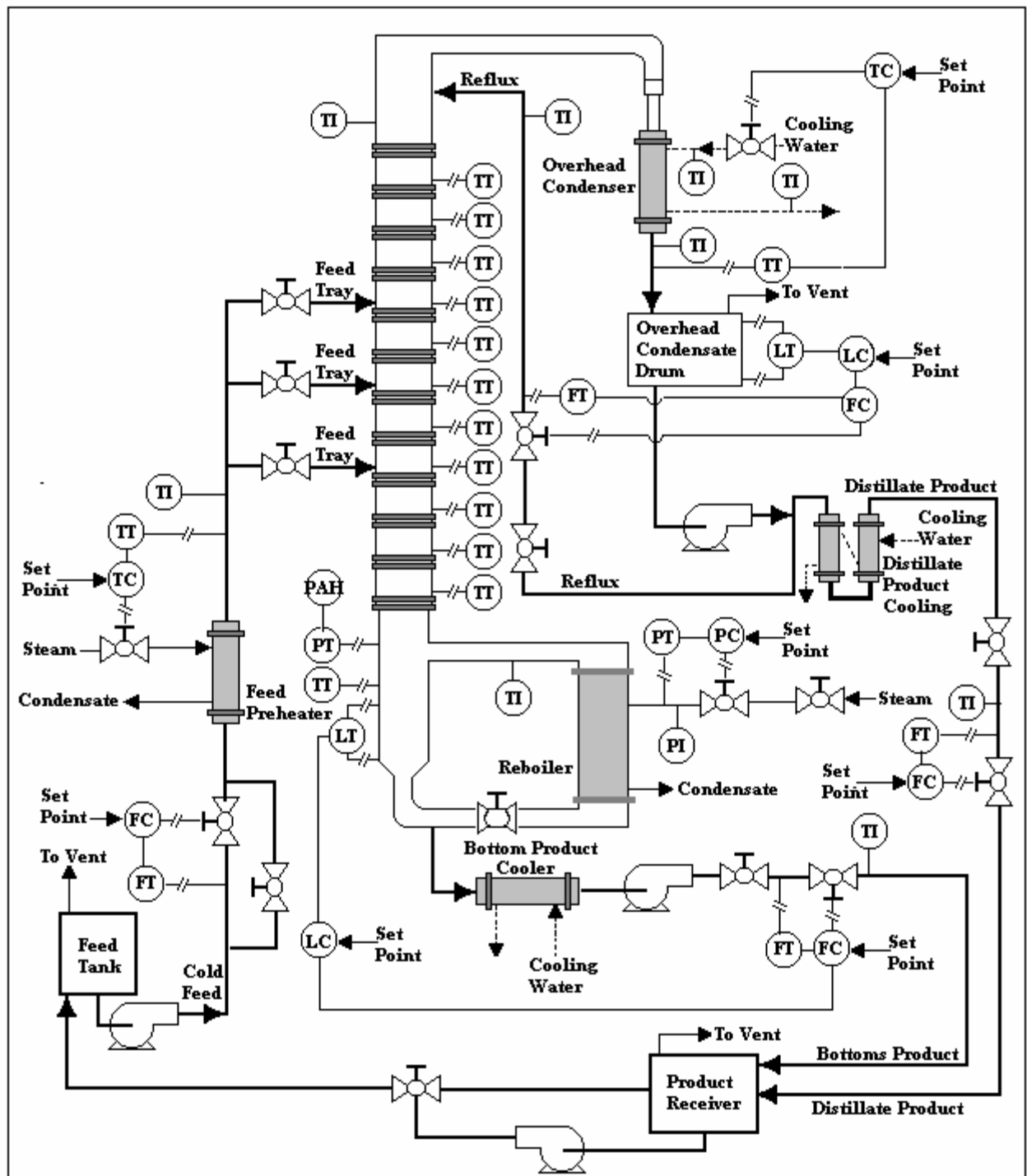


Figure 10: The distillation column used for the experimental tests. The column separated methanol and water and was operated by a DeltaV distributed control system [9].

The input variables to the process include the feed flow rate, feed temperature, reboiler steam pressure, reboiler level and reflux flow rate. Other inputs that were considered were the distillate flow rate, bottoms flow rate and overhead temperature; however, these were not included in the experimental design. The distillate flow and overhead temperature were held constant, and the bottoms flow rate was cascaded with the reboiler level in order to maintain proper control of the column. In addition, although there are three possible feed trays, for these experiments the feed was only introduced on tray 6 in the middle of the column. The output variable examined was the top tray (Tray 12) temperature, from which a composition could be inferred.

A statistical experimental design was determined and carried out on the distillation column. The design was a Box-Behnken design [10] with four factors and three center points, resulting in a total of 27 runs. The four inputs that were manipulated were the feed flow rate, the feed temperature, the reboiler level and the reboiler steam pressure. It is important to note that we also consider reflux flow rate to be an input to the process. It was not specifically manipulated for the experiments because doing so may have caused instability in the operation of the column. Instead, the reflux flow rate is cascaded to an overhead condensate accumulator level controller. In the modeling of the distillation column that will be performed, we will consider this flow as an input, but it could not be included as part of the design due to safety and operational reasons.

The experimental design is shown in Fig. 11. Note that Fig.11 shows the set point changes for each of the inputs. The measured value of each of the inputs that was varied in the experiment showed significant dynamic behavior.

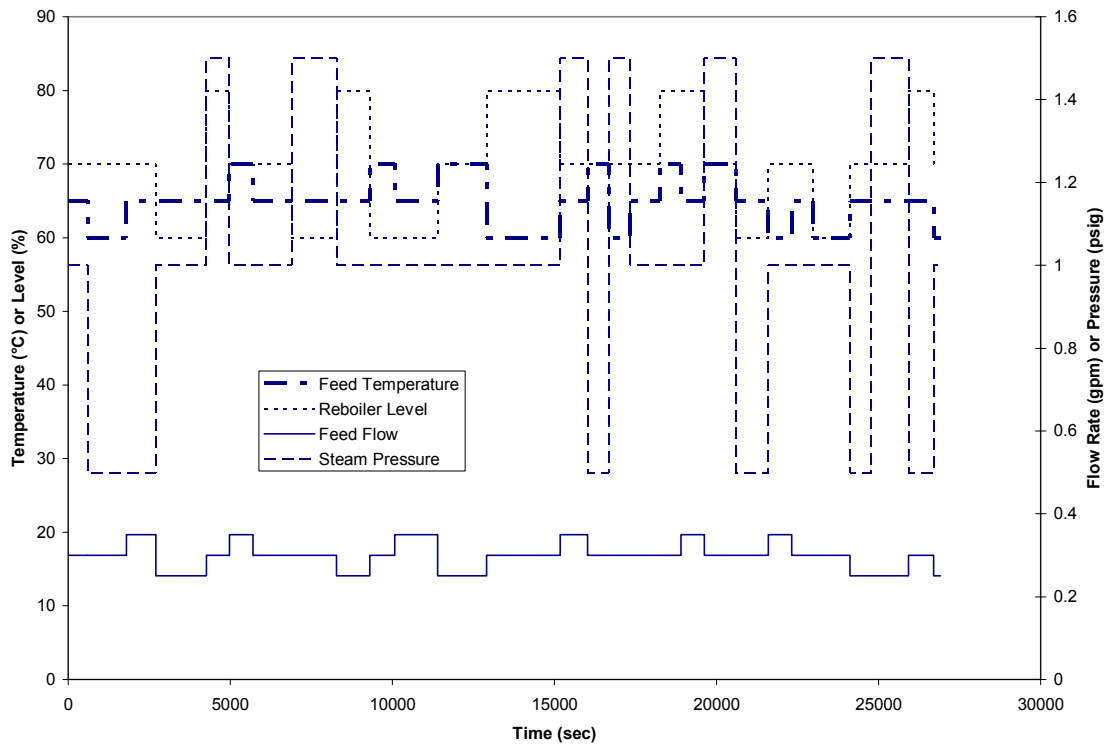


Figure 11: The set point changes used for the experimental design of the distillation column. The design used was a Box-Behnken design with 27 points.

The measured responses of the inputs to their set point changes can be seen in Figures 12 through 15, and the dynamic behavior of these inputs is clearly visible in these plots.

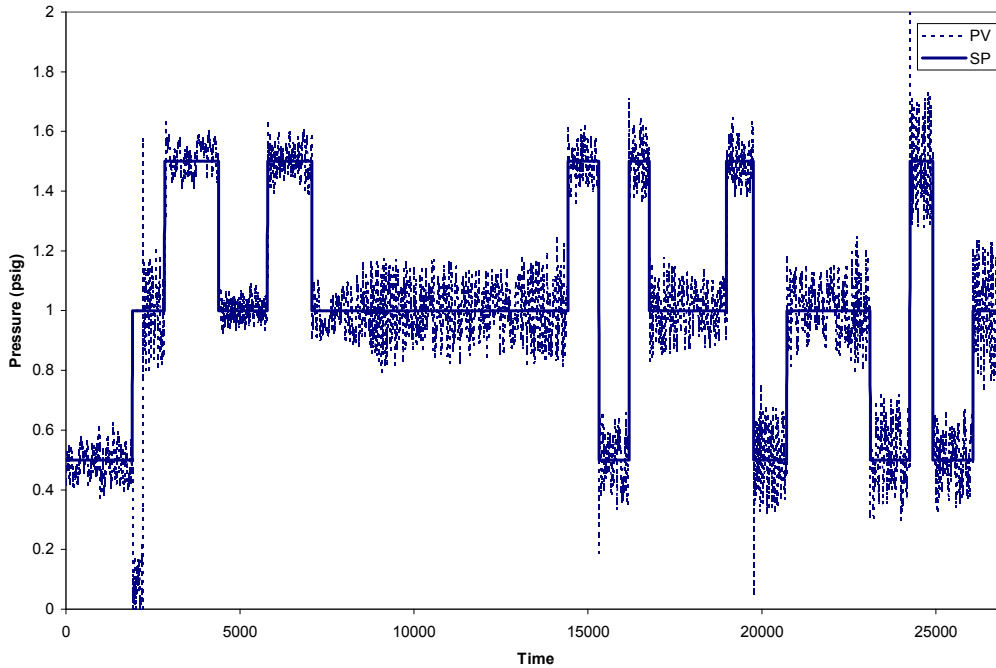


Figure 12: Reboiler steam pressure response to the set point changes made during the experiments that were conducted on the distillation column. SP represents the change in set point and PV represents the measured process value of the reboiler steam pressure.

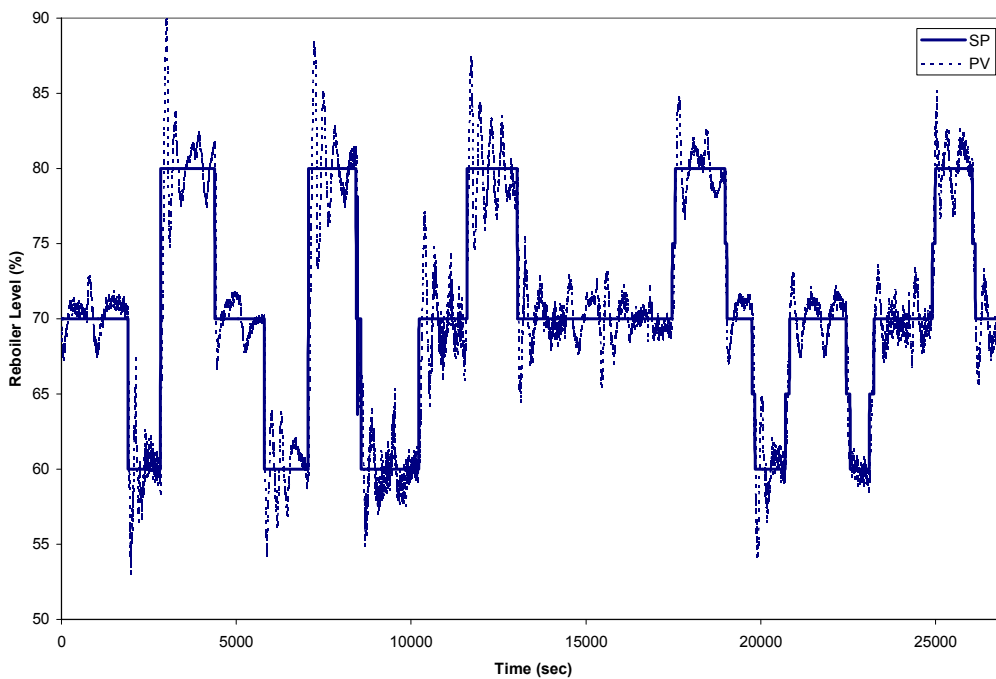


Figure 13: Reboiler level response to the set point changes made during the experiments that were conducted on the distillation column. SP represents the change in set point and PV represents the measured process value of the reboiler level.

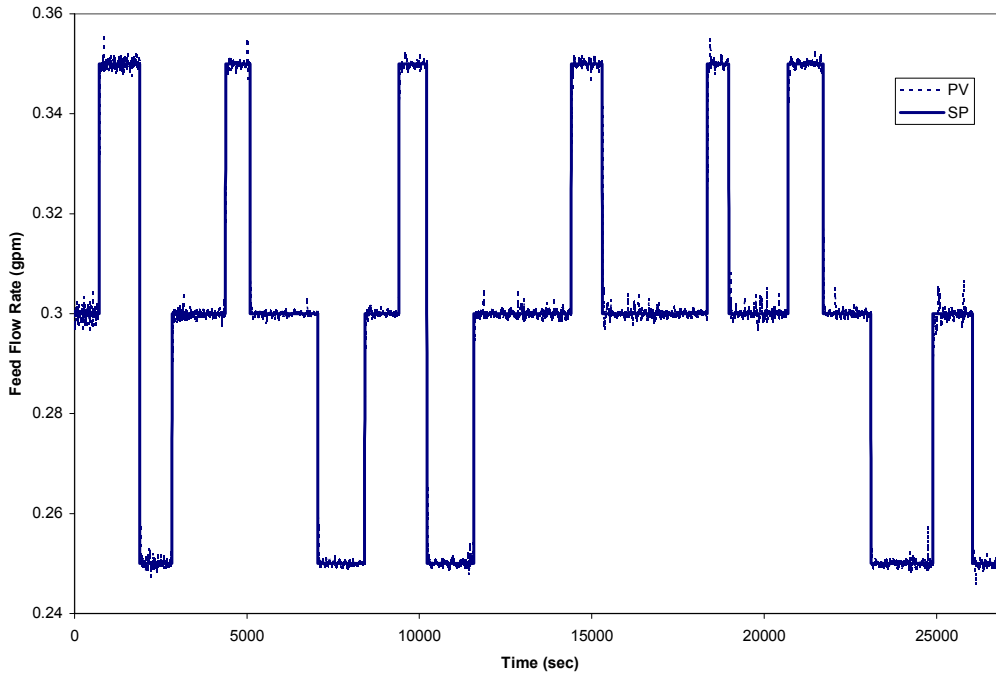


Figure 14: Feed flow response to the set point changes made during the experiments that were conducted on the distillation column. SP represents the change in set point and PV represents the measured process value of the feed flow rate.

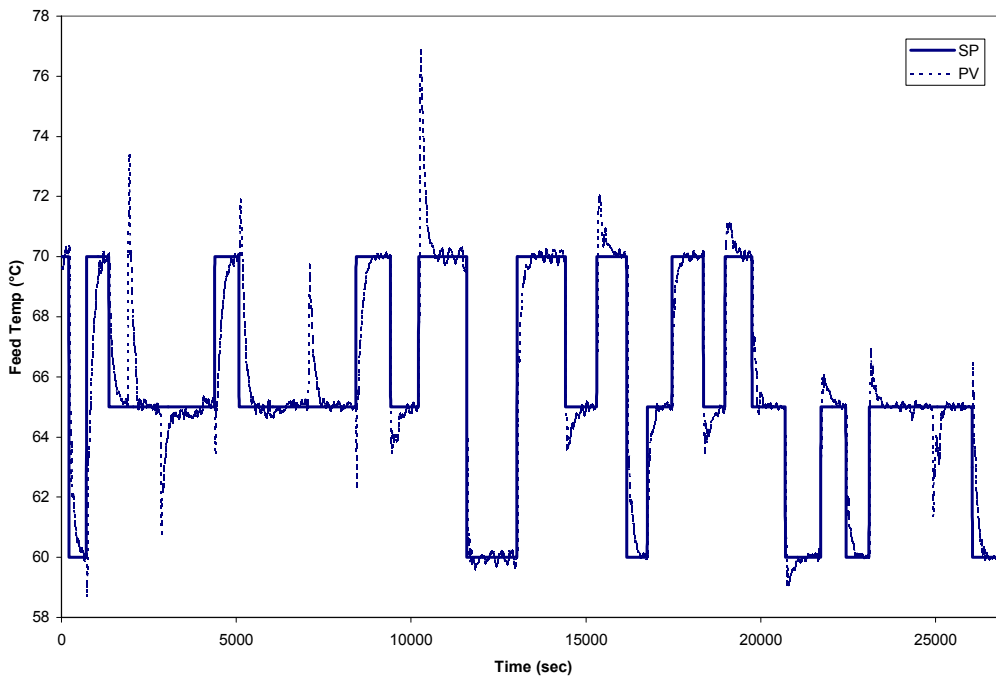


Figure 15: Feed temperature response to set point changes during the experiments that were conducted on the distillation column. SP represents the change in set point and PV represents the measured process value of the temperature.

Based upon our previous discussion of the variability in a process input, we can see from these figures that each of the inputs on the distillation column behave according to different combinations of the three variability contributions. The reboiler level and feed temperature inputs appear to demonstrate significant dynamic behavior, while the feed flow and steam pressure inputs do not.

Let us examine more closely the feed temperature input. This one is of particular interest because the feed temperature is affected not only by the set point changes of the feed temperature controller, but also by changes in the feed flow rate. Fig. 15 shows the input sequence for the set point changes in feed temperature along with the feed temperature that was measured during the experiments.

The H-BEST model algorithm introduced by Rollins, et al. (1998) [11] was used to fit the temperature data. For one change occurring at $t = 0$, this can be written as

$$y(t) = f(u(t); \beta) \cdot g(t; \tau) s(t) \quad (6)$$

where β is the vector of coefficients and the dynamics are described by $g(t; \tau)$. It is important to note that in this case the function $f(u(t); \beta)$ is equal to 1 because the input is a set point and the output is the process response to set point. Therefore, we essentially have only the dynamic block to model the process response. The dynamic behavior of the process was fit to a second-order underdamped model, which is represented as

$$g(t) = 1 - e^{-\zeta t/\tau} \left[\cos\left(\sqrt{1-\zeta^2} t/\tau\right) + \frac{\zeta}{1-\zeta^2} \sin\left(\sqrt{1-\zeta^2} t/\tau\right) \right] \quad (7)$$

The parameters found for this model of the process were $\hat{\tau} = 1.49$ and $\hat{\zeta} = 0.659$. The fit of the model to the process can be seen in Fig. 16. As this demonstrates, the model did a very good job of fitting the process data.

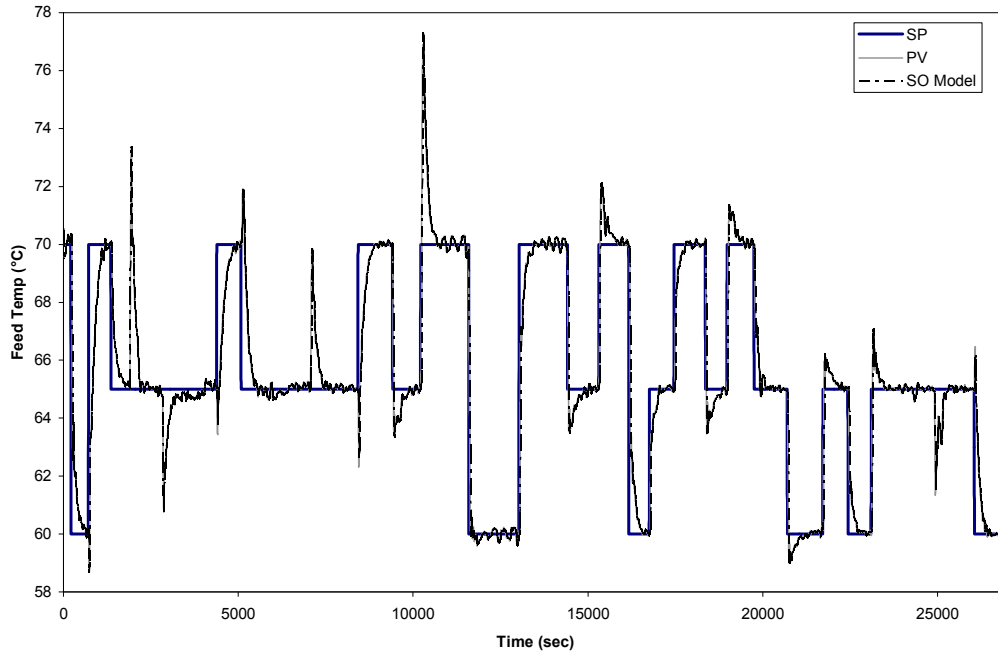


Figure 16: The feed temperature response (PV) to the set point changes (SP) introduced during the experimental runs, along with the second-order underdamped model (SO Model) fit to the feed temperature.

4. Dissertation Research

The questions to be addressed in this research are the following: how do we include this input information into a model-based control algorithm without requiring excessive computational effort? How will this work on a process that has multiple inputs? Can we develop a practical method for identifying the model and implementing it into a model-based control algorithm without requiring any extra model identification effort? These questions will be addressed in detail in the forthcoming chapters.

The goal was to ultimately implement the models developed into a model-based control scheme on the pilot-scale distillation column that was discussed earlier, and use that control algorithm to maintain product quality. The pilot-scale distillation column initially had no overall composition control but instead used several individual controllers to maintain specific operating parameters. Steps will be taken toward achieving the ultimate goal by first testing a new feedforward/feedback control algorithm on a simulated continuous-stirred tank reactor (CSTR) process that can be adequately modeled by an LNL block-oriented model. This is demonstrated in Chapter 4. The control scheme will then be developed further, to show that the models can be identified using data similar in nature to plant historical data, and then implemented into a feedforward/feedback control algorithm that will be applied to the pilot-scale distillation process in the laboratory. Chapter 5 discusses the methods for identifying the model and applying the control scheme to the distillation process.

5. References

- [1] Brosilow, C. and B. Joseph, *Techniques of Model-Based Control*, Prentice Hall PTR, Upper Saddle River, NJ, pp. 387-394.
- [2] Rollins, D.K., L. Pacheco and N. Bhandari, "A Quantitative Measure to Evaluate Competing Designs for Non-linear Dynamic Process Identification," *The Canadian Journal of Chemical Engineering*, Vol. 84, No. 4, 2006
- [3] Hardjasamudra, A., D.K. Rollins, N. Bhandari and S. Chin, "Optimal Experimental Design for Wiener Systems," accepted by *Chemical Engineering Communications*, April, 2006.
- [4] Zhai, D., D.K. Rollins and N. Bhandari, "Compact Block-Oriented Continuous-Time Dynamic Modeling for Nonlinear Systems Under Sinusoidal Input Sequences," *Proceedings of the IASTED Intelligent Systems and Control Conference*, Honolulu, Hawaii, pp. 295-300, 2004.

- [5] Zhai, D., Wu and D.K. Rollins, "Parameter Estimation for the Wiener Dynamic System With Unmeasured Continuous-Time Correlated Stochastic Disturbances," submitted to *Industrial and Engineering Chemistry Research*, September, 2005, in review.
- [6] Zhai, D., D.K. Rollins, N. Bhandari and H. Wu, "Continuous-Time Hammerstein and Wiener Modeling Under Second-Order Static Nonlinearity for Periodic Process Signals," *Computers and Chemical Engineering*, in press.
- [7] Rollins, D.K., N. Bhandari, S. Chin, T. Junge and K. Roosa, "Optimal Deterministic Transfer Function Modeling in the Presence of Serially Correlated Noise," *Chemical Engineering Research and Design*, Vol. 84(A1), pp. 9-21, 2006.
- [8] Pearson, R.K. and B.A. Ogunnaike, "Nonlinear Process Identification," *Nonlinear Process Control*, Prentice-Hall PTR, Upper Saddle River, NJ, pp. 11-110, 1997.
- [9] Loveland, S.D. and L. dela Rosa, "Distillation – A Unit Operations Laboratory Manual," Department of Chemical and Biological Engineering, Iowa State University, Ames, Iowa, 2005.
- [10] Cochran, W.G. and G. Cox, *Experimental Designs*, 2nd ed., Wiley, New York, 1992.
- [11] Rollins, D.K., J.M. Liang and P. Smith, "Accurate Simplistic Predictive Modeling of Non-linear Dynamic Processes," *ISA Transactions*, Vol. 36, pp. 293-303, 1998.

CHAPTER 4. NONLINEAR MULTIPLE INPUT FEEDFORWARD CONTROL UNDER BLOCK-ORIENTED MODELING

A paper to be submitted to the *Journal of Process Control*

Stephanie D. Loveland, Derrick K. Rollins and Nidhi Bhandari

1. Background

The control of chemical processes is a very important part of an industrial plant. Traditional feedback control makes adjustments to some manipulated variable after the process has deviated from its desired operating condition. In the past few decades, more sophisticated control algorithms have been introduced that use predictive models to correct for disturbances before a deviation of the process output from its set point occurs. Many of these are model-based control algorithms, including feedforward control, internal model control and model predictive control (MPC). Each of these types of model-based control uses a model of the process. In most instances, these control algorithms use linear models to predict process behavior based on input changes. However, many real processes exhibit complicated nonlinear behavior so these linear estimations are limited as to when they can be used. Therefore, the use of linear models is often restricted to certain input or output ranges [1, 2].

Some nonlinear models have been proposed for model-based controllers, including artificial neural networks (ANNs) and radial basis functions (RBF) [3, 4], genetic algorithms (GA) [5] and NARMAX models [6, 7, 8]. Another type of nonlinear model that has been used is a block-oriented model (BOM) [9-14], which combines blocks of static nonlinearities with blocks of linear dynamics. The simplest of the block-oriented models are the Hammerstein model, which has a static nonlinear block (N) followed by a linear dynamic

block (L), and the Wiener model, which reverses the order of these two blocks. More complicated block-oriented structures include sandwich models such as the LNL model, which has a linear dynamic block followed by a nonlinear static block followed by a second linear dynamic block. A diagram showing the block-oriented structure of these three models is given in Fig. 1.

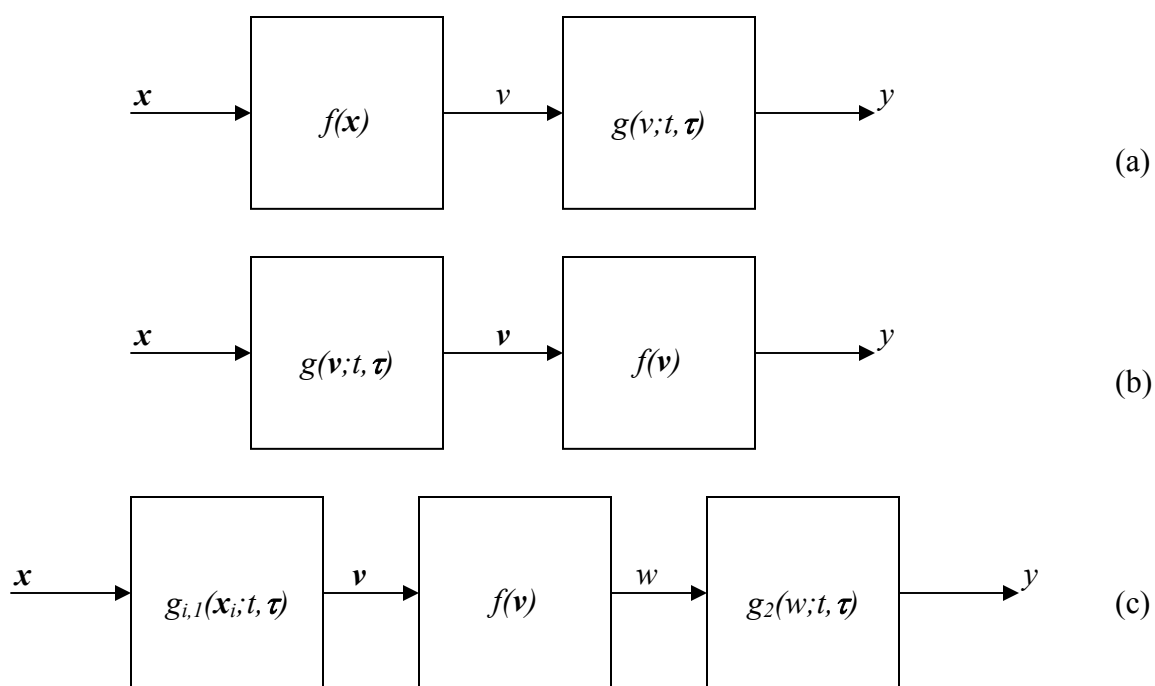


Figure 1: (a) Hammerstein model; (b) Wiener model; (c) LNL model

Many have studied the identification of model parameters for the Hammerstein and Wiener models, including Greblicki [11, 15], Eskinat et al. [16] and Al-Duwaish and Naeem [5]. The LNL process has not gotten as much attention, but some have proposed methods for its parameter identification [17]. In this paper, we present a method for parameter identification for the LNL model that draws from the discrete-time H-BEST and W-BEST identifications presented by Rollins and Bhandari for Hammerstein and Wiener models,

respectively [18]. We will apply the methodology to a simulated continuous-stirred tank reactor (CSTR). In addition, we will implement the model identified into a feedforward-feedback controller and demonstrate its effectiveness in reducing the variability of the process output when the inputs are changing.

The paper is organized as follows. In the next section we will present the method for identifying the LNL model parameters, and introduce the proposed feedforward control algorithm. In Section 3 we will present the simulated CSTR process that was used for the study, as well as the input series that were used for training and testing the model. Finally, we will implement the proposed feedforward controller using the LNL model on the simulated CSTR process, and show how it improves control of the output (reactor tank temperature) as compared to a traditional feedback controller.

2. Methodology

2.1. Building the Proposed LNL model

This section introduces the method for formulating the proposed discrete-time LNL model of a process. For a process such as that shown in Fig. 1(c), the general mathematical form is given by Eqs. 1-3.

$$\begin{aligned} & a_{ij,n} \frac{d^n v_{ij}(t)}{dt^n} + a_{ij,n-1} \frac{d^{n-1} v_{ij}(t)}{dt^{n-1}} + \dots + a_{ij,1} \frac{dv_{ij}(t)}{dt} + v_{ij}(t) \\ & = b_{ij,m} \frac{d^m x_j(t)}{dt^m} + b_{ij,m-1} \frac{d^{m-1} x_j(t)}{dt^{m-1}} + \dots + b_{ij,1} \frac{dx_j(t)}{dt} + x_j(t) \end{aligned} \quad (1)$$

$$w_i(t) = f_i(\mathbf{v}_i(t)) \quad (2)$$

$$\begin{aligned} & c_{ij,n} \frac{d^n \eta_{ij}(t)}{dt^n} + c_{ij,n-1} \frac{d^{n-1} \eta_{ij}(t)}{dt^{n-1}} + \dots + c_{ij,1} \frac{d\eta_{ij}(t)}{dt} + \eta_{ij}(t) \\ & = d_{ij,m} \frac{d^m w_j(t)}{dt^m} + d_{ij,m-1} \frac{d^{m-1} w_j(t)}{dt^{m-1}} + \dots + d_{ij,1} \frac{dw_j(t)}{dt} + w_j(t) \end{aligned} \quad (3)$$

where i refers to the output with $i=1, \dots, q$, j refers to the input with $j=1, \dots, p$, $\mathbf{v}_i(t) = [v_{i1}, v_{i2}, \dots, v_{ip}]^T$, w_i is the unobservable intermediate variable after the nonlinear static function, and η_i is the true value of the output. Eqs. 1 and 3 are written without dead time for simplicity, and the form of Eq. 2 is not restricted. Eqs. 1 and 3 can be converted to a discrete-time form by using a backwards difference approximation, resulting in Eqs. 4 and 5.

$$\begin{aligned} v_{ij,t} = & \delta_{ij,1}v_{ij,t-1} + \delta_{ij,2}v_{ij,t-2} + \dots + \delta_{ij,n}v_{ij,t-n} \\ & + \omega_{ij,1}x_{j,t-1} + \omega_{ij,2}x_{j,t-2} + \dots + \omega_{ij,m}x_{j,t-m} + \omega_{ij,m+1}x_{j,t-(m+1)} \end{aligned} \quad (4)$$

$$\begin{aligned} v_{ij,t} = & \gamma_{ij,1}\eta_{ij,t-1} + \gamma_{ij,2}\eta_{ij,t-2} + \dots + \gamma_{ij,n}\eta_{ij,t-n} \\ & + \lambda_{ij,1}w_{j,t-1} + \lambda_{ij,2}w_{j,t-2} + \dots + \lambda_{ij,m}w_{j,t-m} + \lambda_{ij,m+1}w_{j,t-(m+1)} \end{aligned} \quad (5)$$

where the δ 's, ω 's, γ 's and λ 's are all functions of the dynamic parameters (a's, b's, c's and d's) in Eqs. 1 and 3. They are derived after the form of the linear dynamic block has been chosen by discretizing the differential equation, separating and collecting terms to get the forms given by Eqs. 4 and 5. The output, \hat{y} , is then described by

$$\hat{y}_{i\ell,t} = \hat{\eta}_{i,t} + \varepsilon_{i\ell,t} \quad (6)$$

where $\varepsilon_{i\ell,t}$ is the noise term such that

$$\varepsilon_{i\ell,t} \sim N(0, \sigma_i^2) \quad \forall \ell \quad (7)$$

Nonlinear least squares regression is used to determine the estimates of the δ 's, ω 's, γ 's and λ 's in Equations 4 and 5. This is obtained by

$$SSE = \sum (y_{measured} - \hat{y})^2 \quad (8)$$

The H-BEST and W-BEST model identification methods are described by Rollins et al. and Bhandari and Rollins [19, 20]. These methodologies have been extended to apply to an LNL model structure as follows:

1. Determine the statistical experimental design to be used.
2. Run the experimental design as a series of step tests, allowing steady state to be reached after each change and collect data dynamically over time.
3. Use the steady-state data to determine the ultimate response function, $f(\Delta\mathbf{v};\beta)$ for each output. $\Delta\mathbf{v}$ is a deviation variable, i.e., $\Delta\mathbf{v}(t) = \mathbf{v}(t) - \mathbf{v}_{ss}$, where \mathbf{v}_{ss} is the steady state value.
4. Use the dynamic data to determine both the dynamic response functions: $g_{i,1}(t, \boldsymbol{\tau})$ for the i^{th} input and $g_2(t; \boldsymbol{\tau})$ for each output.

The static nonlinearity is determined using only steady state data, and the dynamic functions $g_{i,1}$ and g_2 are selected from typical linear dynamic forms (i.e., first order, second order plus lead, etc.).

Once the initial parameters for the $f(\cdot)$ and $g(\cdot)$ functions are identified, these are used as initial guesses in a nonlinear parameter estimation routine to simultaneously determine all the parameters to obtain the best fit for the data, if necessary. The identified model is then tested against a new set of experimental or simulated data obtained from the same process. A new sequence of input changes is generated and used to change the inputs of the process and the output response is compared to the predicted output response of the identified model.

2.2. General Feedforward Control

The concept of feedforward control was first applied as early as 1925 to level control systems for boiler drums [21]. It allows for theoretically perfect control of a process system, because it corrects for input disturbances before the process outputs deviate from their desired values. However, this requires timely and efficient measurement of all possible process disturbances, which is nearly impossible, so it is typically used in conjunction with feedback control. The addition of feedback control compensates for any deviation of the process output from its setpoint, regardless of the cause of the deviation. Feedforward controllers are typically found independently for each disturbance variable that is placed on

feedforward control, and the feedforward controller is generally approximated by a linear model [22]. A block diagram of a typical feedforward/feedback controller is shown in Fig. 2.

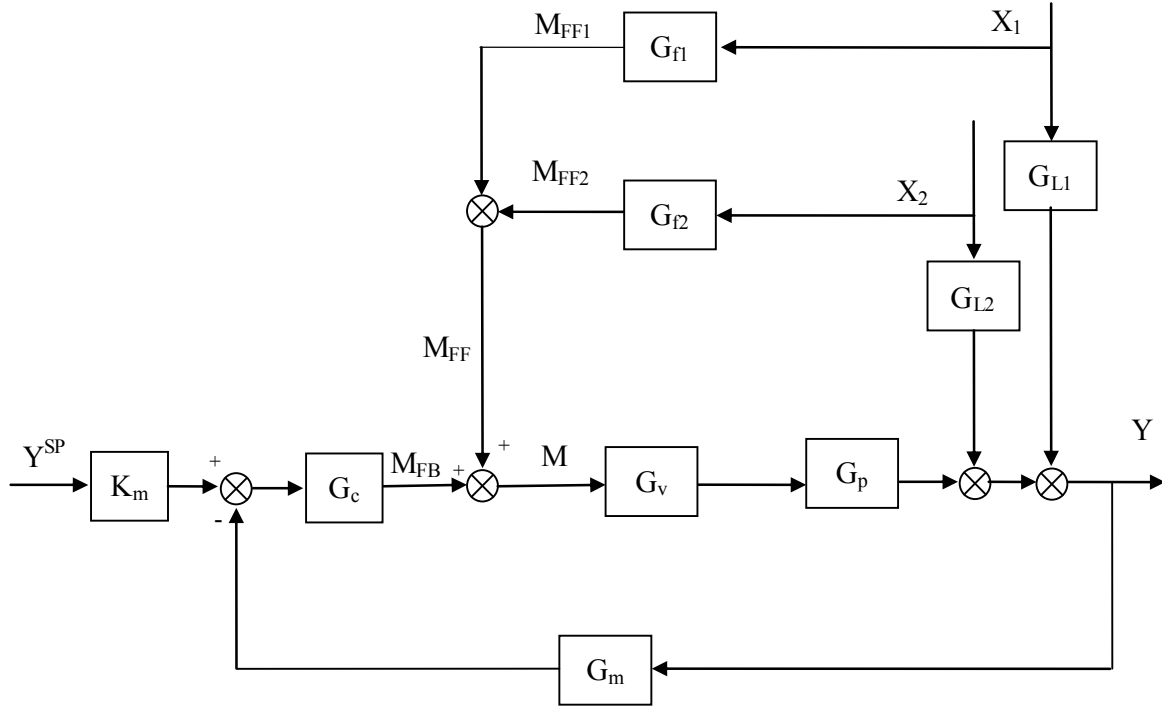


Figure 2: A typical feedforward/feedback control block diagram, with two disturbance variables (X_1 and X_2) on feedforward control. The lower loop is for feedback control and the upper loops are for feedforward control.

Ideal feedforward controllers can be physically unrealizable if the process transfer function, G_p has a longer dead time or is a higher-order transfer function than G_{Li} . In these cases, the feedforward controller (G_f) is typically approximated by a lead-lag unit [21].

2.2. Proposed Feedforward Control Methodology

The block diagram for the proposed feedforward/feedback controller under Hammerstein modeling is shown in Fig. 3. In order for perfect control to be achieved, we must first find the closed-loop response to an arbitrary change in the disturbance variable X_i . Note that all variables are given in terms of deviation from an initial steady state.

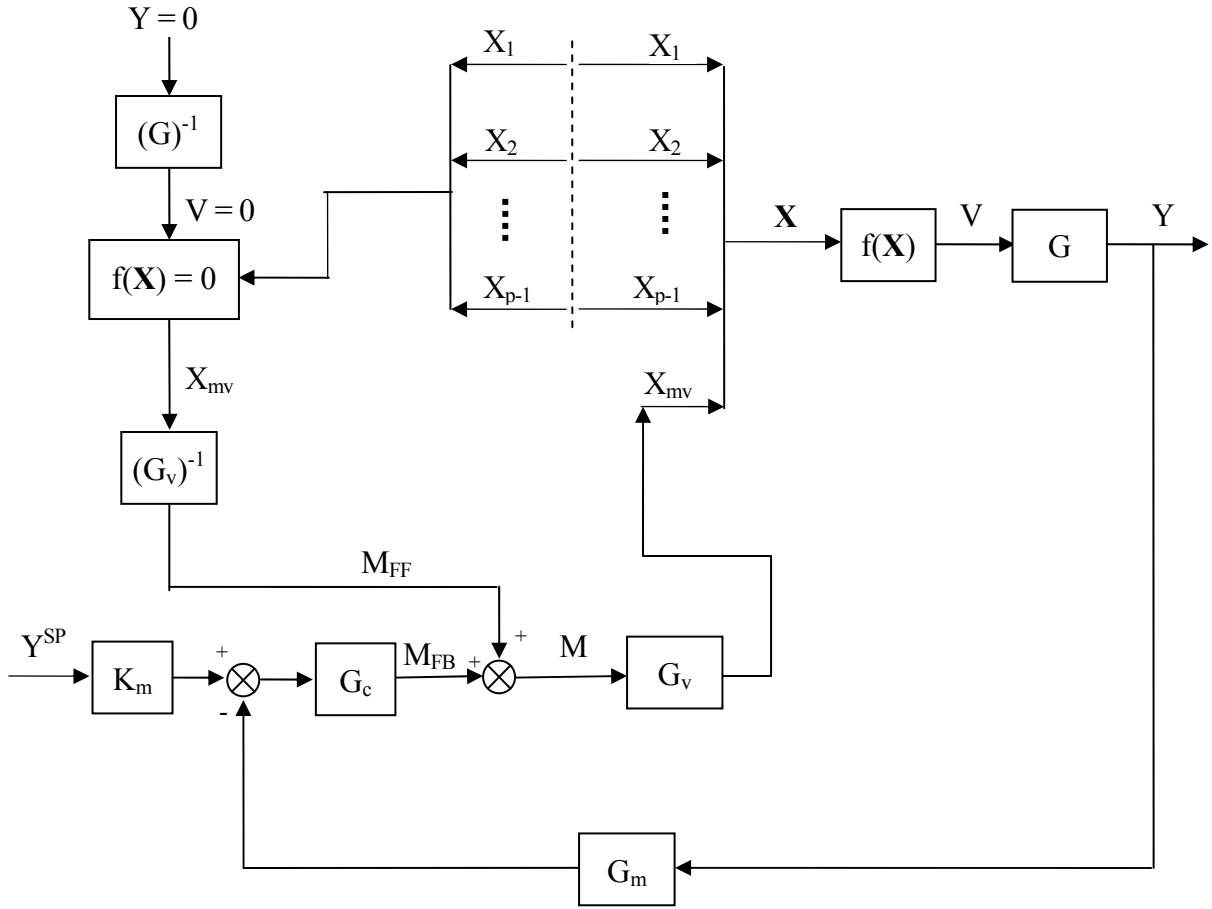


Figure 3: The proposed feedforward/feedback controller under Wiener modeling. The X_i 's represent the input variables, Y represents the controlled variable, M represents the controller signal.

For any and all $X_i \neq 0$, $v_i \neq 0$. The change in M_{FF} required for $Y = f(\mathbf{v}) = 0$ is determined as follows.

$$f(\mathbf{x}) = a_0 + a_1 x_1 + a_2 x_2 + a_{1,mv} x_{mv} + \dots + a_j x_1^2 + \dots + a_{2,mv} x_{mv}^2 + a_k x_1 x_2 + \dots + a_{i,mv} x_i x_{mv} + \dots \quad (9)$$

Rearranging Eq. 9 gives

$$f(x) = ax_{mv}^2 + bx_{mv} + c \quad (10)$$

where

$$\begin{aligned}
a &= a_{2,mv} \\
b &= a_{1,mv}x_1 + a_{2,mv}x_2 + \cdots + a_{i,mv}x_i \\
c &= a_0 + a_1x_1 + a_2x_2 + \cdots
\end{aligned} \tag{11}$$

Therefore, x_{mv} can be determined using the quadratic equation. As shown by Fig. 3, after determining x_{mv} , M_{FF} , the feedforward control law, is determined by

$$M_{FF} = G_v^{-1} X_{mv} \tag{12}$$

which gives $y = 0$ for changes in the measurable loads shown in Figure 3 as required. In the case where G_v^{-1} is physically unrealizable, an approximation will be used. This takes on a form much like a derivative filter in an ideal PID controller, and its use will be demonstrated when we implement the LNL model into a feedforward/feedback controller on the simulated CSTR process.

3. The Process Studied

To test the LNL model identification process above, a simulated continuous-stirred tank reactor (CSTR) was used. The process originally appears in Smith & Corripio [23] and a schematic diagram can be found in Fig. 4. A dynamic model of the process was developed using first principles on the mass, species and energy of the process for the simulation. The assumptions made include the following: densities and heat capacities of the tank and jacket contents are constant, volumes in the tank and jacket are constant, perfect mixing occurs in the tank, the thermal capacitance of the tank wall is negligible, heat capacity at constant volume (C_v , C_{vc}) and heat capacity at constant pressure (C_p , C_{pc}) are approximately equal for both the jacket and reactor contents and are constant, and the internal energy of the system is adequately described by the enthalpy. For this study, we have added valve dynamics to the

coolant flow rate in order to show the LNL model structure. A list of variables and initial values is given in Table 1.

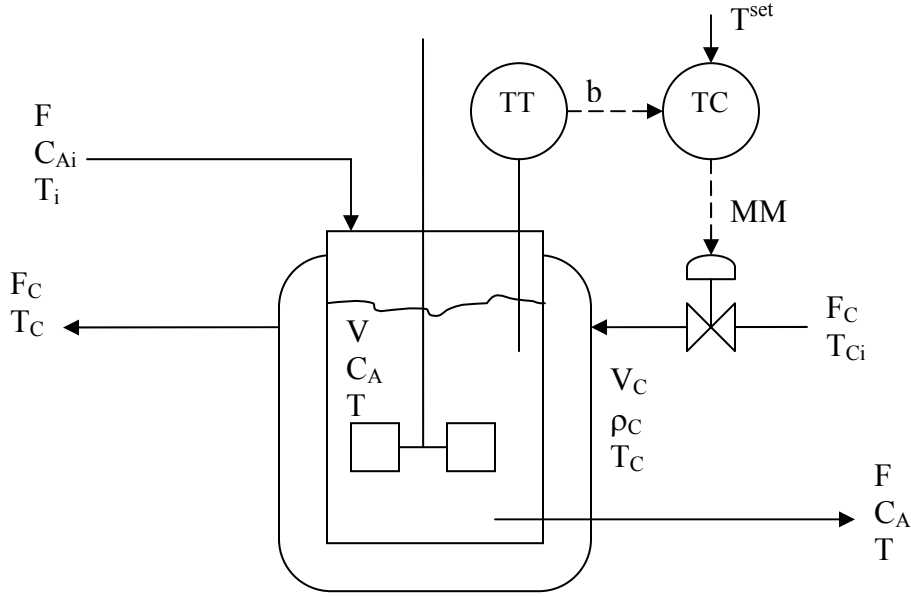


Figure 2: The simulated CSTR process used for this study.

The CSTR process is described mathematically in Eqs. 13-17.

$$\frac{dC_A}{dt} = \frac{F}{V}(C_{Ai} - C_A) - kC_A^2 \quad (13)$$

$$\frac{dT_T}{dt} = \frac{F}{V}(T_T - T_T) - \frac{\Delta H_R}{\rho C_p} kC_A^2 - \frac{UA}{\rho V C_p}(T_T - T_C) \quad (14)$$

$$\frac{dT_C}{dt} = \frac{UA}{V_C \rho_C C_{pC}}(T_T - T_C) - \frac{F}{V_C}(T_C - T_{Ci}) \quad (15)$$

$$k = k_0 \exp\left(\frac{-E}{R(T_T + 273.16)}\right) \quad (16)$$

$$F_C = F_{C_{\max}} \times \alpha^{(-MM)} \quad (17)$$

Table 1: Definition of variables and initial steady-state values for the CSTR process.

Variable	Definition	SS value (units)
A	Heat transfer area	5.40 (m ²)
α	Control valve rangeability parameter	50 (none)
C _A	Concentration of species A in reactor	1.0302 (kgmol/m ³)
C _{Ai}	Concentration of species A in inlet stream	2.88 (kgmol/m ³)
c _p	Heat capacity of feed and product streams	1.815x10 ⁵ (J/kgmol-°C)
c _{pc}	Heat capacity of coolant	4184 (J/kg-°C)
ΔH_R	Heat of reaction	-9.86x10 ⁷ (J/kgmol)
E	Activation energy	1.182x10 ⁷ (J/kgmol)
F	Feed flow rate	0.45 (m ³ /s)
F _C	Coolant flow rate	0.44 (m ³ /s)
F _{Cmax}	Maximum flow rate of coolant through control valve	1.2 (m ³ /s)
k	Reaction rate constant	0.09 (m ³ /s-kgmol)
k _o	Arrhenius frequency parameter	0.0744 (m ³ /s-kgmol)
MM	Controller output signal	0.26 (none)
R	Gas law constant	8314.39 (J/kgmol-K)
ρ	Density of reactor contents	19.2 (kgmol/m ³)
ρ_c	Density of coolant	1000 (kg/m ³)
T _c	Coolant temperature in the jacket	50.48 (°C)
T _{ci}	Coolant inlet temperature	27 (°C)
TT	Reactor temperature	88 (°C)
TT _M	Measured reactor temperature	88 (°C)
U	Overall heat transfer coefficient	2.13x10 ⁵ (J/s-m ² -°C)
V _C	Cooling jacket volume	1.82 (m ³)
V	CSTR volume	7.08 (m ³)

To identify the model parameters for the LNL model, a Box-Behnken experimental design with three center points was chosen using four inputs: feed flow rate, concentration of A in the inlet stream, controller signal, and coolant inlet temperature. This gave a total of 27 input combinations. The input sequence is shown in Fig. 5, and the response of reactor temperature to this series of input changes is given in Fig. 6.

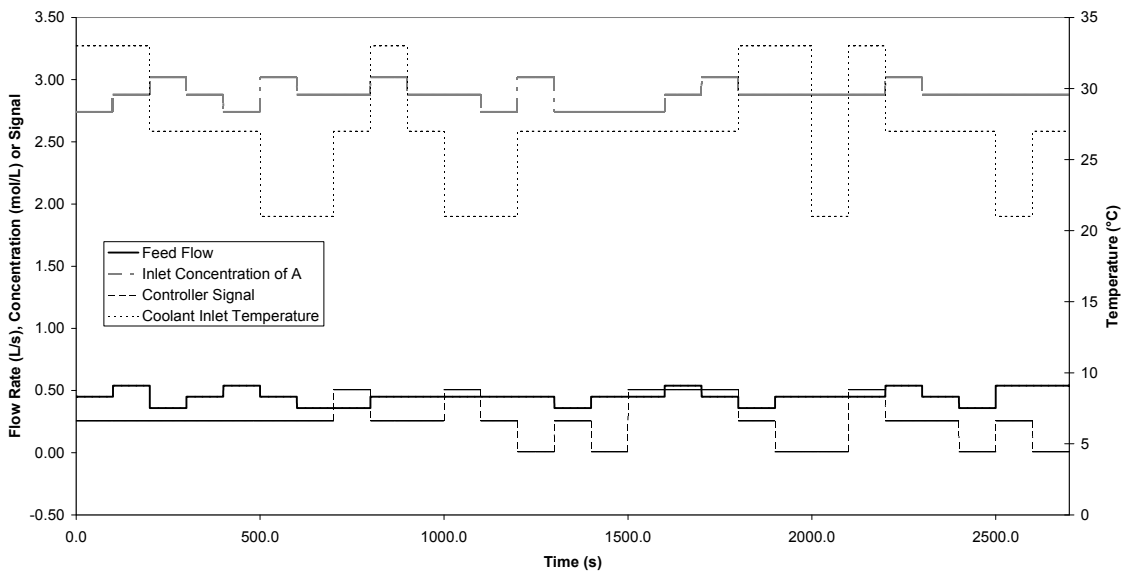


Figure 5: The input sequence used for training the LNL model for the CSTR process.

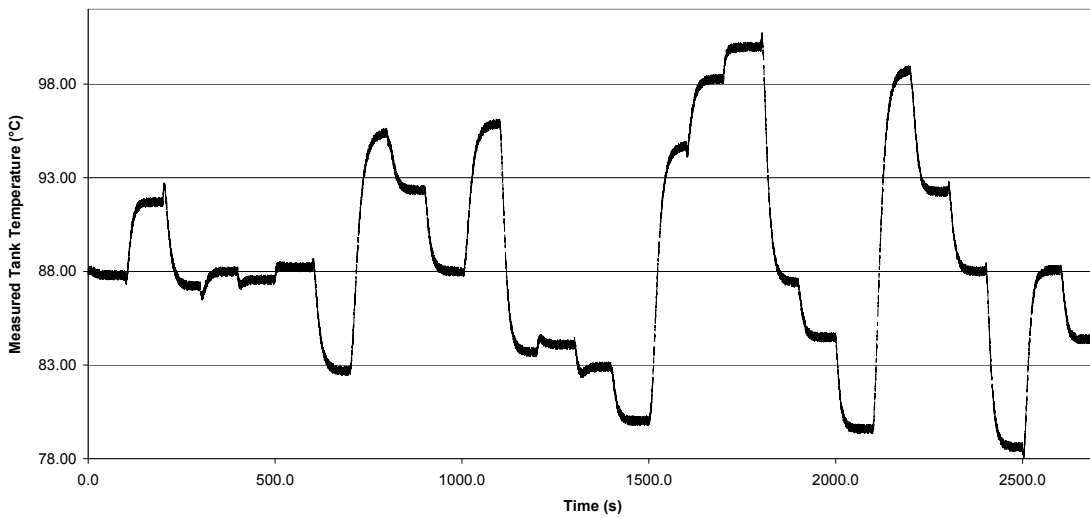


Figure 6: The reactor temperature response to the input sequence shown in Figure 3 above.

The valve dynamics of this process will be estimated using a linear dynamic block.

The LNL model for this process, then, has the structure given in Fig. 7.

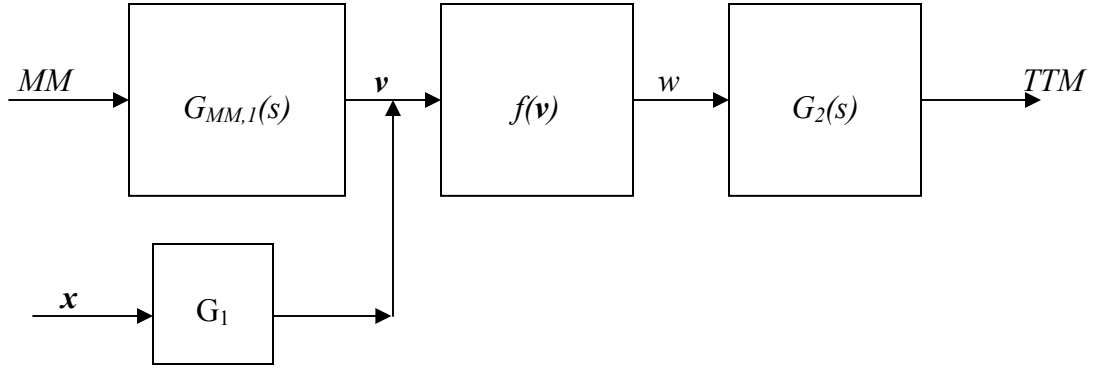


Figure 7: The LNL model for the CSTR process used in this study. MM is the controller signal, the vector \mathbf{x} includes the three input variables TCI, CAI and F.

The fitted model for the process follows the form given in equations 18 through 20.

The G_1 block is equal to unity. The parameters for the model are listed in Table 2.

$$G_{MM,1}(s) = \frac{K_v}{\tau_v s + 1} \quad (18)$$

$$f(\mathbf{v}) = a_0 + a_1 F + a_2 CAI + a_3 MM + a_4 TCI + a_5 F^2 + a_6 MM^2 + a_7 F \cdot MM + a_8 F \cdot TCI + a_9 CAI \cdot MM + a_{10} MM \cdot TCI \quad (19)$$

$$G_2(s) = \frac{\tau_a s + 1}{\tau^2 s^2 + 2\tau\zeta s + 1} \quad (20)$$

Table 2: Fitted model parameters for the LNL block-oriented model used to predict the reactor temperature response to the input changes shown in Figure 7.

Parameter	Value	Parameter	Value
a_0	0	a_8	-0.40434
a_1	26.91867	a_9	11.52124
a_2	16.98205	a_{10}	-0.3336
a_3	30.4157	τ	8.572204
a_4	0.333564	ζ	1.063172
a_5	-64.9391	τ_a	0.17824
a_6	23.30424	K_v	1.003916
a_7	-25.9394	τ_v	3.196657

The fitted model response to the input series is shown in Fig. 8. A test sequence was then applied to test the fitted model, and the input sequence for this is shown in Fig. 9, while the reactor temperature response is shown in Fig. 10.

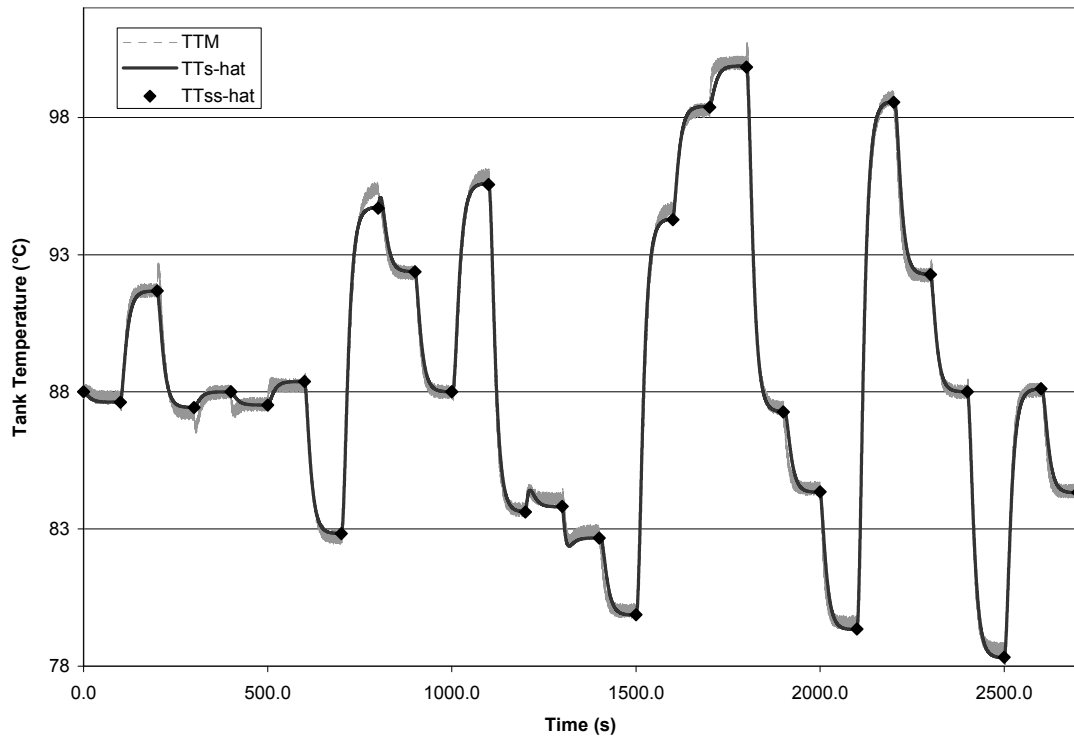


Figure 8: The fitted model response to the training sequence given in Figure 3. TTM is the measured reactor temperature, TTs-hat is the predicted reactor temperature, and TTss-hat is the predicted steady-state value for the reactor temperature.

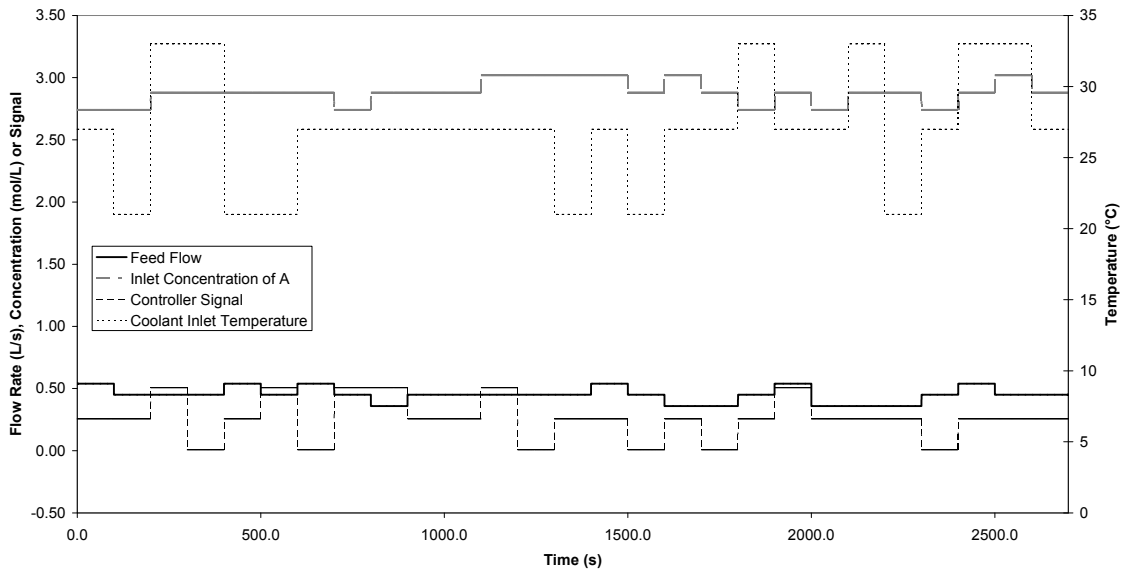


Figure 9: The input sequence used to test the model that was identified for the reactor temperature response to input changes.

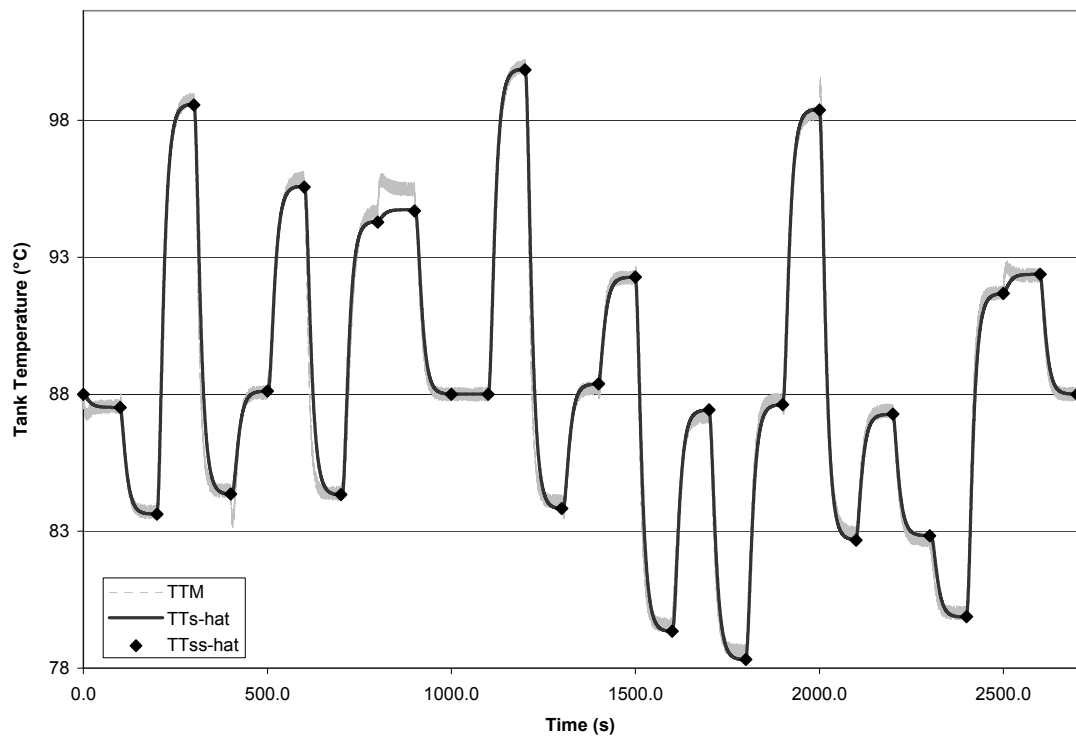


Figure 10: The reactor temperature response to the test input sequence given in Figure 7. TTM is the measured reactor temperature, TTs-hat is the predicted reactor temperature, and TTss-hat is the predicted steady-state values for the reactor temperature.

4. The Feedforward-Feedback Controller

A typical proportional-integral (PI) controller was implemented to control the reactor temperature by manipulating the coolant flow rate. It was tuned to give the best possible response (quick response with minimal overshoot) to a step change of +2 degrees Celsius to the reactor temperature set point.

The LNL model generated from the open-loop training in Section 3 was then used to implement a feedforward controller in conjunction with the feedback PI controller. The manipulated variable chosen to maintain the reactor temperature is the coolant flow rate through the jacket of the CSTR vessel and can be varied by changing the controller signal. Following Eqs. 9-12, the feedforward controller is implemented. Since Eq. 9 gives that $f(\mathbf{x})$ was determined to be a quadratic function, x_{mv} can be found by solving the quadratic equation. The root chosen depends upon the input variables that are changing, and varies with different combinations of inputs. The decision of which root to use is made based on which solution is within the physical limits of the controller output. This was implemented in the simulation by a simple IF statement.

Once x_{mv} has been determined, M_{FF} must be found. Taking the inverse of Eq. 18 will give MM from a known value of x_{mv} , and this is shown in Eq. 20.

$$G^{-1}(s) = \frac{M_{FF}}{x_{mv}} = \frac{\tau_v s + 1}{K_v} \quad (20)$$

Eq. 20 is physically unrealizable, so in order to make this a physically realizable function when transformed into the time domain, the variable τ_{av} is introduced. This is shown in Eq. 21.

$$G^{-1}(s) = \frac{M_{FF}}{x_{mv}} = \frac{\tau_v s + 1}{K_v(\tau_{av} s + 1)} \quad (21)$$

This τ_{av} is a tuning parameter for the feedforward controller, and is similar in function to a derivative filter that is used to make an ideal PID controller physically realizable (see [21]). Its value is chosen to be a very small value, in this case, 0.2. Varying the parameter τ_{av} does not have a considerable effect on the behavior of the controller as long as it remains small.

5. Comparison of Feedback only controller with Feedforward/feedback controller

The feedforward/feedback controller developed in Section 4 was tested and compared to the feedback controller (PI) alone. The input series given in Fig. 9 was applied to the process in closed-loop mode for both controller configurations. The results are shown in Figs. 11-12.

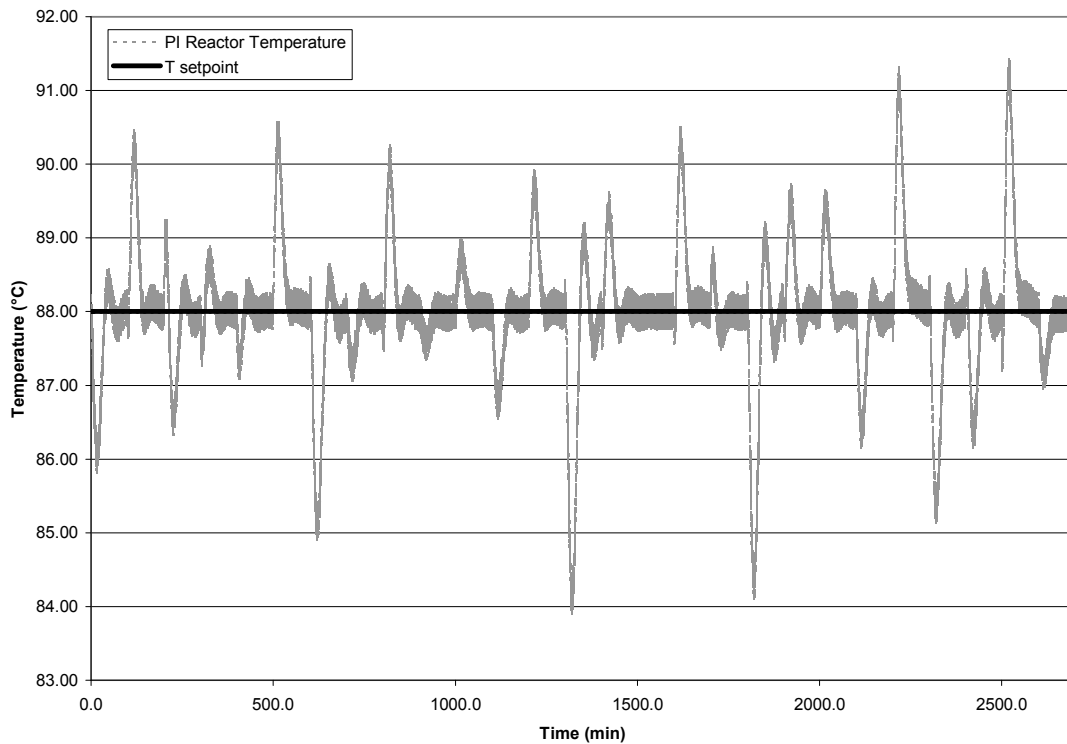


Figure 11: The reactor temperature response under feedback control to the test input sequence given in Fig. 9.

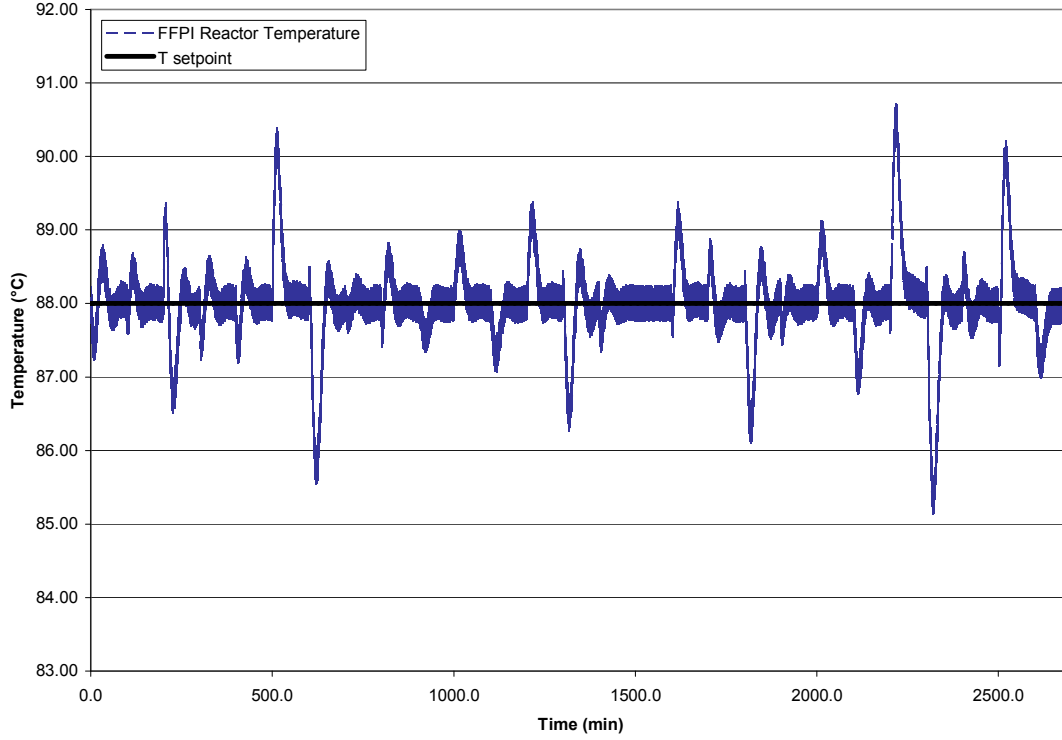


Figure 12: The reactor temperature response under feedforward/feedback control to the test input sequence given in Fig. 9.

We have use the average absolute error (AAE) as the quantitative measure to compare the responses of the two controllers. AAE is given by

$$AAE = \frac{\sum_n |T_{setpoint} - T_{measured}|}{n} \quad (22)$$

where $T_{setpoint}$ is the set point of the reactor temperature, $T_{measured}$ is the measured value of the tank temperature and n is the number of sample points. In this work, for the feedback controller, AAE is equal to 0.4942. For the feedforward/feedback controller, $AAE = 0.3215$. This represents a 35% reduction in process variability by using the proposed feedforward/feedback controller.

6. Conclusions

In this work, we have proposed a new methodology for identifying the models and estimating the parameters therein for an LNL sandwich block-oriented model that takes full advantage of statistical design of experiments to account for input interactions. We have developed a feedforward controller that uses this LNL model to compensate for multiple process input disturbances simultaneously, and have demonstrated its use on a simulated CSTR process. The proposed feedforward/feedback controller has been shown to reduce process variability considerably.

7. References

- [1] Clarke, D.W., C. Mohtadi and P.S. Tuffs, "Generalized Predictive Control- Part 1: The Basic Algorithm," *Automatica*, Vol. 23, pp. 137-148, 1987.
- [2] Muske, K.R. and J.B. Rawlins, "Model Predictive Control with Linear Models," *AIChE Journal*, Vol. 39, pp. 262-287, 1993.
- [3] Alexandridis, A. and H. Sarimveis, "Nonlinear Adaptive Model Predictive Control Based on Self-Correcting Neural Network Models," *AIChE Journal*, Vol. 51. No. 9, September 2005.
- [4] Fischer, M., O. Nelles and R. Isermann, "Adaptive Predictive Control of a Heat Exchanger Based on a Fuzzy Model," *Control Engineering Practice*, Vol. 6, pp. 259-269, 1998.
- [5] Al-Duwaish H. and Naeem, Wasif , "Nonlinear Model Predictive Control of Hammerstein and Wiener Models Using Genetic Algorithms," *Proceedings of the 2001 IEEE International Conference on Control Applications*, September 5-7, 2001, Mexico City, Mexico
- [6] Di Palma, F., L. Magni, "A Multi-Model Structure for Model Predictive Control," *Annual Reviews in Control*, Vol. 28, pp. 47-52, 2004.
- [7] Gao, J, R. Patwardhan, K. Akamatsu, Y. Hashimoto, G. Emoto, S.L. Shah, B. Huang, "Performance Evaluation of Two Industrial MPC Controllers," *Control Engineering Practice*, Vol. 11, pp.1371-1387, 2003.
- [8] Havlena, V. and J. Findejs, "Application of Model Predictive Control to Advanced Combustion Control," *Control Engineering Practice*, Vol. 13, pp. 671-680, 2005.

- [9] Pearson, R.K. and B.A. Ogunnaike, "Nonlinear Process Identification," *Nonlinear Process Control*, Prentice-Hall PTR, Upper Saddle River, NJ, pp. 11-110, 1997.
- [10] Rollins, D.K., N. Bhandari, A.M. Bassily, G.M. Colver and S. Chin, "A Continuous-Time Nonlinear Dynamic Predictive Modeling Method for Hammerstein Processes," *Industrial and Engineering Chemistry Research*, Vol. 42, No. 4, pp. 861-872, 2003.
- [11] Greblicki, W., "Continuous-Time Hammerstein System Identification," *IEEE Transactions on Automatic Control*, Vol. 45, No. 6, pp. 1232-1236, 2000.
- [12] Bhandari, N. and D.K. Rollins, "Continuous-Time Hammerstein Nonlinear Modeling Applied to Distillation," *AIChE Journal*, Vol. 50, No. 2, pp. 530-533, 2004.
- [13] Bhandari, N. and D.K. Rollins, "A Continuous-Time MIMO Wiener Modeling Method," *Industrial and Engineering Chemistry Research*, Vol. 42, No. 22, pp. 5583-5595, 2003.
- [14] Chin, S., N. Bhandari and D.K. Rollins, "An Unrestricted Algorithm for Accurate Prediction of MIMO Wiener Processes," *Industrial and Engineering Chemistry Research*, Vol. 43, pp. 7065-7074, 2004.
- [15] Greblicki, W., "Nonparametric Identification of Wiener Systems," *IEEE Transactions on Information Theory*, Vol. 38, No. 5, pp. 1487-1493, 1992.
- [16] Eskinat, E., S.H. Johnson and W.L. Luyben, "Use of Hammerstein Models in Identification of Nonlinear Systems," *AIChE Journal*, Vol. 37, No. 2, pp. 255-268, 1991.
- [17] Shi, J. and H.H. Sun, "A General Method for Nonlinear System Identification," *Proceedings of the American Control Conference*, Vol. 1, pp. 715-716, 1991.
- [18] Rollins, D.K. and N. Bhandari, "Constrained MIMO dynamic Discrete-Time Modeling Exploiting Optimal Experimental Design," *Journal of Process Control*, Vol. 14, No. 6, pp. 671-683, 2004.
- [19] Rollins, D.K., N. Bhandari, A.M. Bassily, G.M. Colver and S. Chin, "A Continuous-Time Nonlinear Dynamic Predictive Modeling Method for Hammerstein Processes," *Industrial and Engineering Chemistry Research*, Vol. 42, No. 4, pp. 861-872, 2003.
- [20] Bhandari, N. and D.K. Rollins, "A Continuous-Time MIMO Wiener Modeling Method," *Industrial and Engineering Chemistry Research*, Vol. 42, No. 22, pp. 5583-5595, 2003.
- [21] Seborg, D.E., T.F. Edgar and D.A. Mellichamp, *Process Dynamics and Control*, 2nd edition, John Wiley and Sons, 2003.

- [22] Zhang, J. and R. Agustriyanto, "Inferential Feedforward Control of a Distillation Column," Proceedings of the American Control Conference, pp. 2555-2560, Arlington, VA, June 25-27, 2001.
- [23] Smith, C.A. and A.B. Corripio, *Principles and Practice of Automatic Process Control*, Wiley, New York, 1985.

CHAPTER 5. DEVELOPMENT OF NONLINEAR FEEDFORWARD CONTROL FROM CLOSED-LOOP FREELY-EXISTING TYPE DATA WITH APPLICATION TO A PILOT-SCALE DISTILLATION COLUMN

A paper to be submitted to *Industrial and Engineering Chemistry Research*

Stephanie D. Loveland, Nidhi Bhandari and Derrick K. Rollins

1. Introduction

The control of chemical processes in industry is a very important aspect of everyday operations. The ability to maintain control has an impact on process safety, product quality and plant profitability. In recent years, many different advanced control techniques have been developed. Included among these are many types of model-based control schemes, including Smith predictors, feedforward controllers and model predictive control schemes [1].

In order to use any of these model-based control schemes, several obstacles must be overcome. Many chemical and biological processes exhibit nonlinear behavior, but model-based control schemes have often used linear models, which can be sufficient if the process is operated over a small range of inputs [2, 3]. Real processes also often exhibit complicated dynamic responses to changes in the process inputs, including nonlinear dynamics. In the past decade, advances in computational capabilities have allowed for nonlinear models to be used for the process response prediction. Some of the types of models that have been proposed include Radial Basis Functions (RBFs) and Artificial Neural Networks (ANNs) [4, 5], ARMAX models [6, 7, 8], Genetic Algorithms [9], Feedforward Neural Networks (FNNs) [10] and Block-Oriented Models (BOMs) [11-16].

The performance of any model-based controller is highly dependent on the model that is used to predict process behavior. The procedures for developing the model can be time-consuming and costly, requiring the process to be perturbed in order to determine cause-and-effect behavior between the process inputs and outputs. It is desirable to be able to identify the process model without causing significant upsets to everyday operations. Ideally, historical data from the plant database could be used to develop the models to be used for prediction of process output response to changes in the inputs. The advantages of using this historical data are numerous. The data is readily available, is collected frequently, covers the “typical” operating space of the process, and does not require specific perturbations of the process inputs. However, several problems can be encountered if plant historical data is used. The process inputs are likely to be highly correlated, and the range of the inputs may not be very broad. For purely empirical models such as neural networks, this can be a significant shortcoming because the model cannot be used outside the input space that was used in the model identification procedure. The ability of the model to accurately predict behavior deteriorates if extrapolation occurs.

Distillation is an example of a process that would benefit from a model-based controller that can be built using plant historical data. Distillation is one of the most commonly used processes in industry. The high degree of interaction between process variables makes it a complicated problem for control. Many different approaches have been applied to the product composition control problem. Use of feedforward control algorithms along with standard feedback controllers was proposed as early as 1969 [17]. Since that time, there have been many applications of feedforward control to distillation processes. Among these, several have attempted to address the process response of product composition

to various input disturbances such as feed flow and feed composition [18-20], but none have attempted to compensate for multiple input disturbances occurring simultaneously. Most of the work done has focused on one or two input disturbances, occurring at separate times. In addition, most of the examples found in the literature are those of simulated distillation processes, not real processes.

The purpose of this work is to demonstrate a method of developing a nonlinear process model under highly correlated inputs that can be used for a feedforward controller that will compensate for multiple input disturbances simultaneously. The model can be developed using historical plant data collected under closed-loop conditions and still effectively determine cause-effect behavior between the inputs and output of the process. To present this advancement, this paper is organized as follows. The next section will present the methodology for developing the process model that will be used for the design of the proposed feedforward/feedback controller. We will also discuss the methodology for typical feedforward/feedback control schemes, and then introduce the proposed feedforward/feedback control scheme. In Section 3 we will present the distillation process that was used to evaluate the proposed methodology. Then we will discuss the procedures for building the model on the distillation process, the implementation of a standard feedback controller and then the implementation of the proposed feedforward/feedback controller. We will present the responses of the distillation process to a set of input disturbances for both feedback and feedforward/feedback control and demonstrate the improvement in control by using the proposed feedforward/feedback controller. Finally, in Section 4 we will discuss the implications of this work for other types of processes.

2. Methodology

2.1 Modeling Methodology

Block-oriented models have been used to accurately describe many types of nonlinear process behavior. The two most common block-oriented models are the Hammerstein and Wiener models, which have simple arrangements of two blocks, as shown in Fig. 1. The Hammerstein model consists of a nonlinear static block (N) followed by a linear dynamic block (L), and the Wiener model has these two blocks reversed. More complicated block-oriented models consist of multiple blocks in various arrangements. In this paper, we will discuss the LNL block-oriented model shown in Fig. 1(c), which has a linear dynamic block followed by a nonlinear static block and then another linear dynamic block.

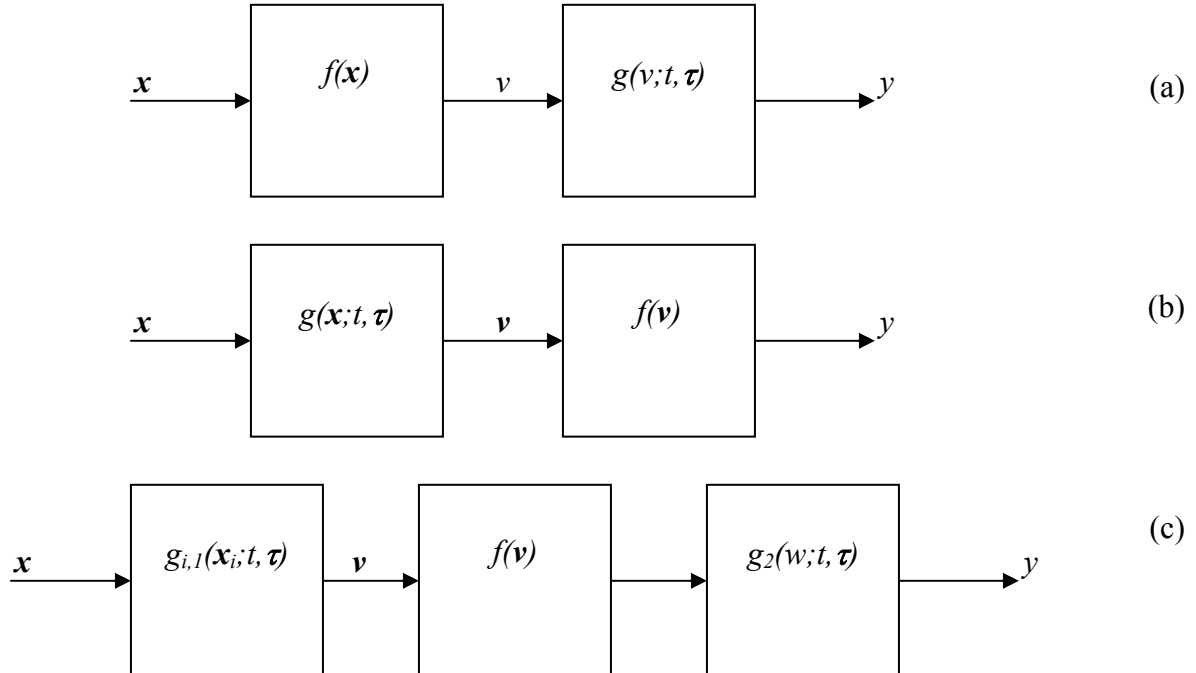


Figure 1: (a) Hammerstein block-oriented model structure; (b) Wiener block-oriented model structure; (c) LNL sandwich block-oriented model structure.

Closed-form solutions to the Hammerstein and Wiener processes have been proposed by Rollins et al. [21] and Bhandari and Rollins [22] for continuous-time modeling (CTM), and are called the H-BEST and W-BEST methodologies, respectively. A discrete-time modeling (DTM) method has also been developed by Rollins and Bhandari [23] that follows the CTM procedures for H-BEST and W-BEST. This work is an extension of the DTM method for the W-BEST methodology. This work also extends the developments of Rollins, et al. [24] in modeling diabetic subjects under free-living data collection to the modeling of real process data under freely existing conditions such as plant data. In addition, it applies the principles used by Rollins et al. [25] to address inputs that are serially correlated.

2.1.1. The Wiener model

This section presents the formulation for the proposed discrete-time W-BEST method. For a process such as that shown in Fig. 1(b), the general mathematical form is shown in Eqs. 1-2.

$$\begin{aligned} & a_{ij,n} \frac{d^n v_{ij}(t)}{dt^n} + a_{ij,n-1} \frac{d^{n-1} v_{ij}(t)}{dt^{n-1}} + \dots + a_{ij,1} \frac{dv_{ij}(t)}{dt} + v_{ij}(t) \\ & = b_{ij,m} \frac{d^m u_j(t)}{dt^m} + b_{ij,m-1} \frac{d^{m-1} u_j(t)}{dt^{m-1}} + \dots + b_{ij,1} \frac{du_j(t)}{dt} + u_j(t) \end{aligned} \quad (1)$$

$$\eta_i(t) = f_i(\mathbf{v}_i(t)) \quad (2)$$

where i refers to the output with $i=1, \dots, q$, j refers to the input with $j=1, \dots, p$, and $\mathbf{v}_i(t) = [v_{i1}, v_{i2}, \dots, v_{ip}]^T$.

Eq. 1 is written without dead time for simplicity, and there are no restrictions on the form of Eq. 2. These can be converted to a discrete-time form by using a backwards difference approximation, resulting in Eq. 3.

$$\begin{aligned} v_{ij,t} = & \delta_{ij,1}v_{ij,t-1} + \delta_{ij,2}v_{ij,t-2} + \cdots + \delta_{ij,n}v_{ij,t-n} \\ & + \omega_{ij,1}u_{j,t-1} + \omega_{ij,2}u_{j,t-2} + \cdots + \omega_{ij,m}u_{j,t-m} + \omega_{ij,m+1}u_{j,t-(m+1)} \end{aligned} \quad (3)$$

where the δ 's and ω 's are functions of the dynamic parameters (a's, and b's) in Eq. 1.

They are derived after the form of the linear dynamic block has been chosen by discretizing the differential equation, separating and collecting terms to get the form given by Eq. 3.

The predicted output, \hat{y} , is then described by

$$\hat{y}_{i\ell,t} = \hat{\eta}_{i,t} + \varepsilon_{i\ell,t} \quad (4)$$

under the assumption that

$$\varepsilon_{i\ell,t} \sim N(0, \sigma_i^2) \quad \forall \ell \quad (5)$$

Under the condition of white noise, this is referred to as Model 1 [25]. In the presence of serially correlated inputs, the output \hat{y} is given by

$$\hat{y}_t = \hat{\eta}_t + N_t \quad (6)$$

where

$$\begin{aligned} N_t &= \frac{\theta_q(B)}{\varphi_p(B)} a_t \quad \forall t, \\ \theta_q(B) &= 1 - \theta_1 B - \theta_2 B^2 - \cdots - \theta_q B^q, \\ \varphi_p(B) &= 1 - \phi_1 B - \phi_2 B^2 - \cdots - \phi_p B^p, \\ B^r x_t &= x_{t-r} \end{aligned} \quad (7)$$

Thus, the noise term N_t is ARMA(p,q). If we let

$$\frac{\varphi_p(B)}{\theta_q(B)} = \Phi(B) = 1 - \phi_1 B - \phi_2 B^2 - \cdots \quad (8)$$

then from Eqs. 7-8 we will get

$$\begin{aligned} \Phi(B)y_t &= \Phi(B)\eta_t + a_t \Rightarrow \\ y_t &= \eta_t + \phi_1(y_{t-1} - \eta_{t-1}) + \phi_2(y_{t-2} - \eta_{t-2}) + \cdots + a_t \end{aligned} \quad (9)$$

And this is now in the white noise form, and Eq. 6 (the estimate of the output) becomes

$$\hat{y}_t = \hat{\eta}_t + \phi_1(y_{t-1} - \hat{\eta}_{t-1}) + \phi_2(y_{t-2} - \hat{\eta}_{t-2}) + \dots \quad (10)$$

This is now referred to as Model 2 [25]. In practice, the number of terms in Eq. 10 is finite because ϕ_i dies out as i increases. Nonlinear least squares regression is used to determine the estimates of the δ 's, and ω 's in Eq. 3. Note that the structures of the Model 1 and Model 2 estimators (\hat{y}) are equivalent, but the coefficients will be different because the objective function for obtaining the SSE for each case is different. In the case of Model 1, the nonlinear least squares objective function is

$$SSE^{(1)} = \sum (y_{measured} - \hat{y})^2 \quad (11)$$

And in the case of Model 2, it is

$$SSE^{(2)} = \sum (y_{measured} - \hat{\eta})^2 \quad (12)$$

2.1.2. Procedure for Model-Building

The following is the procedure we developed for model building under freely existing data, and is a modification of the experimental design method in Rollins et al. [25]:

1. Select the dynamic model form for Eq. 1, and estimate the static and dynamic model parameters under Model 1. This is repeated until an acceptable model form is found.
2. Using the residuals from step 1, determine the ARMA (p,q) form of Eq. 7 and estimates of the θ_p and ϕ_q parameters.
3. Simultaneously refit the dynamic, ultimate response, and ARMA parameters under Model 2 if necessary.
4. Check the residuals in step 3 for compliance to white noise

The form of the ARMA (p,q) model is found using the autocorrelation function (ACF) and partial autocorrelation function (PACF). Box and Jenkins [26] gives more complete information on how to use these to find the form and initial estimates of the

parameters p and q . Note that in Rollins et al. [25], statistical design of experiments (SDOE) was used to determine input changes to the process. In this case, we will be using historical plant data so no additional experiments need to be determined.

2.2. Feedforward Control Methodology

2.2.1. General Feedforward Controller Methods

Feedforward control has been used in many industrial applications since the 1960s, including boilers, evaporators, dryers, waste neutralization plants and distillation processes. The basic concept was applied as early as 1925 in level control systems for boiler drums [1].

The concept of feedforward control allows for theoretically perfect control of a process system. By measuring the disturbances (loads) of a process and modeling how these disturbances affect the process outputs, corrective action can be taken before the process outputs deviate from their desired values [1]. However, because there are many process disturbances that cannot be measured in a timely or efficient manner, feedforward control is typically used in conjunction with standard feedback control, which compensates for any deviation of the output variable from its setpoint, regardless of what caused the deviation.

A typical feedforward/feedback control block diagram is shown in Fig. 2 . The feedforward controller, G_f , is generally approximated by a linear model [27], but nonlinear process models can also be used [28, 29]. The model is found by determining how the process output responds to a given input disturbance. By ignoring interactive behavior, a different G_f is typically found independently for each disturbance that is implemented into the feedforward control scheme [1], as shown in Fig. 2.

In order for the feedforward/feedback controller to provide perfect control of the output variable Y , we must first find the closed-loop response to an arbitrary change in the disturbance variable X_i . The result is given by Eq. 13.

$$\frac{Y(s)}{X_i(s)} = \frac{G_{Li} + G_{fi}G_vG_p}{1 + G_cG_vG_pG_m} \quad (13)$$

In the case of perfect control, Eq. 13 is set equal to zero and can be solved for G_f , the feedforward controller, as follows:

$$\frac{Y(s)}{X_i(s)} = 0 = \frac{G_{Li} + G_{fi}G_vG_p}{1 + G_cG_vG_pG_m} \quad (14)$$

$$G_{fi} = \frac{-G_{Li}}{G_vG_p} \quad (15)$$

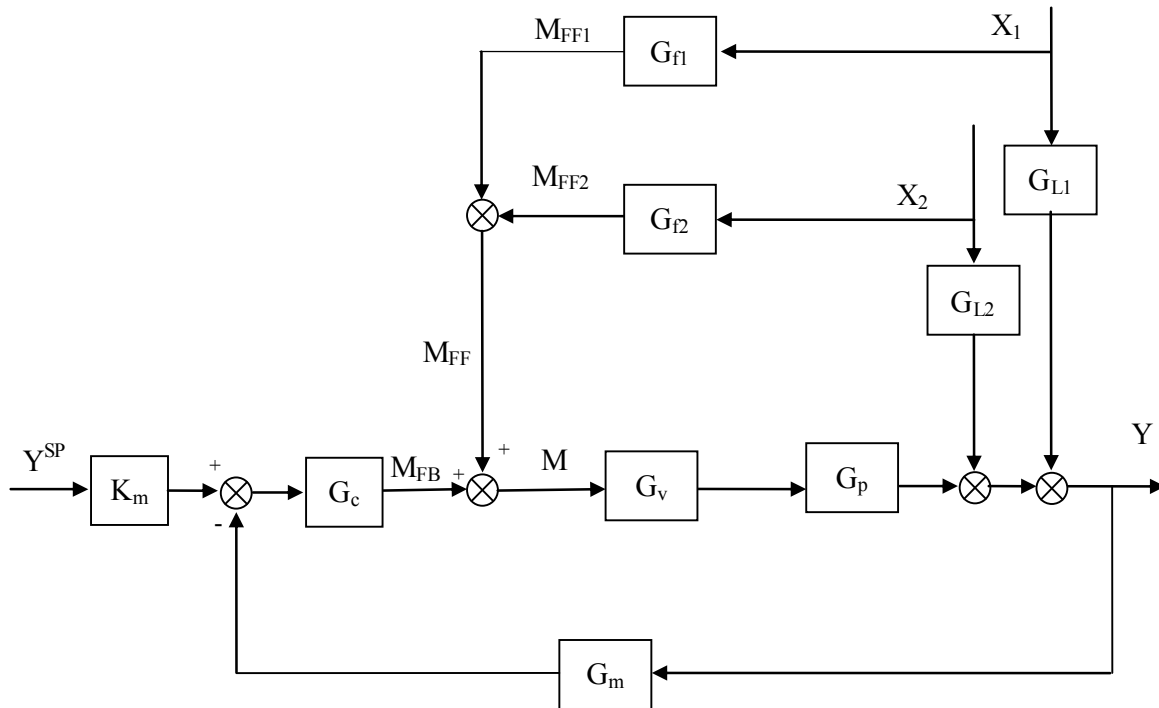


Figure 2: A typical feedforward/feedback control block diagram, with two disturbance variables on feedforward control.

Ideal feedforward controllers are physically unrealizable if G_p has a longer dead time than G_{Li} or if G_p is a higher-order transfer function than G_{Li} . In these cases, the feedforward controller is often approximated by a lead-lag unit [1]. We will discuss how this problem is addressed with the feedforward controller of the proposed approach in the next section.

2.2.2. Proposed Feedforward Controller Methodology

The block diagram for the feedforward/feedback controller under Wiener modeling is shown in Fig. 3. The first step in implementing this version of feedforward control is to identify the model parameters for the process being studied. Once the model has been identified, the feedforward controller is designed.

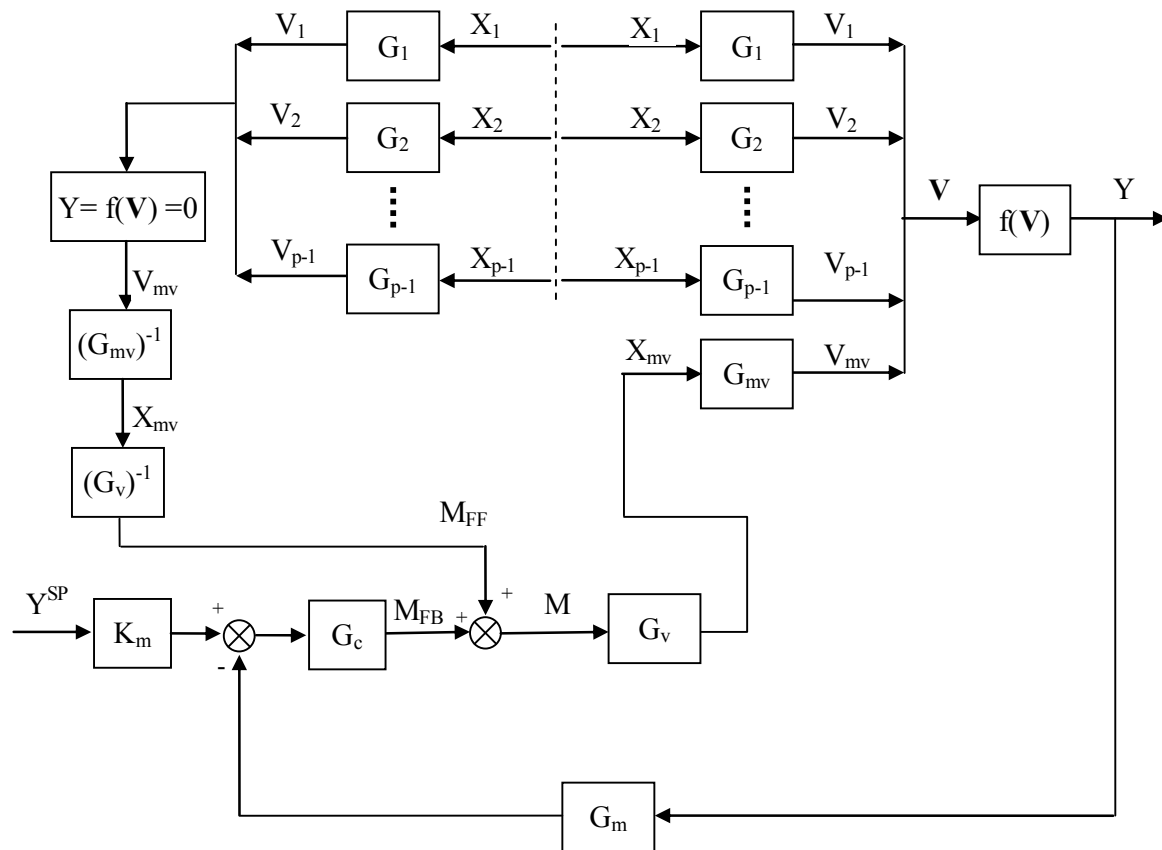


Figure 3: The proposed feedforward/feedback controller under Wiener modeling. The X_i 's represent the input variables, Y represents the controlled variable, M represents the controller signal.

As in the case of the traditional feedforward controller, we can find the closed-loop output response to a change in the input disturbance X_i . Note that all variables are given in terms of deviation from an initial steady state.

For any and all $X_i \neq 0$, $v_i \neq 0$. The change in M_{FF} required for $Y = f(\mathbf{v}) = 0$ is determined as follows.

$$f(\mathbf{v}) = a_0 + a_1 v_1 + a_2 v_2 + a_{1,mv} v_{mv} + \dots + a_j v_1^2 + \dots + a_{2,mv} v_{mv}^2 + a_k v_1 v_2 + \dots + a_{i,mv} v_i v_{mv} + \dots \quad (16a)$$

Rearranging Eq. 16a gives

$$f(\mathbf{v}) = a v_{mv}^2 + b v_{mv} + c \quad (16b)$$

where

$$\begin{aligned} a &= a_{2,mv} \\ b &= a_{1,mv} v_1 + a_{2,mv} v_2 + \dots + a_{i,mv} v_i \\ c &= a_0 + a_1 v_1 + a_2 v_2 + \dots \end{aligned}$$

Therefore, v_{mv} can be determined using the quadratic equation. As shown by Fig. 3, after determining v_{mv} , M_{FF} , the feedforward control law, is determined by

$$M_{FF} = G_{mv}^{-1} G_v^{-1} v_{mv} \quad (17)$$

which gives $y = 0$ for changes in the measurable loads shown in Fig. 3 as required. In the case where $G_{mv}^{-1} G_v^{-1}$ is physically unrealizable, an approximation will be used that takes on a form much like a derivative filter in an ideal PID controller. For example, if

$$G(s) = G_{mv} G_v = \frac{v_{mv}}{M_{FF}} = \frac{K}{\tau s + 1} \quad (18)$$

then the approximation takes on the form of

$$G^{-1}(s) = \frac{M_{FF}}{v_{mv}} = \frac{\tau s + 1}{K(\phi s + 1)} \quad (19)$$

3. The Distillation Process

The distillation process used was a pilot-scale methanol/water distillation column consisting of 12 trays, with an inside diameter of 6 inches. Feed was introduced at Tray 4 and had a concentration of 15% (mol) methanol. A process instrumentation diagram of the column is shown in Fig. 4. The column is connected to a DeltaV distributed control system from Emerson Process Management.

3.1. Open-Loop Model Building

3.1.1. Training Phase

In order to first determine the feasibility of developing a Wiener model under highly correlated inputs for the distillation process, training and test data were collected in the open-loop mode. The input variables chosen for the experimental tests that were conducted included feed flow rate, feed temperature set point, reboiler level and reboiler steam pressure. Other variables that were measured on-line and used as input variables included reflux flow rate, column pressure, bottoms product flow rate, distillate product flow rate and overhead condensate temperature. The output response of the process was the top tray (Tray 12) temperature, which was also measured on-line.

An experimental design was chosen for three levels of the first four input variables, using a Box-Behnken statistical design (see [32]), with the feed flow rate and feed temperature set point having a correlation coefficient of 0.94. This was done to give the effect of highly correlated inputs to demonstrate effective modeling of the proposed approach

under conditions typical of plant data. The input changes used for the training of the model are shown in Figs. 5-9.

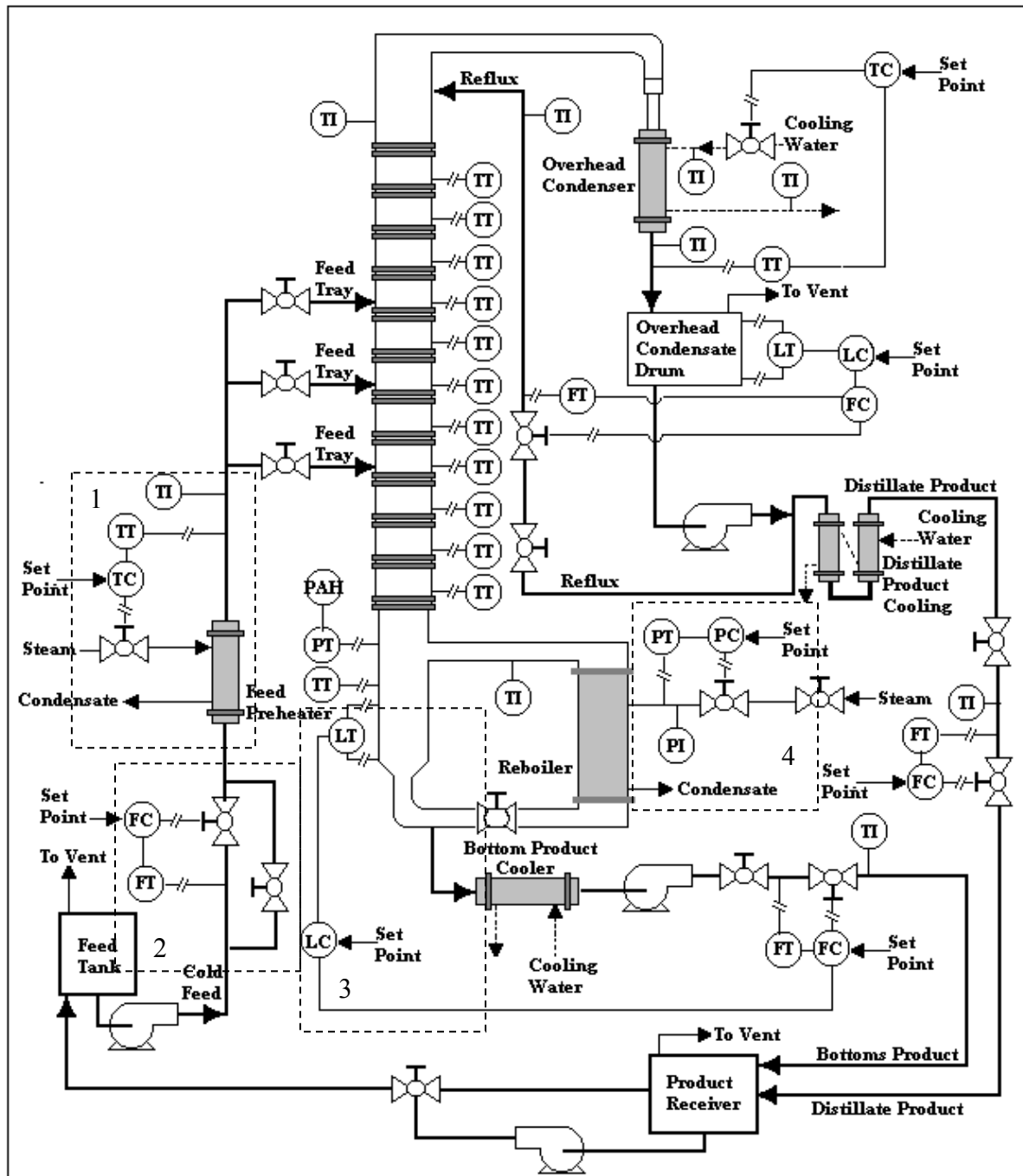


Figure 4: Process instrumentation diagram of the distillation process used for the experimental tests [30]. The column is connected to a DeltaV control system from Emerson Process Management. The dashed boxes indicate the four input variables that were deliberately changed. (1-feed temperature, 2-feed flow, 3-reboiler level, 4-steam pressure)

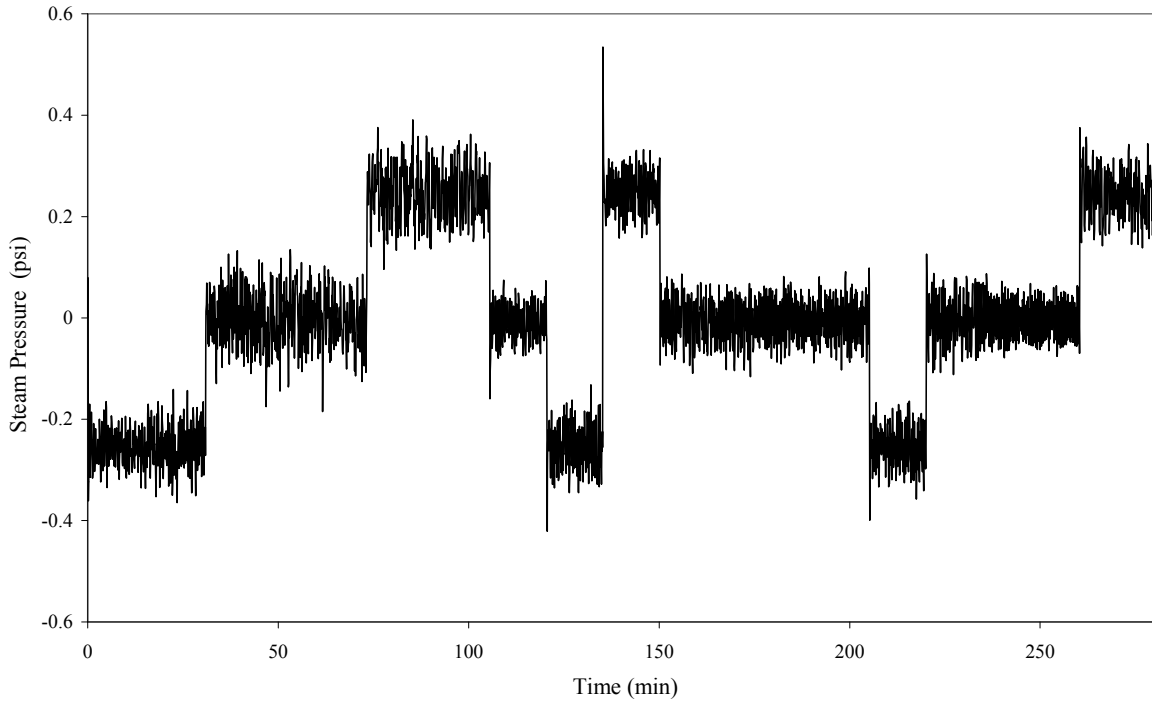


Figure 5: The input changes in steam pressure that occurred during the open-loop model identification. The changes are in terms of deviation variables.

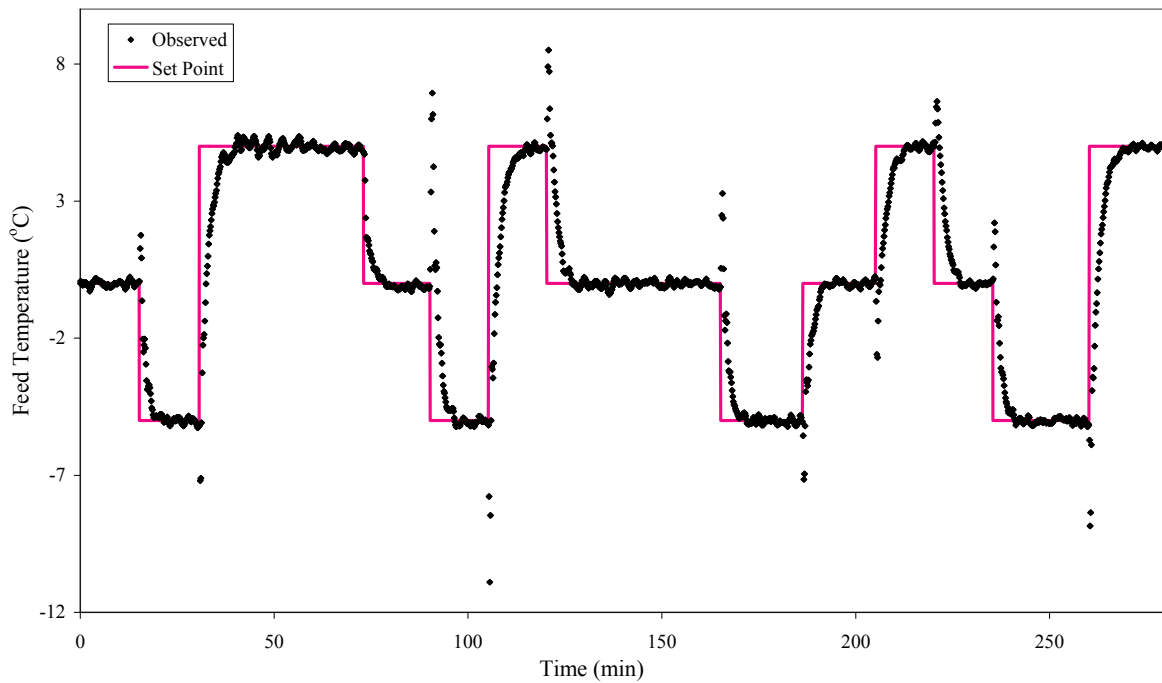


Figure 6: The feed temperature set point input changes that occurred during the open-loop model identification. The changes are in terms of deviation variables.

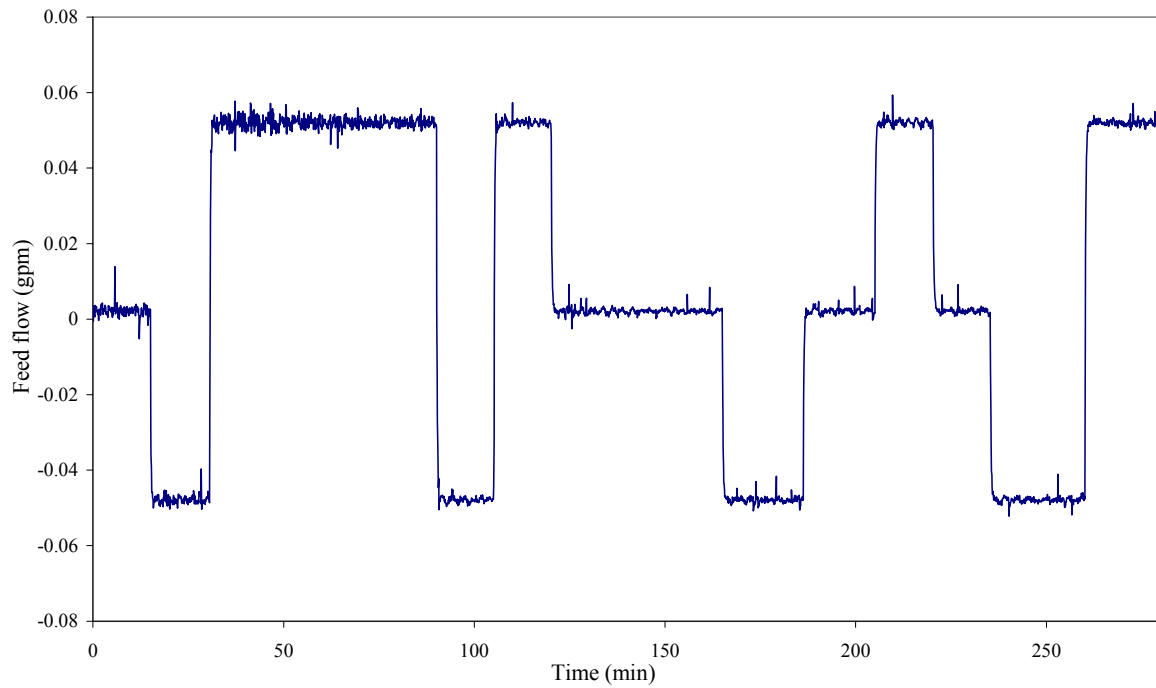


Figure 7: The feed flow input changes that occurred during the open-loop model identification. The changes are in terms of deviation variables.

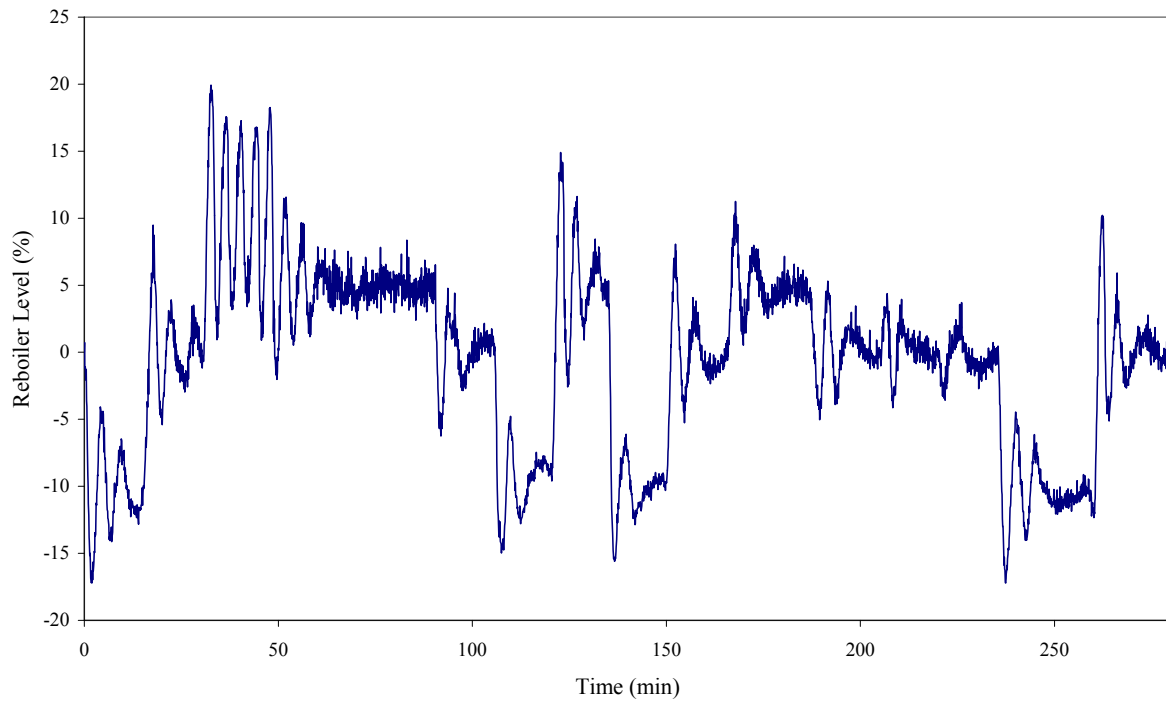


Figure 8: The reboiler level input changes that occurred during the open-loop model identification. The changes are in terms of deviation variables.

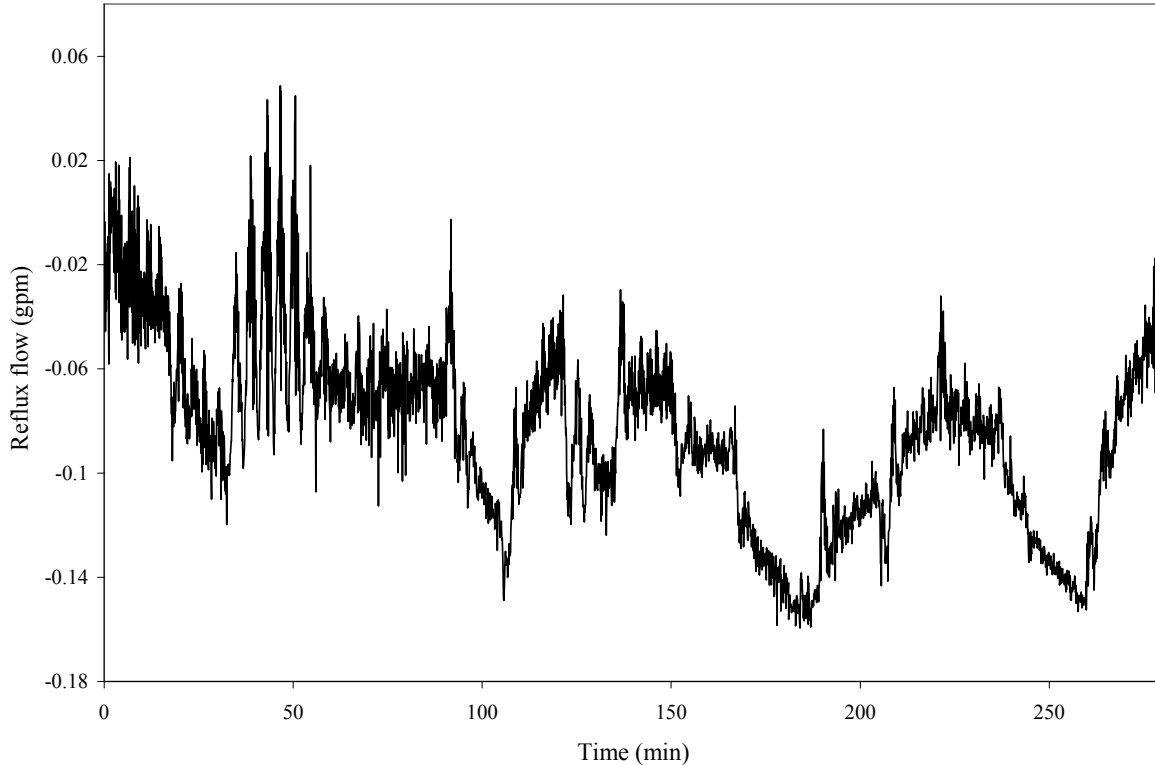


Figure 9: The reflux flow rate input changes that occurred during the open-loop model identification. The changes are in terms of deviation variables.

Note that in Fig. 6 the feed temperature set point was the input variable, but the feed temperature displays significant dynamic response to the set point changes and also to the feed flow changes. Because of this, we included dynamics on the feed temperature set point which relate the observed feed temperature with the feed temperature set point and feed flow changes. The other input changes displayed very little dynamic response to set point changes, so the measured values of those input variables were used directly in the model building process. The block diagram for the open-loop process is shown in Fig. 10.

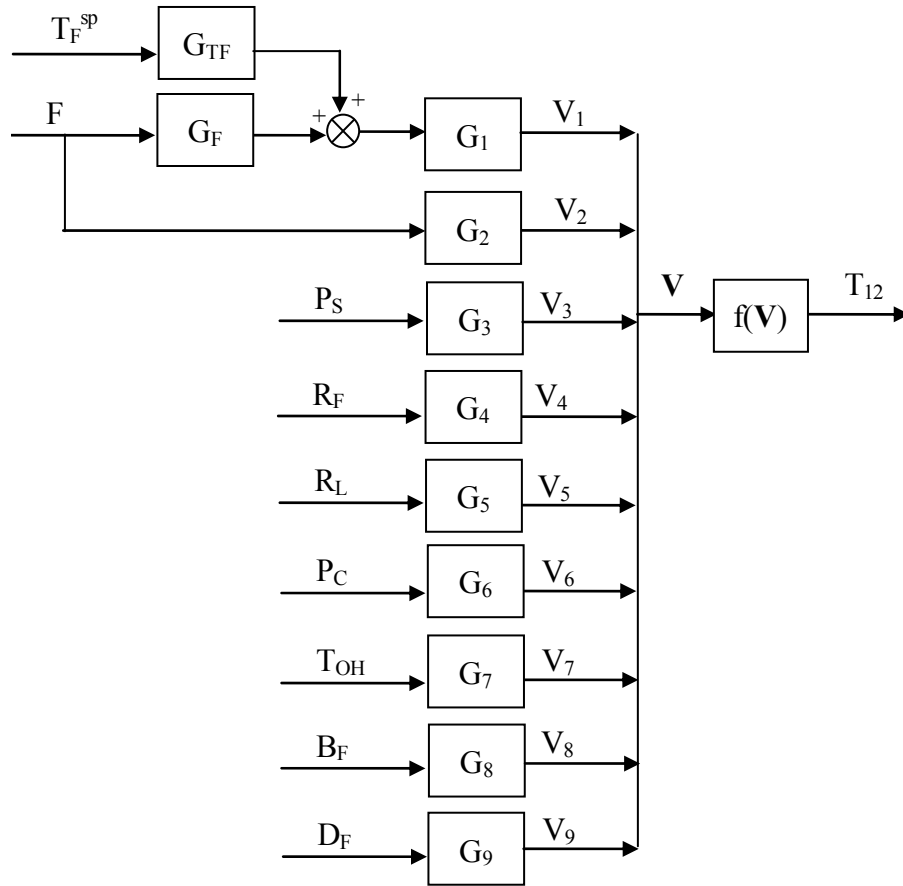


Figure 10: The block diagram for the open-loop distillation process. T_{12} is the Tray 12 temperature, T_F^{set} is the feed temperature set point, F is the feed flow rate, R_L is the reboiler level, R_F is the reflux flow rate, P_s is the steam pressure, P_C is the column pressure, D_F is the distillate flow rate, B_F is the bottoms flow rate and T_{OH} is the overhead condensate temperature.

Using the procedures listed in Section 2 above, the dynamic blocks were chosen to be second-order-plus-lead forms. That is, in the Laplace domain, all the dynamic blocks have the form

$$G_i(s) = \frac{V_i(s)}{X_i(s)} = \frac{\tau_{ai}s + 1}{\tau_i^2 s^2 + 2\tau_i\zeta_i s + 1} \quad (20)$$

where $i=1, \dots, p$, p is the number of inputs, τ_{ai} is the lead (or zero) parameter, τ_i is the time constant and ζ_i is the damping coefficient. For the static nonlinear block, we used a second-order regression model that included interactions between the inputs, given by

$$y(t) = a_0 + a_1 v_1(t) + \dots + a_p v_p(t) + b_1 v_1^2(t) + \dots + b_p v_p^2(t) + c_{1,2} v_1(t) v_2(t) + \dots + c_{p-1,p} v_{p-1}(t) v_p(t) \quad (21)$$

All of the variables represent deviations from an initial steady state. In order for the system to be dynamically stable and physically meaningful, the parameters are restricted to $\tau_i > 0$ and $\zeta_i > 0$. It should be noted that the use of the discrete-time model equations given by Equations 4 and 5 allow for the linear dynamics to vary between underdamped (i.e., $0 < \zeta_i < 1$) and overdamped behavior (i.e., $\zeta_i > 1$) during the optimization process to estimate the parameters [24]. It should also be noted that parameter estimation for the training phase of the open-loop model identification was done under Model 1.

Given the model form chosen, the differential equation representing the linear dynamic blocks is of the form

$$\tau_i^2 \frac{d^2 v_i(t)}{dt^2} + 2\tau_i \zeta_i \frac{dv_i(t)}{dt} + v_i(t) = \tau_{ai} \frac{dx_i(t)}{dt} + x_i(t) \quad (22)$$

This results in a discrete-time solution for $v_i(t) = v_{i,t}$ at sampling time t of

$$v_{i,t} = \delta_{1,i} v_{i,t-1} + \delta_{2,i} v_{i,t-2} + \omega_{1,i} x_{i,t-1} + \omega_{2,i} x_{i,t-2} \quad (23)$$

where $\omega_{2,i} = 1 - \delta_{1,i} - \delta_{2,i} - \omega_{1,i}$ in order to satisfy the requirement of unity gain, and

$$\begin{aligned}
\delta_{1,i} &= \frac{2(\tau - \tau_a \Delta t)}{\tau} \\
\delta_{2,i} &= \frac{2\tau\zeta\Delta t - \tau^2 - \Delta t^2}{\tau^2} \\
\omega_{1,i} &= \frac{\tau_a \Delta t}{\tau^2} \\
\omega_{2,i} &= \frac{\Delta t^2 - \tau_a \Delta t}{\tau^2}
\end{aligned} \tag{24}$$

where Δt is the sampling interval. For a complete overview of how to do derive these parameters from Eq. 25, see Rollins et al. [24]. The optimization routine changed the parameters τ_i , τ_{ai} and ζ_i under the constraints for dynamic stability given above, calculated the dynamic discrete-time parameters using Eq. 24, determined the values for $v_{i,t}$ using Eq. 23, and finally, computed the predicted value of the output, \hat{y}_t using Eq. 21.

The fitted model parameters from the open-loop model identification process are shown in Table 1. The fit of the feed temperature based upon feed temperature set point and feed flow rate changes are shown in Fig. 10, and the output response (Tray 12 temperature) to the input changes made during the model identification process are shown in Fig. 11.

Table 1: Fitted model parameters from the open-loop model identification process.

Input Parameter (i)	τ_i	ζ_i	τ_{ai}
Steam Pressure	1.396978	2.820889	-3.03288
Feed Temperature	4.58391	5.402179	-0.67471
Feed Flow Rate	0.165333	2.157524	1.274657
Reflux Flow Rate	4.377505	1.399567	-0.70564
Reboiler Level	1.572078	3.431548	0.743615
Column Pressure	0.02197	1.192745	-0.01899
Overhead Temperature	3.11355	2.491256	0.683125
Bottoms Flow Rate	2.425401	1.497818	0.71684
Distillate Flow Rate	0.99697	1.998645	0.000325

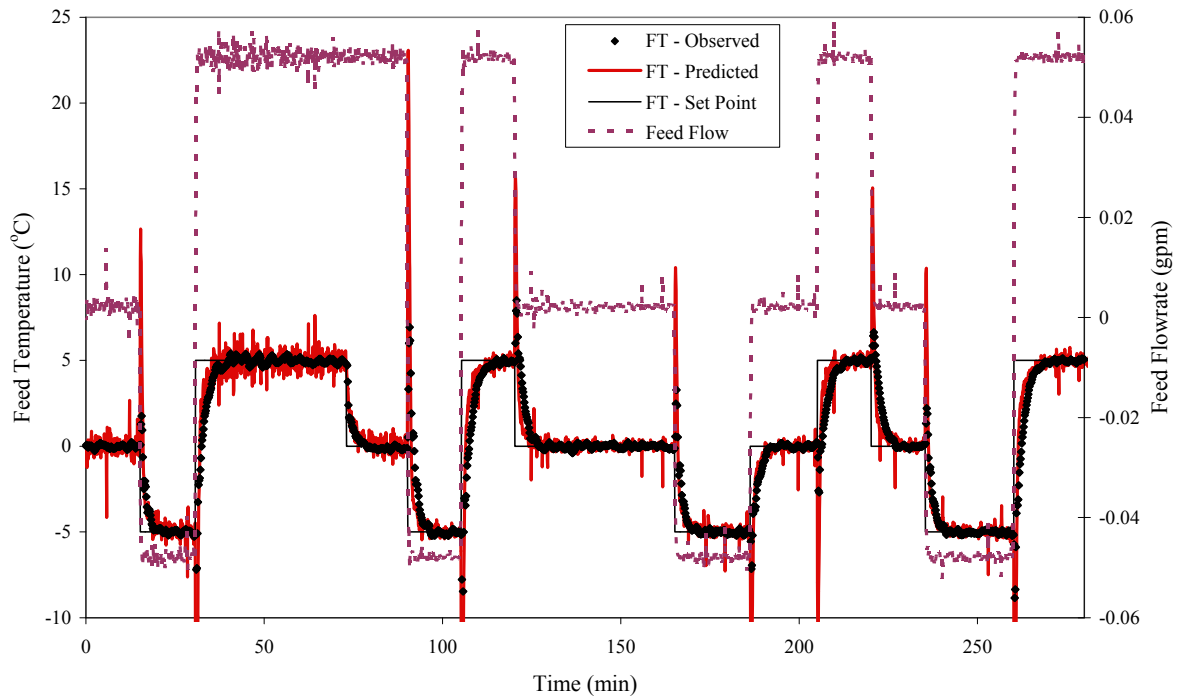


Figure 10: The feed temperature input changes made during the open-loop model identification process. The feed flow rate and feed temperature setpoint inputs are used to fit a model to represent the observed feed temperature.

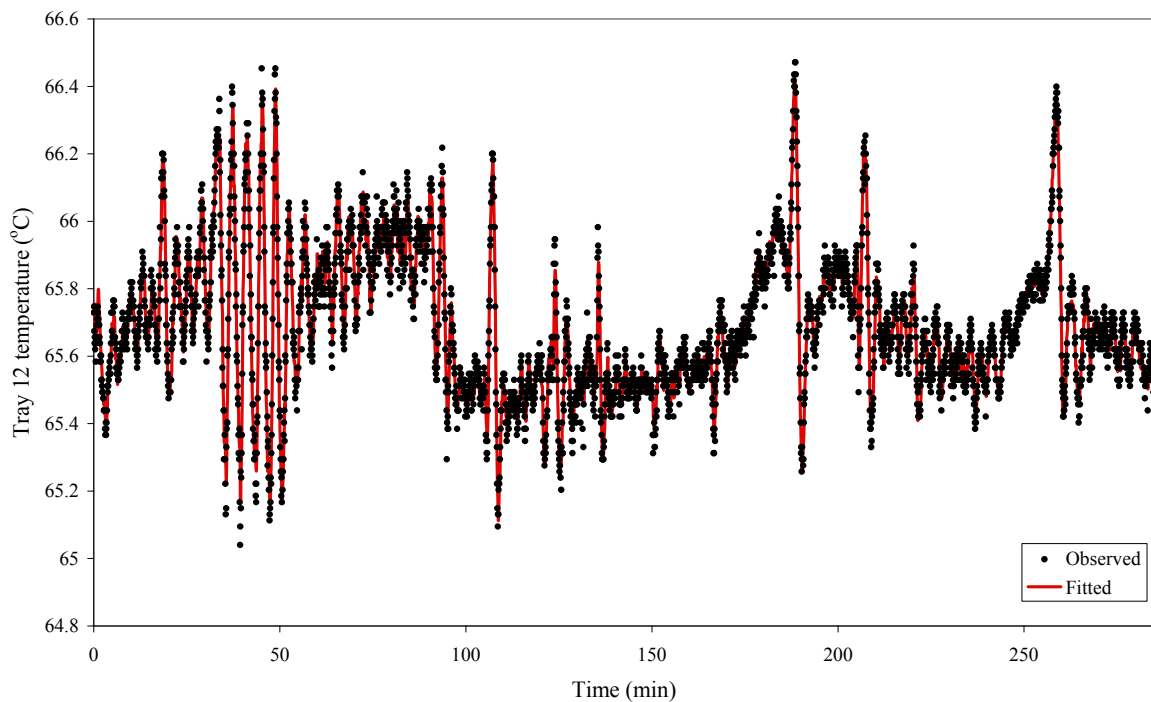


Figure 11a: The observed top tray temperature response and fitted (Model 1) response to the input changes made during training for the open-loop model identification process.

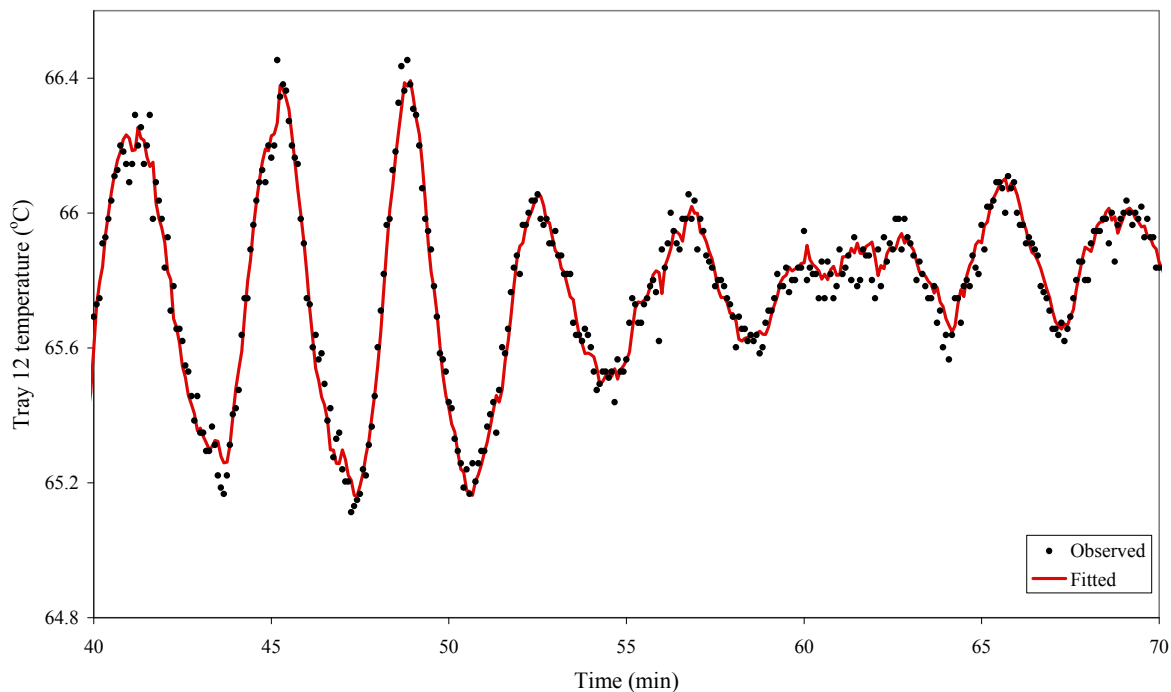


Figure 11b: A close-up look at Fig. 11a with time ranging from 40-70 minutes.

3.1.2. Testing Phase

In order to test the model that was built during the training phase, another series of input changes was made to the distillation process. In this case, a Box-Behnken design with four factors and three center points was run, but this time the correlation between the feed flow rate and feed temperature set point was zero. This was done to demonstrate that the model built under high correlation was able to determine accurate cause-and-effect behavior between the input and output variables. As in the training phase, only four inputs were deliberately changed, but an additional five inputs were measured on-line and used in the prediction of the output response. The input sequence used for the testing phase is shown in Fig. 12.

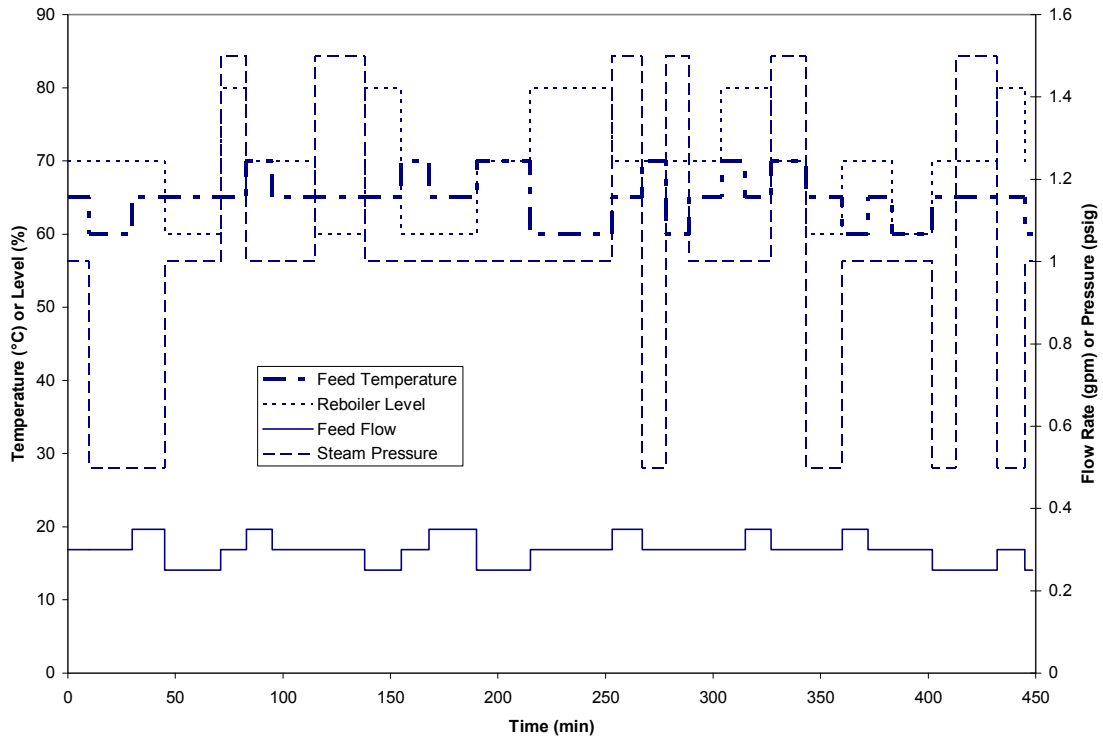


Figure 12: The input changes made during the testing phase of the open-loop model identification process.

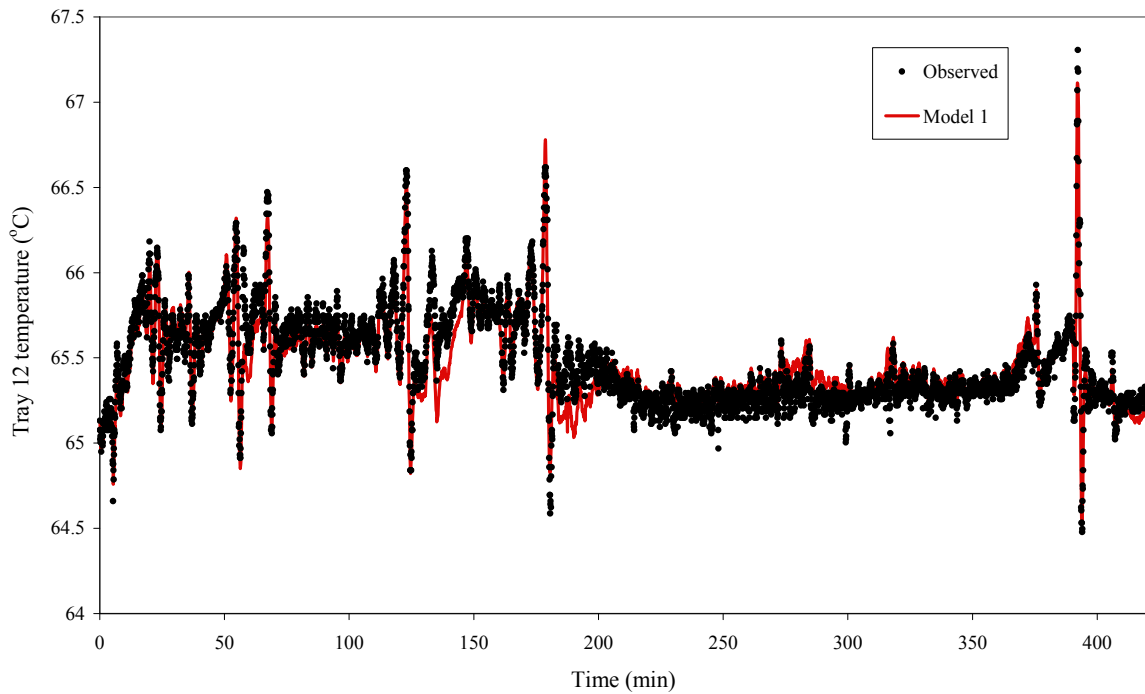


Figure 13a: The observed and predicted values of the Tray 12 temperature under Model 1 during the testing phase of the open-loop model identification process.

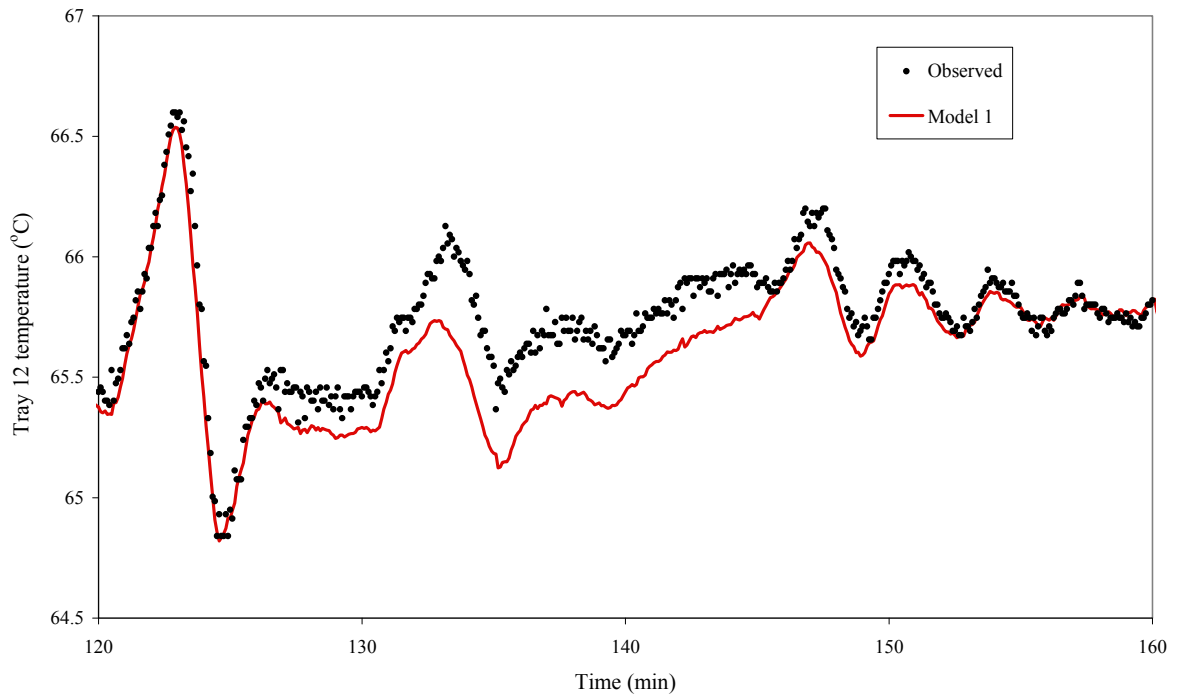


Figure 13b: Close-up look at the observed and predicted values of the Tray 12 temperature under Model 1 during the testing phase for time ranging from 120-160 min

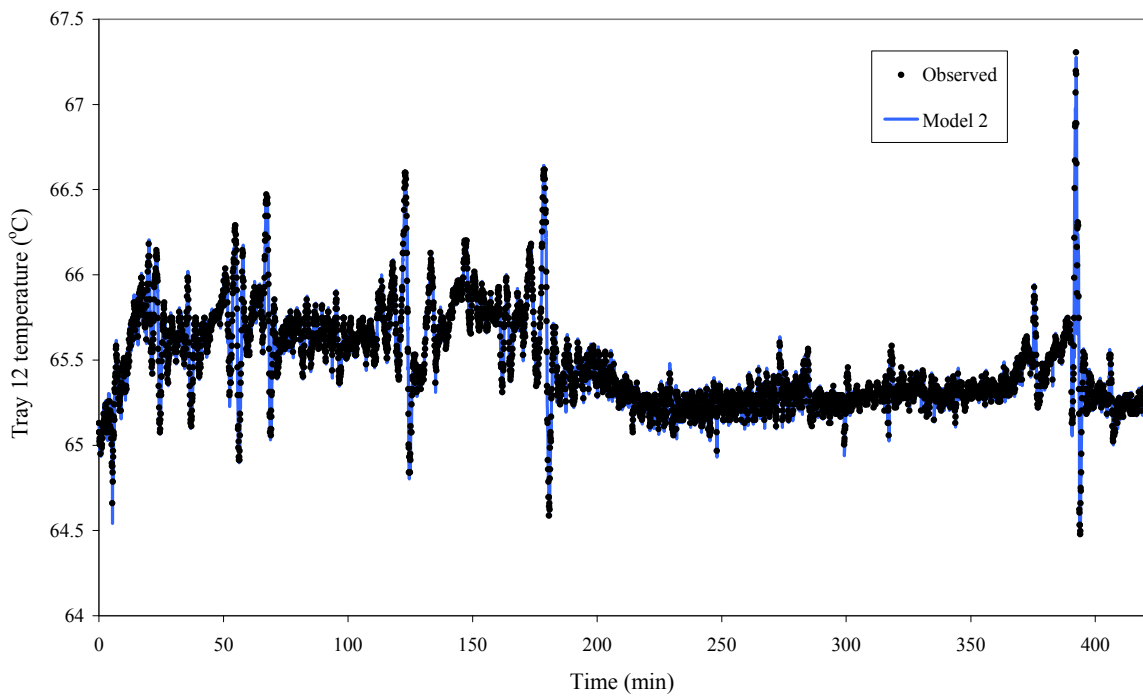


Figure 14a: The observed and predicted values of the Tray 12 temperature under Model 2 during the testing phase of the open-loop model identification process.

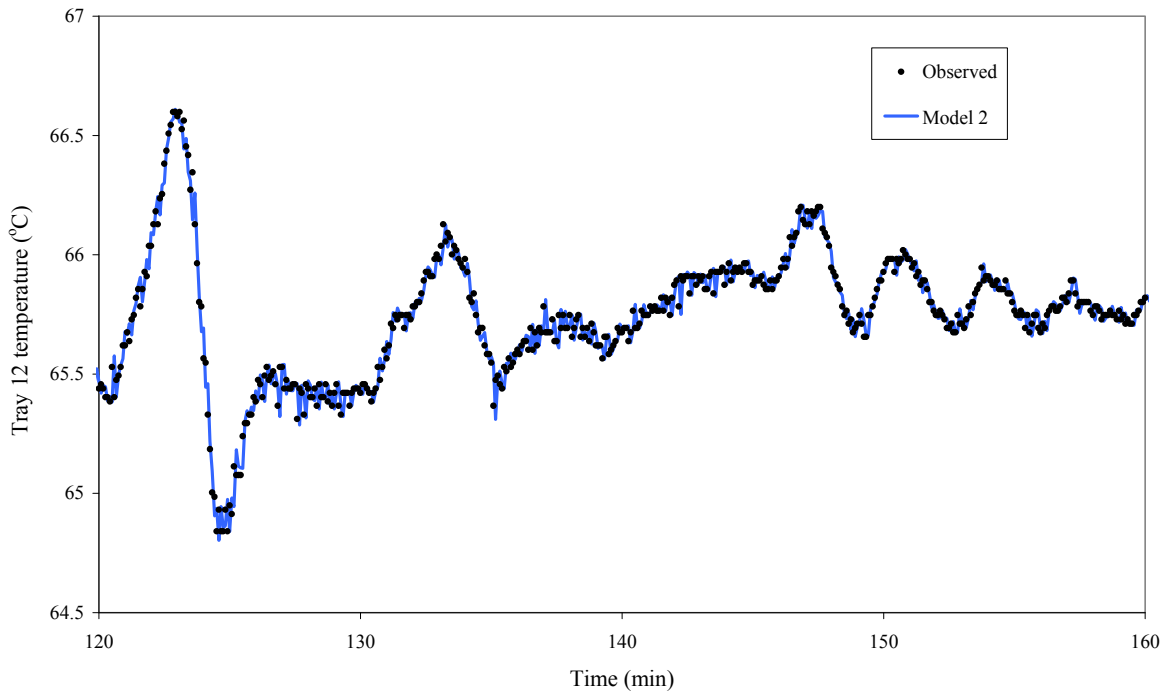


Figure 14b: Close-up look at the observed and predicted values of the Tray 12 temperature under Model 2 during the testing phase for time ranging from 120-160 min.

Under Model 1, the testing phase of the model identification process in open-loop showed that there was some small but observable bias between the predicted and observed values of the output variable. This can be seen in Fig. 13b. As a result, Model 2 was implemented and the fit of the predicted values was much better, and is shown in Fig. 14b. Quantitatively, this can be summarized by the coefficient of determination, defined as $r^2 = 1 - (SSE / SST)$. For Model 1, $r^2 = 0.832$ and for Model 2, $r^2 = 0.965$. Therefore, Model 2 was chosen for the closed-loop model building process.

3.2. Closed-Loop Feedback Control and Model Building

A standard proportional-integral (PI) feedback controller was implemented using the DeltaV software connected to the distillation column. The controlled variable was the Tray 12 temperature, and the manipulated variable that we chose was the reflux flow rate. Tuning

parameters for the PI controller were found using the “DeltaV Tune” feature built in to the control system. This feature made small changes to the reflux flow valve, determined the process dynamics, and provided suggested values for the tuning parameters based upon Ziegler-Nichols estimations [31, 1].

Given that we were able to accurately model the column behavior with large cross-correlations in open-loop mode, we felt confident in our ability to develop a model under closed-loop control. For the closed-loop model identification, the input series was the same as that used during the training phase of the open-loop model building. The model parameters that were identified are given in Table 2, and the process response to the input changes is shown in Fig. 15. This model was developed from data collected from the column on March 18, 2008. Once again, the model identified is able to accurately predict the output behavior, and this is seen in Fig. 15.

Table 2: Model parameters identified during the closed-loop model identification process.

Input Parameter (i)	τ_i	ζ_i	τ_{ai}
Steam Pressure	1.056943	0.546046	-1.05117
Feed Temperature	3.0194371	2.7537438	-1.0203227
Feed Flow Rate	0.593302	0.07315	0.616065
Reflux Flow Rate	0	0	0
Reboiler Level	1.364168	0.409419	0.196817
Column Pressure	0.365075	2.643698	-4.66672
Overhead Temperature	1.685189	0.700723	0.887374
Bottoms Flow Rate	1553132	0.365697	0.553574
Distillate Flow Rate	1.986547	0.844026	-1.07884

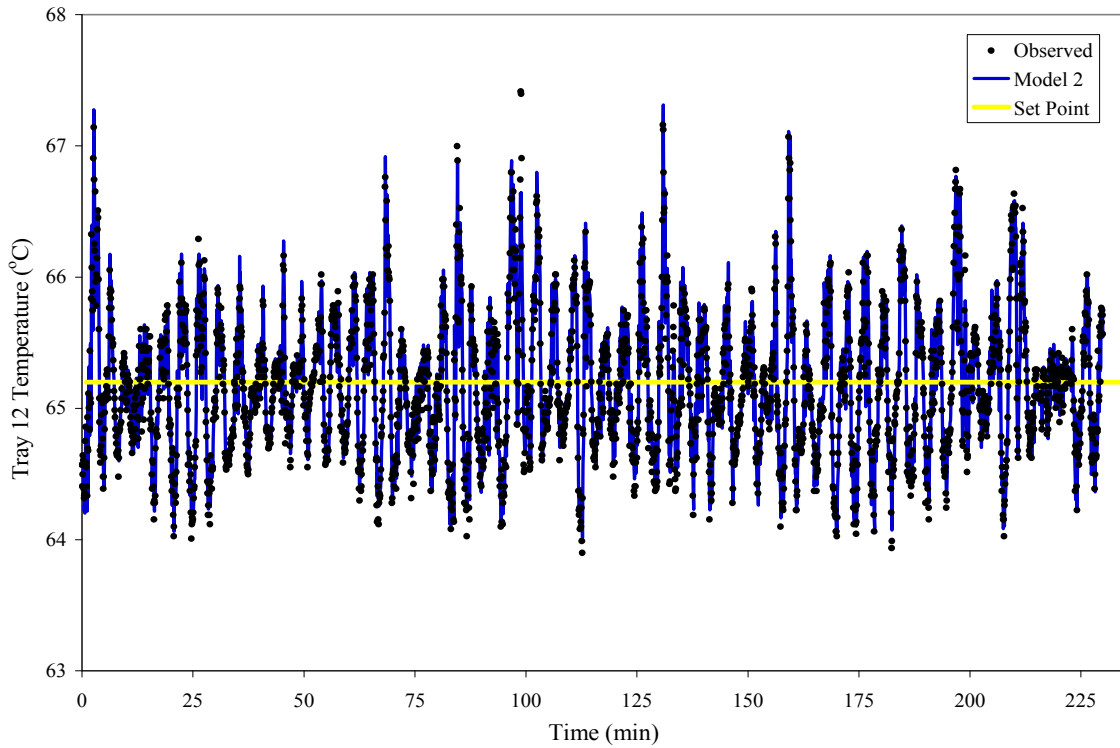


Figure 15a: The observed and predicted values of the Tray 12 temperature under Model 2 during the training phase of closed-loop model identification on March 18, 2008.

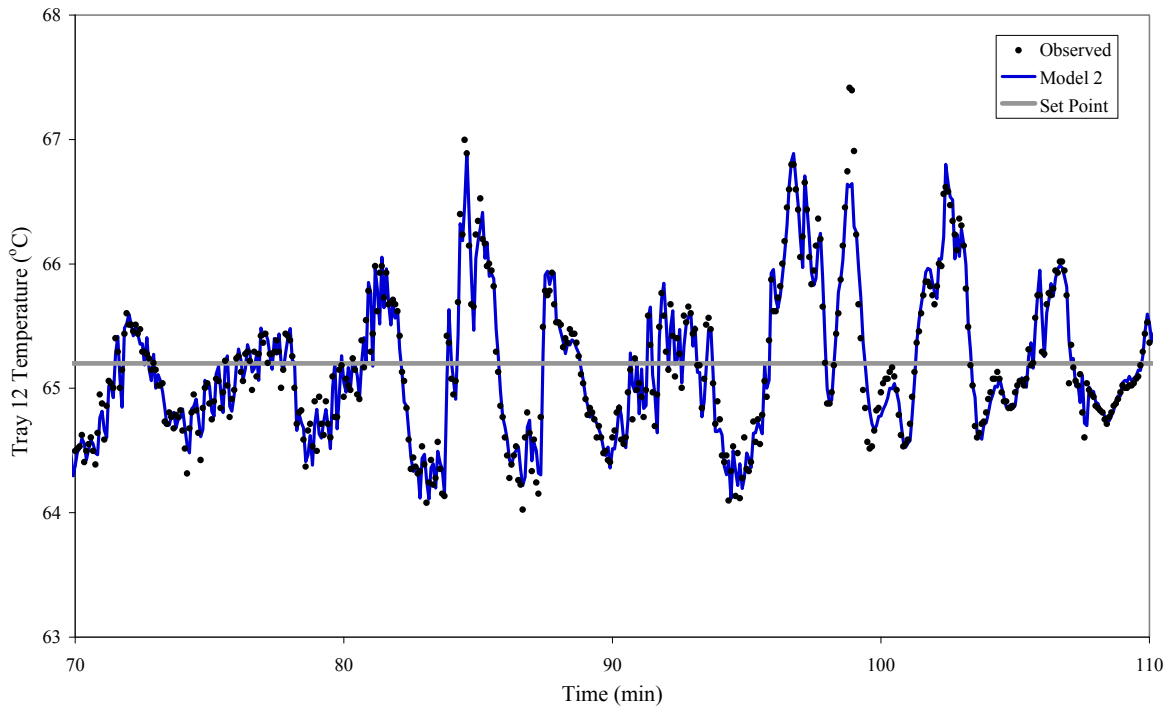


Figure 15b: The observed and predicted values of the Tray 12 temperature under Model 2 during the training phase of closed-loop model identification for time between 70-110 min.

To evaluate this model, test data collected on March 8, 2008 were used. As shown in Fig. 16, even though there are 10 days separating these runs, the agreement is excellent, verifying that the model can hold up over time, despite the fact that the distillation column is shut down in between runs.

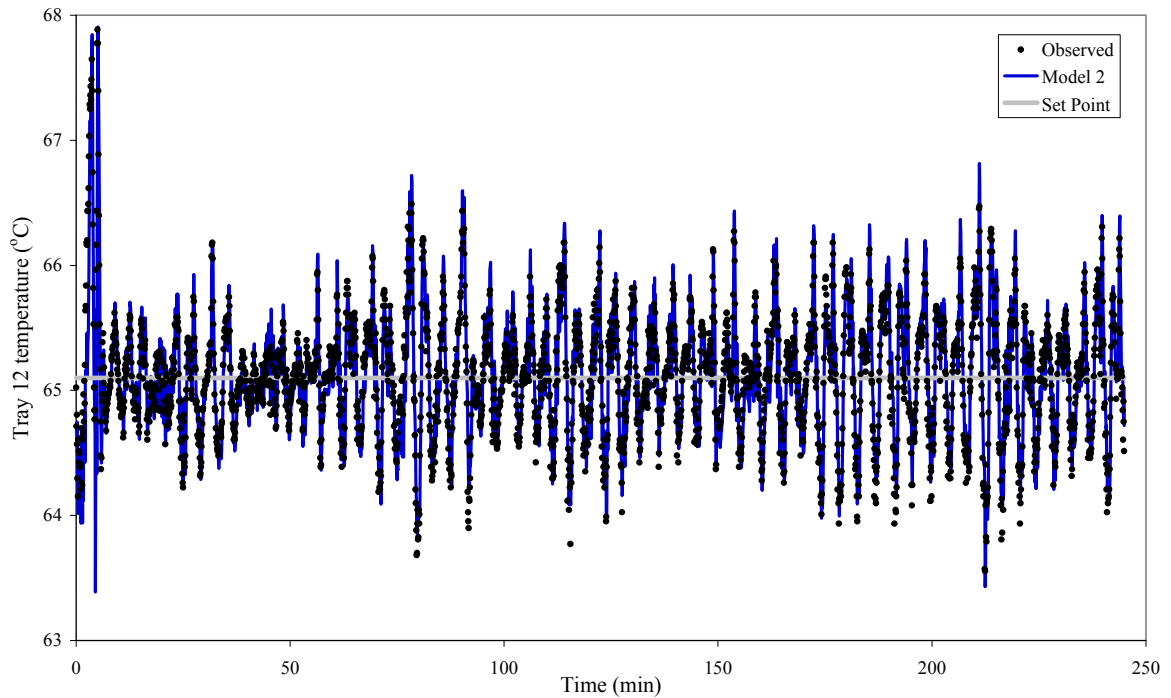


Figure 16a: The observed and predicted values of the Tray 12 temperature under Model 2. This data was collected from the tests run on March 8, 2008.

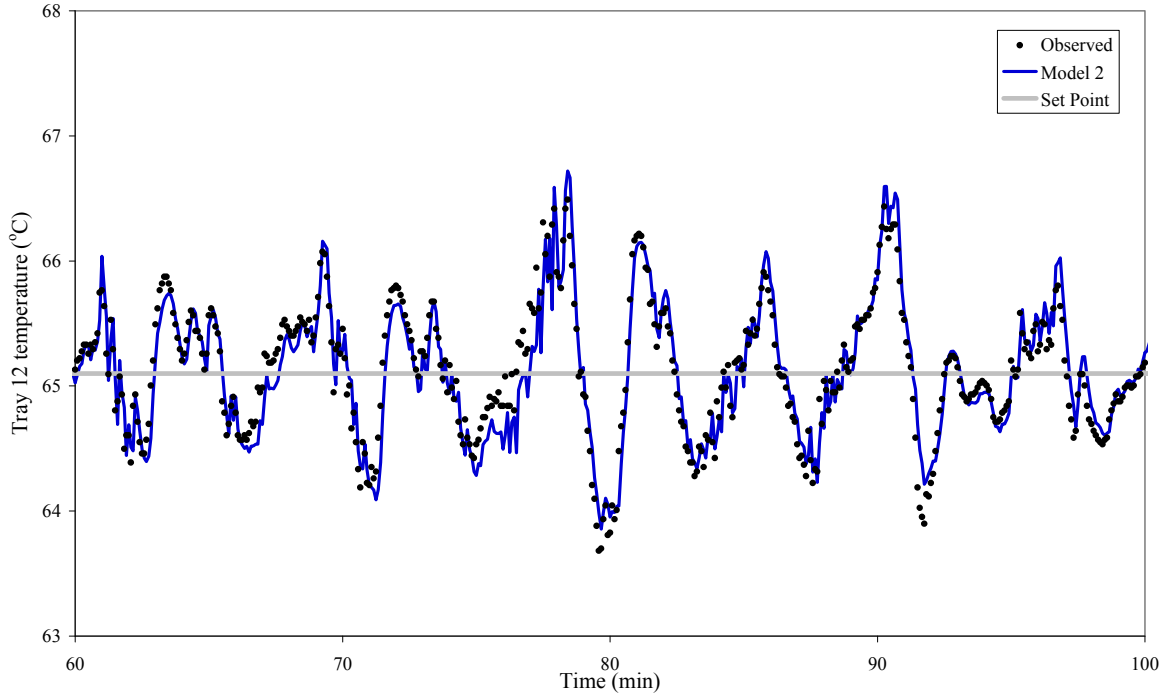


Figure 16b: The observed and predicted values of the Tray 12 temperature under Model 2 for time between 60-100 min. This data was collected from the test run on March 8, 2008.

3.3. Implementation of the proposed feedforward/feedback control scheme

The controller parameters (gain, reset) for the PI controller were not changed when the feedforward controller was implemented, for the sake of demonstrating the effect of the feedforward controller on the process output. The feedforward controller was implemented using Eqs. 21-22 above.

For this particular case, the reflux flow rate had virtually no dynamics associated with it. Because of this, the linear dynamic function G_{mv}^{-1} is essentially equal to unity, and

$$v_{mv} \approx x_{mv} \quad (25)$$

In addition, the valve dynamic function in this case is a simple static nonlinear function given by

$$out\% = ax_{mv}^2 + bx_{mv} + c \quad (26)$$

where $out\%$ represents the position of the control valve (0 = fully closed, 100 = fully open) and x_{mv} is the desired value of the reflux flow rate, as determined by the feedforward controller. In cases where the manipulated variable has significant process dynamics, the implementation of the feedforward controller will become slightly more complex.

3.4. PI controller vs. FFPI controller process responses

The feedforward/feedback controller that we developed was tested and compared to the feedback controller alone. The column was tested first under regulatory control, where all inputs only varied as a result of normal process operations. In this case, by turning the feedforward part of the controller on, a significant reduction in process variability was observed. This is shown in Fig. 17. To test the feedforward/feedback controller under more extreme conditions, a series of three input changes was made to the process with the feedforward controller active, and this input sequence can be seen in Fig. 18. After the three changes were made, the feedforward controller was turned off and the system was allowed to reach steady state before introducing the same three input changes again. Fig. 19 shows the response of the tray 12 temperature in both feedforward/feedback and feedback only control to the input changes that were made under these conditions.

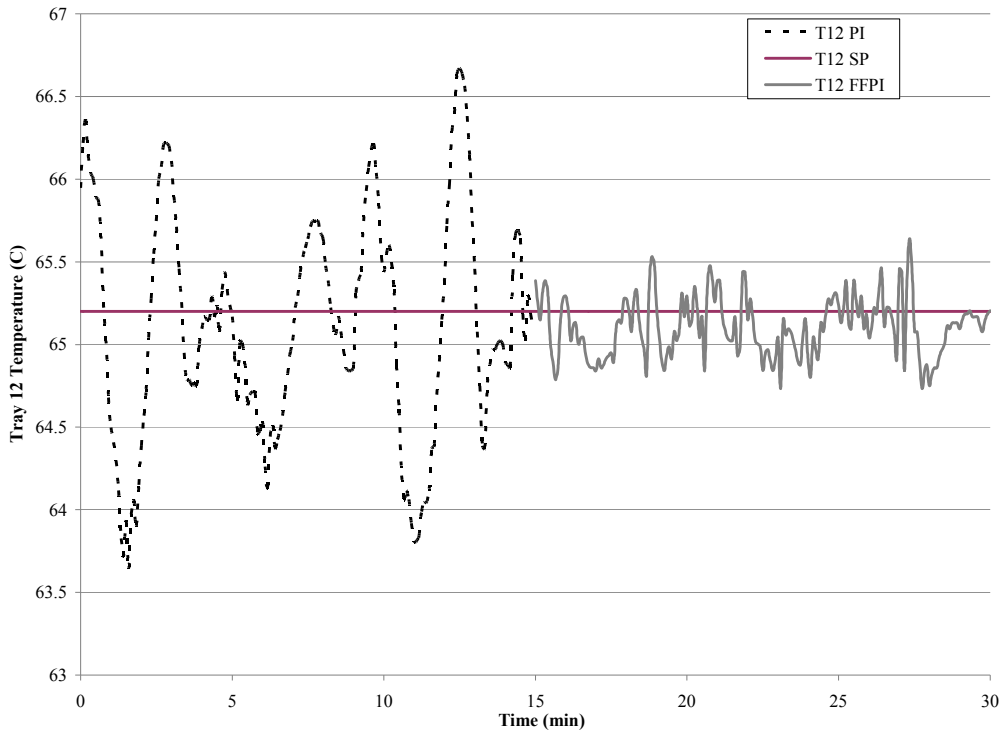


Figure 17: The observed Tray 12 temperatures under feedback only (PI) and feedforward/feedback (FFPI) control when process inputs are not deliberately being disturbed. Changes in the inputs are a result of only normal operational variability.

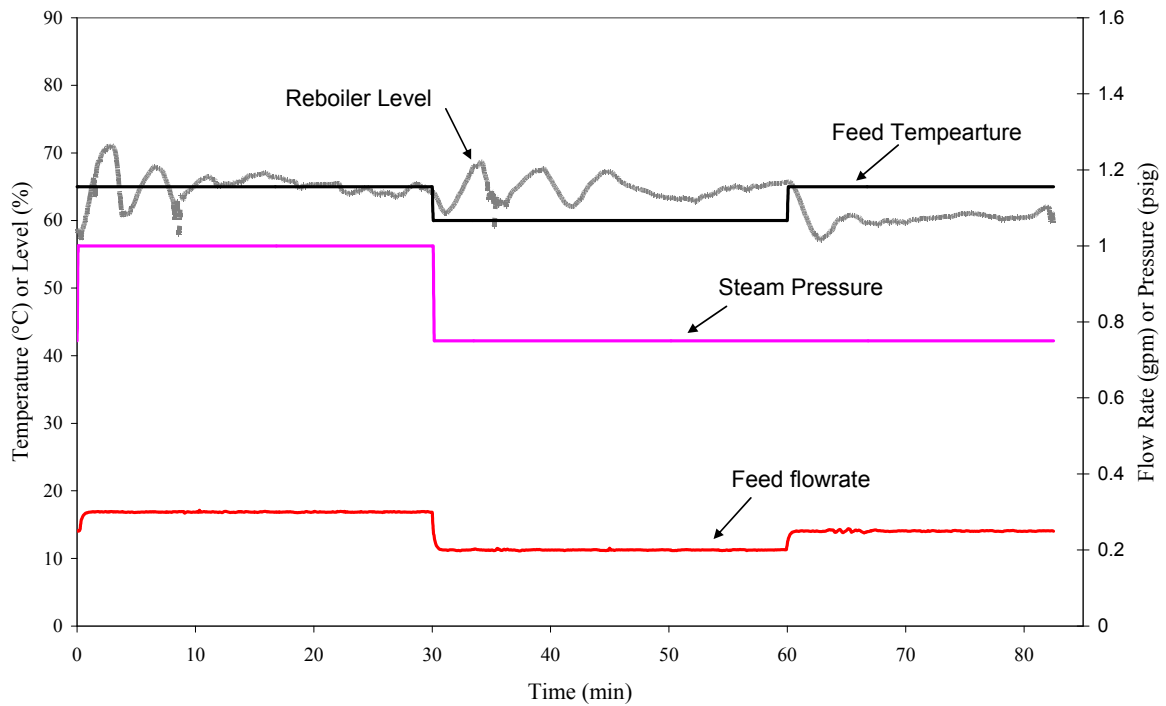


Figure 18: The input changes made to test the proposed feedforward/feedback controller and the feedback only controller.

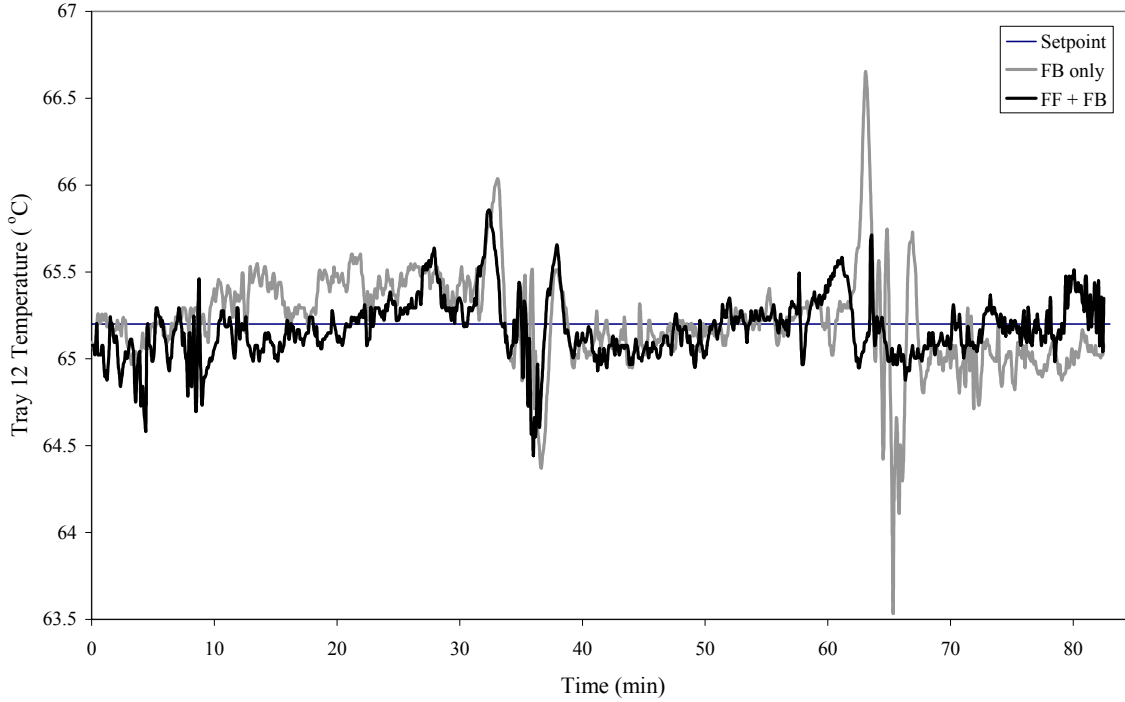


Figure 19: The output responses of the tray 12 temperature under feedforward/feedback (FF + FB) control and feedback (FB) only control to the series of input changes that is given in Fig. 17.

In order to quantitatively compare the results of implementing the feedforward controller, the average absolute error (AAE) term is used. This is defined as

$$AAE = \frac{\sum_n |T_{setpoint} - T_{measured}|}{n} \quad (27)$$

Under regulatory control, for the PI only controller, $AAE = 0.563$ and for the FFPI controller, $AAE = 0.168$. This represents a reduction in process variability of 70.1%. In the case where inputs were deliberately changed to test more extreme process conditions, for the PI controller the $AAE = 0.192$, while in the case of the FFPI controller, $AAE = 0.134$. This represents a 42.8% reduction in the variability of the Tray 12 temperature. In addition, we can also examine the range of the temperature that is measured on Tray 12. Under the more extreme process conditions, for the PI controller the temperature varies from 63.5°C to

66.7°C (3.11° range), and for the FFPI controller the temperature varies from 64.4°C to 65.8°C (1.41° range). Thus, the range of the temperature measured on Tray 12 is reduced by 54.6%.

4. Conclusions

In this paper, we have presented a methodology for developing a Wiener block-oriented model from plant data that accurately predicts process response behavior to multiple input disturbances that are occurring simultaneously. The model was implemented into a feedforward/feedback control scheme and demonstrated marked improvements over traditional feedback control. The ability to develop the model with plant historical data under closed-loop conditions represents a significant advantage over traditional model-building techniques, which require specific perturbations of the process that can affect plant operations.

This work will be extended to other types of chemical and biological process systems for further investigation. Specifically, the work done by Rollins et al. [24] to predict glucose response in type 2 diabetics will be extended to close the loop on glucose concentration. The implications of this for persons with type 1 and type 2 diabetes are tremendous, as the ability to control glucose levels at a desired level will greatly affect their longevity and quality of life.

5. Acknowledgements

The authors would like to thank Utkarsh Singh and Setche Kwamu-Nana for their assistance in running tests on the distillation column. They would also like to thank Tracy Junge and Terry Blevins from Emerson Process Management for their suggestions and expertise in programming the DeltaV control system.

6. References

- [1] Seborg, D.E., T.F. Edgar and D.A. Mellichamp, *Process Dynamics and Control*, 2nd edition, John Wiley and Sons, 2003.
- [2] Clarke, D.W., C. Mohtadi and P.S. Tuffs, "Generalized Predictive Control- Part 1: The Basic Algorithm," *Automatica*, Vol. 23, pp. 137-148, 1987.
- [3] Muske, K.R. and J.B. Rawlins, "Model Predictive Control with Linear Models," *AIChE Journal*, Vol. 39, pp. 262-287, 1993.
- [4] Alexandridis, A. and H. Sarimveis, "Nonlinear Adaptive Model Predictive Control Based on Self-Correcting Neural Network Models," *AIChE Journal*, Vol. 51. No. 9, September 2005.
- [5] Fischer, M., O. Nelles and R. Isermann, "Adaptive Predictive Control of a Heat Exchanger Based on a Fuzzy Model," *Control Engineering Practice*, Vol. 6, pp. 259-269, 1998.
- [6] Di Palma, F., L. Magni, "A Multi-Model Structure for Model Predictive Control," *Annual Reviews in Control*, Vol. 28, pp. 47-52, 2004.
- [7] Gao, J, R. Patwardhan, K. Akamatsu, Y. Hashimoto, G. Emoto, S.L. Shah, B. Huang, "Performance Evaluation of Two Industrial MPC Controllers," *Control Engineering Practice*, Vol. 11, pp.1371-1387, 2003.
- [8] Havlena, V. and J. Findejs, "Application of Model Predictive Control to Advanced Combustion Control," *Control Engineering Practice*, Vol. 13, pp. 671-680, 2005.
- [9] Al-Duwaish H. and Naeem, Wasif , "Nonlinear Model Predictive Control of Hammerstein and Wiener Models Using Genetic Algorithms," *Proceedings of the 2001 IEEE International Conference on Control Applications*, September 5-7, 2001, Mexico City, Mexico
- [10] Gao, F., F. Wang and M. Li, "Predictive Control for Processes with Input Dynamic Nonlinearity," *Chemical Engineering Science*, Vol. 55, pp. 4045-4052, 2000.
- [11] Pearson, R.K. and B.A. Ogunnaike, "Nonlinear Process Identification," *Nonlinear Process Control*, Prentice-Hall PTR, Upper Saddle River, NJ, pp. 11-110, 1997.
- [12] Rollins, D.K., N. Bhandari, A.M. Bassily, G.M. Colver and S. Chin, "A Continuous-Time Nonlinear Dynamic Predictive Modeling Method for Hammerstein Processes," *Industrial and Engineering Chemistry Research*, Vol. 42, No. 4, pp. 861-872, 2003.
- [13] Greblicki, W., "Continuous-Time Hammerstein System Identification," *IEEE Transactions on Automatic Control*, Vol. 45, No. 6, pp. 1232-1236, 2000.

- [14] Bhandari, N. and D.K. Rollins, "Continuous-Time Hammerstein Nonlinear Modeling Applied to Distillation," *AIChE Journal*, Vol. 50, No. 2, pp. 530-533, 2004.
- [15] Bhandari, N. and D.K. Rollins, "A Continuous-Time MIMO Wiener Modeling Method," *Industrial and Engineering Chemistry Research*, Vol. 42, No. 22, pp. 5583-5595, 2003.
- [16] Chin, S., N. Bhandari and D.K. Rollins, "An Unrestricted Algorithm for Accurate Prediction of MIMO Wiener Processes," *Industrial and Engineering Chemistry Research*, Vol. 43, pp. 7065-7074, 2004.
- [17] Luyben, W.L., "Distillation, Feedforward Control with Intermediate Feedback Control Trays," *Chemical Engineering Science*, Vol. 24, No. 6, pp. 997-1007, 1969.
- [18] Rix, A., K. Loewe and H. Gelbe, "Feedforward Control of a Binary High Purity Distillation Column," *Chemical Engineering Communications*, Vol. 159, pp. 105-118, 1997.
- [19] Castellanos-Sahagun, E., J. Alvarez-Ramirez and J. Alvarez, "Two-Point temperature Control Structure and Algorithm Design for Binary Distillation Columns," *Industrial and Engineering Chemistry Research*, Vol. 44, pp. 142-152, 2005.
- [20] Baratti, R., S. Corti and A. Servida, "Feedforward Control Strategy for Distillation Columns," *Artificial Intelligence in Engineering*, vol. 11, No. 4, pp. 405-412, 1997.
- [21] Rollins, D.K., N. Bhandari, A.M. Bassily, G.M. Colver and S. Chin, "A Continuous-Time Nonlinear Dynamic Predictive Modeling Method for Hammerstein Processes," *Industrial and Engineering Chemistry Research*, Vol. 42, No. 4, pp. 861-872, 2003.
- [22] Bhandari, N. and D.K. Rollins, "A Continuous-Time MIMO Wiener Modeling Method," *Industrial and Engineering Chemistry Research*, Vol. 42, No. 22, pp. 5583-5595, 2003.
- [23] Rollins, D.K. and N. Bhandari, "Constrained MIMO dynamic Discrete-Time Modeling Exploiting Optimal Experimental Design," *Journal of Process Control*, Vol. 14, No. 6, pp. 671-683, 2004.
- [24] Rollins, D.K., J. Kleinedler, A. Strohhahn, L. Boland, M. Murphy, D. Andre, D. Wolf and W.E. Franke, "Modeling Glucose Noninvasively Using Wiener Simulation Modeling for Type 2 Diabetic Patients Under Free-living Conditions," submitted to *IEEE Transactions on Biomedical Engineering*, in review.
- [25] Rollins, D.K., N. Bhandari, S. Chin, T. Junge and K. Roosa, "Optimal Deterministic Transfer Function Modeling in the Presence of Serially Correlated Noise," *Chemical Engineering Research and Design*, Vol. 84(A1), pp. 9-21, 2006.

- [26] Box, G.P. and G.M. Jenkins, *Time Series Analysis: Forecasting and Control*, Revised edition (Holden-day, Oakland, California), 1976.
- [27] Zhang, J. and R. Agustriyanto, "Inferential Feedforward Control of a Distillation Column," *Proceedings of the American Control Conference*, pp. 2555-2560, Arlington, VA, June 25-27, 2001.
- [28] Smith, C.A. and A.B. Corripio, *Principles and Practice of Automatic Process Control*, Wiley, New York, 1985.
- [29] Luyben, W.L., *Process Modeling, Simulation and Control for Chemical Engineers*, 2nd ed., McGraw-Hill, New York, 1990.
- [30] Loveland, S.D. and L. dela Rosa, "Distillation – A Unit Operations Laboratory Manual," Department of Chemical and Biological Engineering, Iowa State University, Ames, Iowa, 2005.
- [31] Emerson Process Management, *DeltaV Books online*, DeltaV version 7.4, 2004.
- [32] Cochran, W.G. and G. Cox, *Experimental Designs*, 2nd ed., Wiley, New York, 1992.

CHAPTER 6. CONCLUSIONS AND FUTURE WORK

1. Conclusions

The increasing pressure in industry to maintain tight control of processes has led to the development of many advanced control algorithms. Many of these are model-based control schemes, which require an accurate predictive model of the process to achieve good controller performance. Because of this, research in the field of nonlinear process modeling has advanced over the past several decades. Included among the types of nonlinear models that have been developed are block-oriented models, which combine linear dynamic blocks (L) with static nonlinear blocks (N) in varying configurations.

As we have seen, the Hammerstein Block-oriented Exact Solution Technique (H-BEST) and Wiener Block-oriented Exact Solution Technique (W-BEST) modeling methodologies have been shown to give accurate and efficient predictions of process output behavior for several different types of processes. The methodologies can be easily extended to include other types of block-oriented models, such as LNL “sandwich” type models, and accurately predict process output behavior in these systems as well. The initial studies into using these methods were presented in Chapter 3.

In Chapter 4, the complete methodology for identifying the LNL block-oriented model was presented. It used statistical design of experiments to determine the input changes to be made to the process in order to identify model parameters. The methodology was demonstrated on a simulated continuous-stirred tank reactor (CSTR) process and accurately predicted the reactor temperature response to changes in four input variables. A new feedforward/feedback control algorithm was introduced that uses the identified LNL model to compensate for multiple input disturbances that were occurring simultaneously. This

represents a significant advancement in model-based control, because it is able to account for interactions between process inputs, nonlinearities in the process dynamics and does not require the process model to be invertible.

Chapter 5 presents an extension of the W-BEST modeling methodology to include the ability to identify a process model using highly correlated input data, such as that which would be found in a plant historical database. It was shown that a model could be built under open- or closed-loop process conditions, and still give accurate predictions of process behavior. In this case, real data from a pilot-scale distillation column was used to develop the model. A new feedforward/feedback control algorithm based upon the identified Wiener model was presented, and it is able to compensate for multiple input disturbances simultaneously. It was implemented on the real distillation column with excellent results - the feedforward/feedback controller performance was compared to standard feedback control, and showed a significant reduction in process output variability.

The work in Chapter 5 introduces an exciting possibility for control engineers in industry. Using the proposed methodology, they will have the ability to retrieve data from their plant historical database, use it to build a model of the process, and implement this model into a feedforward control algorithm that compensates for multiple input disturbances simultaneously. This eliminates the sometimes tedious and costly task of introducing perturbations to an industrial process, which may cause significant process upsets and pose a risk to the safety of the plant operations personnel.

2. Future Work

Along with the successful implementation of the proposed model identification methodologies and feedforward/feedback control algorithms, there have been numerous questions raised that require further extension of this work.

Although the feedforward/feedback control scheme makes a significant improvement in the process variability and can compensate for multiple input disturbances simultaneously, it can only address those inputs that are measurable in a timely and efficient manner. Many other variables exist that may not be able to be addressed. Because of this, further research should be done to apply the concepts of model predictive control in conjunction with the feedforward algorithms proposed here. Doing this could result in an even greater improvement in the control of the process output variables. Ideally, this work will be implemented on a real process in an industrial setting, and will contribute to greater efficiency in plant operations, and a higher level of safety, quality and production yield.

In addition, other types of processes should be investigated. In this work, only a CSTR and a distillation process were examined. Some preliminary work has been done by Rollins et al. [1, 2] to predict blood glucose response in type 1 and type 2 diabetic patients using the principles of the W-BEST methodology. Understanding how different input variables affect the glucose response is the first step toward being able to control glucose levels. By using the feedforward control principles developed here, one could essentially “close the loop” on glucose response in patients. For type 1 diabetics, this would include manipulating the flow from an insulin pump that currently operates only on feedback control. For type 2 diabetics, this would be more indirect, but it would help them to understand how to eat, exercise, etc. to best control blood glucose levels on a given day.

3. References

- [1] Rollins, D.K., N. Bhandari and K.R. Kotz, “Critical Modeling Issues for Successful Feedforward Control of Blood Glucose in Insulin Dependent Diabetics,” accepted for publication in the *Proceedings of the American Control Conference*, June 2008.
- [2] Rollins, D.K., J. Kleinedler, A. Strohhahn, L. Boland, M. Murphy, D. Andre, D. Wolf and W.E. Franke, “Modeling Glucose Noninvasively Using Wiener Simulation Modeling for Type 2 Diabetic Patients Under Free-living Conditions,” submitted to *IEEE Transactions on Biomedical Engineering*, in review.

ACKNOWLEDGEMENTS

There are many people I would like to thank for their support, help and encouragement during the course of this work. Brian, you are the best husband anyone could ever ask for. Your love, patience and encouragement through all of this has been tremendous. Words can't express how thankful I am to have you as my partner on this life's journey. My children, Josh, Nate and LilyAnna, you bring so much joy to all who know you. I hope this is an inspiration to you to achieve all of your life's goals. Thank you to my parents and siblings for your encouragement and your help with everything from babysitting to editing my writing. To Derrick, thank you for all your support and for pushing me to achieve what I once thought was impossible. I am proud to call you not just my major professor, but my friend.

To all my group-mates who have been on this long journey with me, I am grateful for your friendship and camaraderie. It has been an adventure. I am especially thankful for the help and friendship of Nidhi and Swee-Teng. To the undergrad researchers who have helped along the way: Lewis, Andy, Singh and Setche, among many others, I appreciate your hard work in the lab and your ability to lighten the mood when things were difficult. Also, thank you to Tracy Junge and Terry Blevins from Emerson Process Management, who provided some suggestions for implementing the feedforward controller on the DeltaV system.

Above all, I must thank my God and Savior, for without His provision and guidance this would have never been possible. *Soli Deo Gloria.*